Port of Weipa Ambient Marine Water Quality Monitoring Program (July 2018 – July 2019)

Nathan Waltham, Christina Buelow, Jordan Iles, James Whinney, Blake Ramsby, and Rachael Macdonald

Report No. 19/32

December 2019

Port of Weipa Ambient Marine Water Quality Monitoring Program (July 2018 – July 2019)

A Report for North Queensland Bulk Ports Corporation

Report No. 19/32

December 2019

Prepared by Nathan Waltham, Christina Buelow, Jordan Iles, James Whinney, Blake Ramsby, and Rachael Macdonald

EXECUTIVE SUMMARY

Background

1. North Queensland Bulk Ports has implemented an ambient marine water quality monitoring program surrounding the Port of Weipa. The objectives of the program are to establish a long term water quality dataset to characterise marine water quality conditions within the waters around this port operation, necessary in order to support future planned activities.
2. This program has incorporated a combination of spot field measurements and high frequency continuous data loggers, laboratory analysis for a range of nutrient, herbicides and heavy metals.

Climatic conditions

1. The 2018-2019 wet season was in the order of the 80th percentile for rainfall in the region. Total wet season rainfall for the monitoring period was 1918 mm, with Tropical Cyclone Trevor being an important feature to the season.
2. The daily average wind speed and direction recorded at Weipa airport for the reporting period (2018-2019) was predominantly from the south east and east and rarely reached speeds exceeding 24 km h^{-1}

Water chemistry

1. Field water quality conditions were measured at all sites for water temperature, electrical conductivity, pH, dissolved oxygen, and Secchi disk depth on a 6 weekly basis, for three depth horizons: surface (0.25 m), mid water, and bottom (1 m above substrate).
2. The water column is well mixed, with depth profiles for dissolved oxygen, temperature, electrical conductivity and pH showing only minor gradients of change.
3. Water column was well mixed during each survey, with little differences among the three horizons examined.
4. Turbidity values are generally higher at depth, contributing to a difference in water clarity between the surface and bottom water horizons. Higher turbidity values at the bottom water horizon is probably related to RMS wave height, currents, and sediment resuspension processes. The elevated turbidity in the bottom horizon becomes an important consideration when examining sensitive receptor habitats, such as seagrass which are sensitive to water clarity changes. Measuring bottom horizon turbidity is a very relevant component of this program; surface measurements for turbidity, or indeed suspended solid concentrations, might not be an entirely relevant measure when the objective is to protect and enhance benthic habitats.
5. Particulate nitrogen (PN) and phosphorus (PP) concentrations exceed guideline values during all 2018-2019 surveys and at all sites.
6. Chlorophyll-*a* concentrations exceed guideline values during all 2018-2019 surveys and at all sites.
7. Phytoplankton and zooplankton communities had a very different species composition between surveys completed so far, which could reflect local seasonal conditions – this pattern will be further explored as more data becomes available for the region.
8. Trace metals were generally well below guideline values throughout the reporting year. Zinc was detected across all sites in April 2018 and Zinc concentrations at WP_AMB4 exceeded guideline values in January 2019.
9. The major pesticide and herbicide concentrations were not detected above the limit of reporting

Sediment deposition and turbidity

1. Continuous sediment deposition and turbidity logging data supports the pattern found more broadly in North Queensland coastal marine environments, that during dry periods with minimal rainfall, elevated turbidity along the coastline is driven by the re-suspension of sediment and this has been most notable here given the links drawn between RMS water depth and NTUe/SSC. Large peaks in NTUe/SSC and RMS water depth were recorded over periods longer than a week.
2. Sediment deposition rates around Weipa were much higher than measured across other north Queensland coastal marine sites investigated during the same period.

Photosynthetically active radiation (PAR)

1. Patterns of light were similar among all the coastal sites. Generally, shallow inshore sites reached higher levels of benthic PAR and were more variable than deeper water coastal sites and sites of closer proximity to one another were more similar than distant sites.
2. At many of the sites where both turbidity and benthic light were measured, the concentration of suspended solids in the water column explained less than half of the variation in PAR. As PAR is more biologically relevant to the health of photosynthetic benthic habitats such as seagrass, algae and corals it is becoming more useful as a management response tool when used in conjunction with known thresholds for healthy growth for these habitats (e.g., Chartrand et al., 2012). For this reason, it is important to include photosynthetically active radiation (PAR) in the suite of water quality variables when capturing local baseline conditions of ambient water quality.

Recommendations

1. Given this monitoring program commenced in January 2018, and is now only into its 2nd full year of operation it is recommended that the program remain in its current form for the 2019/20 period.

TABLE OF CONTENTS

TABLE OF FIGURES

1   INTRODUCTION

1.1   Port operations

The Port of Weipa is situated on the western side of Cape York Peninsula in northern Queensland (Figure 1.1). It is located within the township of Weipa, where the Embley, Mission and Pine River's converge and discharge into the Gulf of Carpentaria. The port has a series of operational and associated loading/unloading facilities. The port is operated by North Queensland Bulk Ports Corporation (NQBP). Along with other NQBP ports in Queensland, Port of Weipa requires routine maintenance dredging to maintain declared navigational depths within the swing basin and berth areas, departure path and aprons. Any dredging activity necessary in the operating ports in the region are undertaken in accordance with Commonwealth and State approvals.

1.2   Program outline

In order to better define the potential impacts associated with port operations and to characterise the natural variability in key water quality parameters within the adjacent sensitive habitats, NQBP committed to an ambient marine water quality monitoring program in and around the coastal waters of Weipa (Figure 1.1; Table 1.1). As part of this program, water quality parameters are being investigated at a range of sites to build on 19 years of seagrass monitoring and three years of monitoring of photosynthetically active radiation (PAR) that has already been undertaken by NQBP. This monitoring program contains a range of ambient water quality components that collectively continue to characterise the natural variability in key water quality parameters, including those experienced at the nearest sensitive receiving habitat, predominately seagrass (Taylor et al., 2015).

Figure 1.1   Locations of the marine water quality monitoring program sites during 2018/19 program

Table 1.1   Locations of the ambient marine water quality monitoring program sites

Location	AMB site no.	Latitude	Longitude	Water quality	Deposition / PAR logger
WQ1	WP_AMB1	-12.668283	141.846133	Yes	Yes
WQ2	WP_AMB2	-12.673778	141.777081	Yes	Yes
WQ3	WP_AMB3	-12.94905	141.59835	Yes	Yes
WQ4	WP_AMB4	-12.701431	141.8667	Yes	Yes

1.3   Rainfall and river flows

The total wet season rainfall during the reporting period was 1918 mm (Figure 1.2). High rainfall occurred in March 2019 when Tropical Cyclone Trevor crossed the region. The influence of rainfall and therefore catchment flow can clearly change from year to year, which highlights precisely the reason for long term commitment to ambient marine monitoring programs.
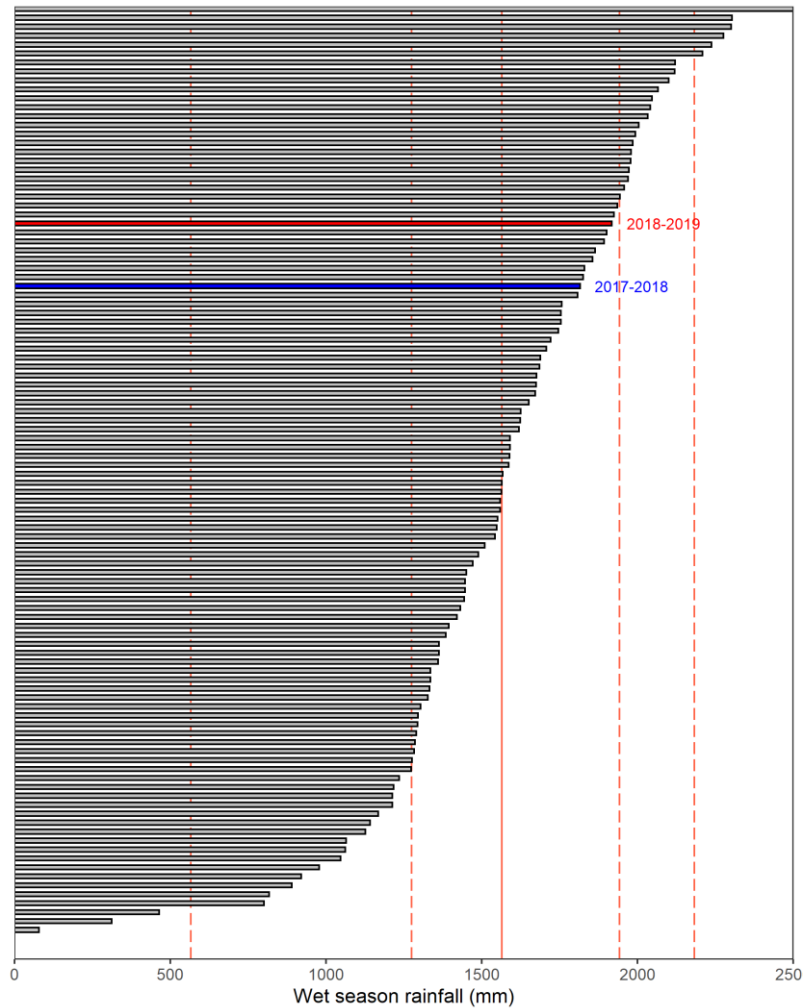
Figure 1.2   BOM wet season (Nov – March) rainfall data for Eastern Av Station (Weipa, station number 27042) ranked in order of decreasing total rainfall (mm). Blue bars show total rainfall over the past monitoring period, and the red bar represents the 2018/19 ambient marine water quality monitoring period. Vertical solid line represents median rainfall, while dashed lines represent 5th, 20th, 80th, and 95th percentiles.

The only local river gauging station near to Weipa is on the Watson River, which is located ~75 km south and does not discharge into the Mission River system where the Port is located. Therefore, although Watson River water flow (ML day^{-1}) has been used throughout this report to provide context for Port water quality conditions, results regarding the influence of water discharge on water quality variability should be interpreted with caution.

The hydrograph for Watson River (Figure 1.3) shows a distinct rise in the hydrograph during wet season months in both the current monitoring period (July 2018 – July 2019) and the previous monitoring period (January 2018 – July 2018). The hydrograph displays typical monsoonal rainfall patterns for this region. Weipa is located in a tropical environment where wet season rainfall can result in prolonged and elevated river discharge during November to April. A peak in water discharge can also be seen in late March 2019, corresponding with Cyclone Trevor (Figure 1.4).
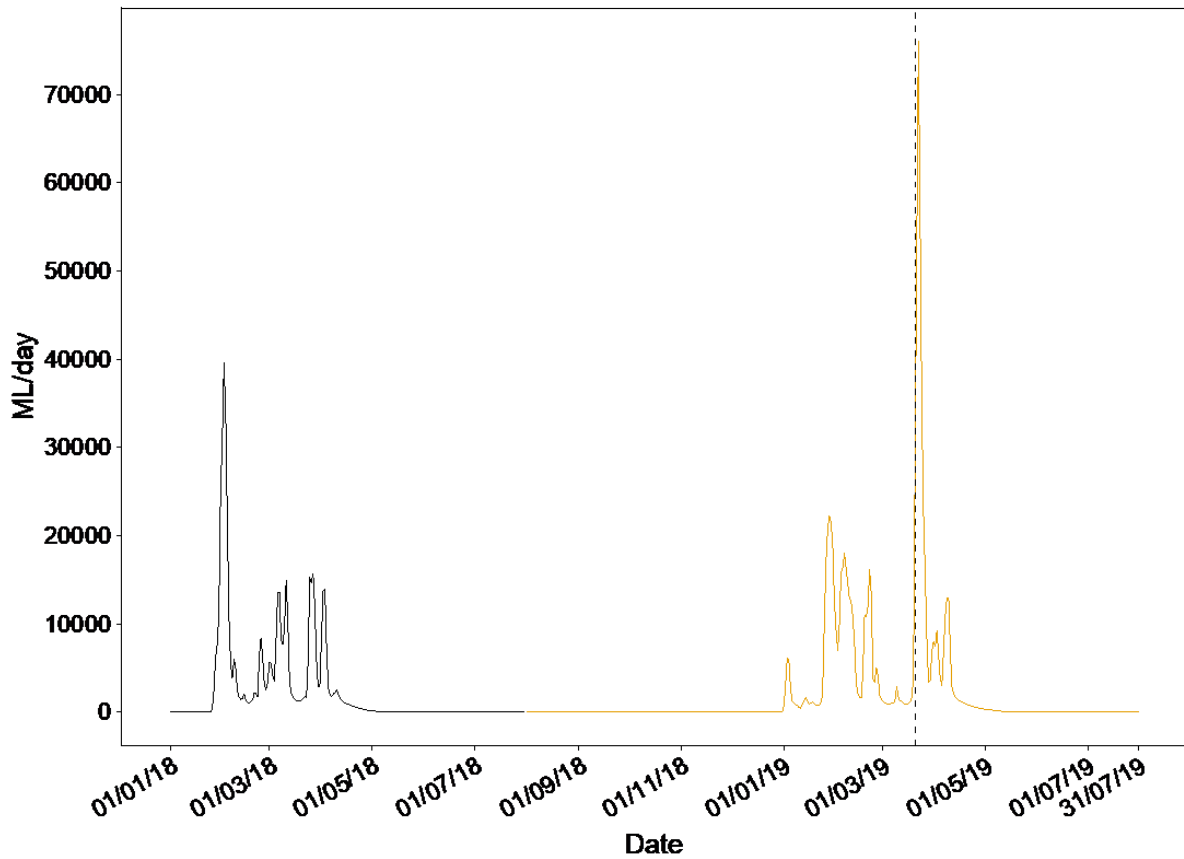
Figure 1.3   Flow (Megalitres/day) recorded for Watson River during January 2018 – July 2018. Colours relate to different monitoring periods (black = January 2018 – July 2018, orange = July 2018 – July 2019). The dashed line indicates a period of heavy rainfall associated with Tropical Cyclone Trevor on March 20th, 2019.
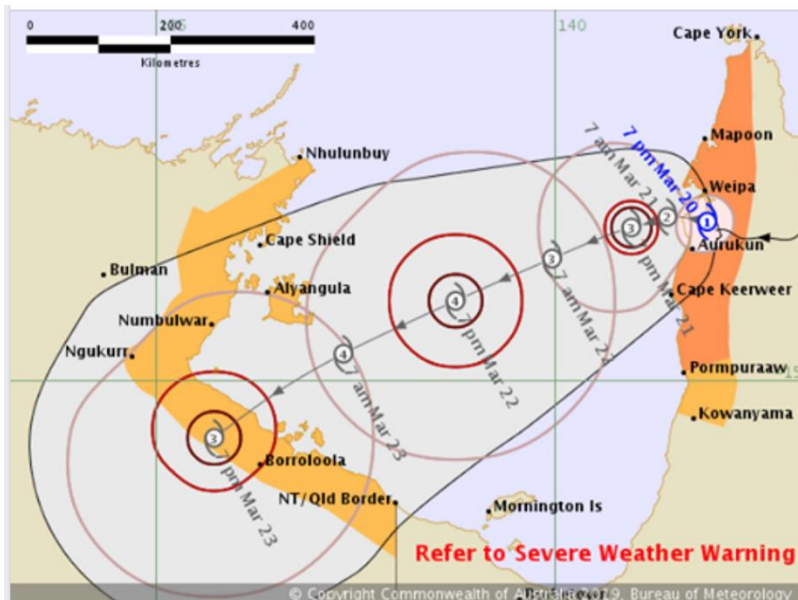
Figure 1.4   Cyclone Trevor path forecast (BOM; March 2019)

1.4   Wind

The daily average wind direction recorded at Weipa airport for the 2018/2019 reporting period was predominantly from the south east and east and rarely reached speeds > 24 km h^{-1} (Figure 1.5).
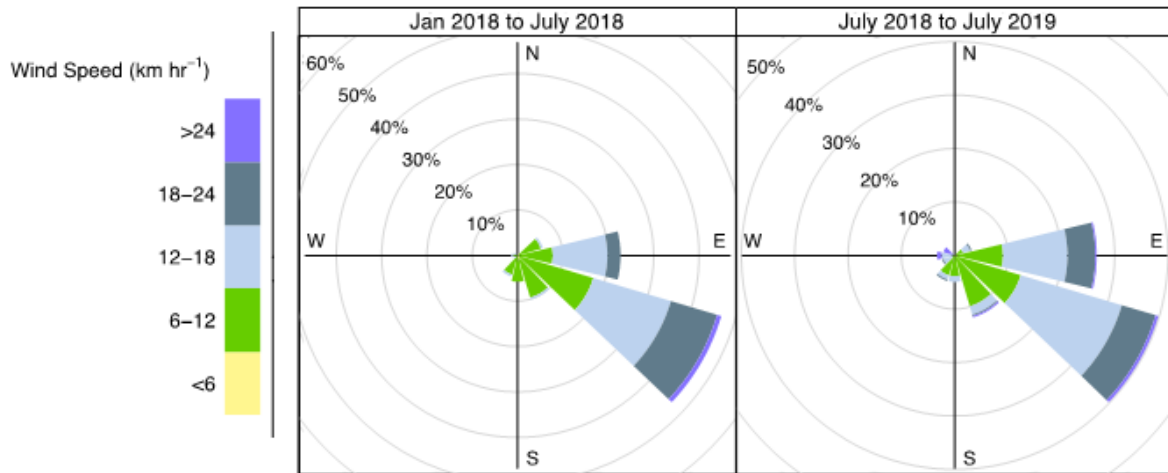
Figure 1.5   Daily average wind direction and strength recorded at the Weipa Airport during each monitoring period

1.5   Project objectives

The goal of the program is to characterise the ambient marine water quality monitoring within the region within and adjacent to Port of Weipa. This report provides a review and analysis of data collected between July 2018 and July 2019. These data are part of a longer term commitment to monitor and characterise receiving water quality conditions, to support future planned asset management and protection of this coastal port.

2   METHODOLOGY

2.1   Ambient water quality

Spot water quality samples were collected at sites approximately on a 6 week basis (Table 2.1) from a research vessel. At each site, a calibrated multiprobe is used to measure water temperature, salinity, dissolved oxygen (%), pH, and turbidity (Figure 2.1). In addition to spot measurements, secchi disk depth is recorded, as a measure of the optical clarity of the water column, along with light attenuation using a LiCor meter. These field in-situ measurements are recorded at three depth horizons: a) surface (0.25m); b) mid-depth; and c) bottom horizon.

In aligning with the ambient marine water quality monitoring in other NQBP ports (Ports of Mackay and Hay Point, and Port of Abbott Point) the water quality program design below was completed. The list of parameters examined consisted:

- Ultra-trace dissolved metals : arsenic (As), cadmium (Cd), copper (Cu), mercury (Hg), nickel (Ni), lead (Pb), and zinc (Zn);
- Nutrients (particulate nitrogen and phosphorus);
- Chlorophyll-*a*; and
- Pesticides/herbicides (Low LOR suite (EP234(A-I)) including: diuron, ametryn, atrazine, terbutryn. Note that pesticides are suspected to be in low concentrations during periods of low rainfall runoff, and only detectable following rainfall. As a consequence sampling of only two events at all sites for pesticides, one during the dry and a wet season – though note that the timing of each are dependent on prevailing weather conditions, so the timing of each survey could differ from year to year.

Figure 2.1   TropWATER staff conducting field water quality sampling

Table 2.1   Summary of instrument maintenance and water quality surveys completed during the 2017/18 reporting period

Date	Nutrients, Chlorophyll-*a*	Metals, herbicides	Plankton	Logger maintenance
July 2018	Yes	-	-	Yes
September 2018	Yes	Yes	Yes	Yes
October 2018	Yes	-	-	Yes
November 2018	Yes	-	Yes	Yes
January 2019	Yes	Yes	-	Yes
February 2019	Yes	-	Yes	Yes

April 2019	Yes	-	-	Yes
May 2019	Yes	-	Yes	Yes
June 2019	Yes	-	-	Yes
July 2019	Yes	-	-	Yes

Sampling methodology, sample bottles, preservation techniques and analytical methodology (NATA accredited) were in accordance with standard methods (i.e., DERM 2009b; APHA 2005; Standards Australia 1998). Field collected water samples were stored on ice in eskies immediately during field trips aboard the vessel, and transported back to refrigeration, before delivery to the TropWATER laboratory. For chlorophyll analysis, water was placed into a 1L dark plastic bottle and placed on ice for transportation back to refrigeration. For dissolved metals and nutrients, water was passed through a 0.45 µm disposable membrane filter (Sartorius), fitted to a sterile 60 mL syringe (Livingstone), and placed into 60 mL bottles (metals) and 10 mL bottles (nutrients) for posterior analysis in the laboratory. (The use of these field sampling equipment and procedures have been previously shown to reduce the risk of contamination of samples, contributing to false positive results for reporting; TropWATER (2015). Unfiltered sample for total nitrogen and total phosphorus analysis were frozen in a 60 mL tube. All samples are kept in the dark and cold until processing in the laboratory, except nutrients which are stored frozen until processing.

Water for chlorophyll determination was filtered through a Whatman 0.45 µm GF/F glass-fibre filter with the addition of approximately 0.2 mL of magnesium carbonate within (less than) 12 hours after collection. Filters are then wrapped in aluminium foil and frozen. Pigment determinations from acetone extracts of the filters were completed using spectrophotometry, method described in 'Standard Methods for the Examination of Water and Wastewater, 10200 H. Chlorophyll'.

Water samples are analysed using the defined analysis methods and detection limits outlined in Table 2.2. In summary, all nutrients were analysed using colorimetric method on OI Analytical Flow IV Segmented Flow Analysers. Total nitrogen and phosphorus and total filterable nitrogen and phosphorus are analysed simultaneously using nitrogen and phosphorous methods after alkaline persulphate digestion, following methods as presented in 'Standard Methods for the Examination of Water and Wastewater, 4500-NO3- F. Automated Cadmium Reduction Method' and in 'Standard Methods for the Examination of Water and Wastewater, 4500-P F. Automated Ascorbic Acid Reduction Method'. Nitrate, Nitrite and Ammonia were analysed using the methods 'Standard Methods for the Examination of Water and Wastewater, 4500-NO3- F. Automated Cadmium Reduction Method', 'Standard Methods for the Examination of Water and Wastewater, 4500-NO2- B. Colorimetric Method', and 'Standard Methods for the Examination of Water and Wastewater, 4500-NH3 G. Automated Phenate Method', respectively. Filterable Reactive Phosphorous is analysed following the method presented in 'Standard Methods for the Examination of Water and Wastewater, 4500-P F. Automated Ascorbic Acid Reduction Method'. Filterable heavy metals, and herbicides are analysed by Australian Laboratory Service (ALS).

For all water quality plots, boxes are 20th and 80th quantile, centre line is median, and whiskers represent the 5th and 95th percentile.

Table 2.2   Water analyses performed during the program

Parameter		APHA method number	Reporting limit
Routine water quality analyses			
	pH	4500-H+ B	-
	Conductivity (EC)	2510 B	5 µS cm^{-1}

	Total Suspended Solids (TSS)	2540 D @ 103 - 105°C	0.2 mg L^{-1}
	Turbidity	2130 B	0.1 NTU
	Salinity		
	Dissolved Oxygen		
	Light Attenuation		
Pesticides/herbicides			
	Organophosphate pesticides	In house LC/MS method: EP234A	0.0002-0.001 µg L^{-1}
	Thiocarbamates and Carbamates - Thiobencarb	In house LC/MS method: EP234B	0.0002 µg L^{-1}
	Dinitroanilines - Pendimethalin	In house LC/MS method: EP234C	0.001 µg L^{-1}
	Triazinone Herbicides - Hexazinone	In house LC/MS method: EP234D	0.0002 µg L^{-1}
	Conazole and Aminopyrimidine Fungicides - Propiconazole, Hexaconazole, Difenoconazole, Flusilazole, Penconazole	In house LC/MS method: EP234E	0.0002 µg L^{-1}
	Phenylurea Thizdiazolurea Uracil and Sulfonylurea Herbicides - Diuron, Ametryn, Atrazine, Cyanazine, Prometryn, Propazine, Simazine, Terbuthylazine, Terbutryn	In house LC/MS method: EP234F	0.0002 µg L^{-1}
Nutrients			
	Total Nitrogen and Phosphorus (TN, TP)	Simultaneous 4500-NO3- F and 4500-P F analyses after alkaline persulphate digestion	25 µg N L^{-1}, 5 µg P L^{-1}
	Filterable nutrients (nitrate, nitrite, ammonia, NO$_x$)	4500-NO3- F	1 µg N L^{-1}
	Ammonia	4500- NH3 G	1 mg N L^{-1}
	Filterable Reactive Phosphorus (FRP)	4500-P F	1 µg P L^{-1}
	Chlorophyll	10200-H	0.1 µg L^{-1}
Trace Metals			
	Arsenic, Cadmium, Copper, Lead, Nickel, Silver, Zinc, Mercury	3125B ORC/ICP/MS	0.05 to 100 µg L^{-1}

2.2   Plankton community

At all sites, a 60 μm plankton net (for phytoplankton) and a 500 μm plankton net (for zooplankton) was towed behind the survey vessel for approximately 100 m. The boat speed is reduced to approximately 6 knots, with a GPS waypoint taken at the start and end of each plankton tow. At the end of each plankton tow, the nets are retrieved, and the contents retained in the plastic jar attached to the net was immediately transferred to preservation containers. Samples were identified to the lowest possible taxon.
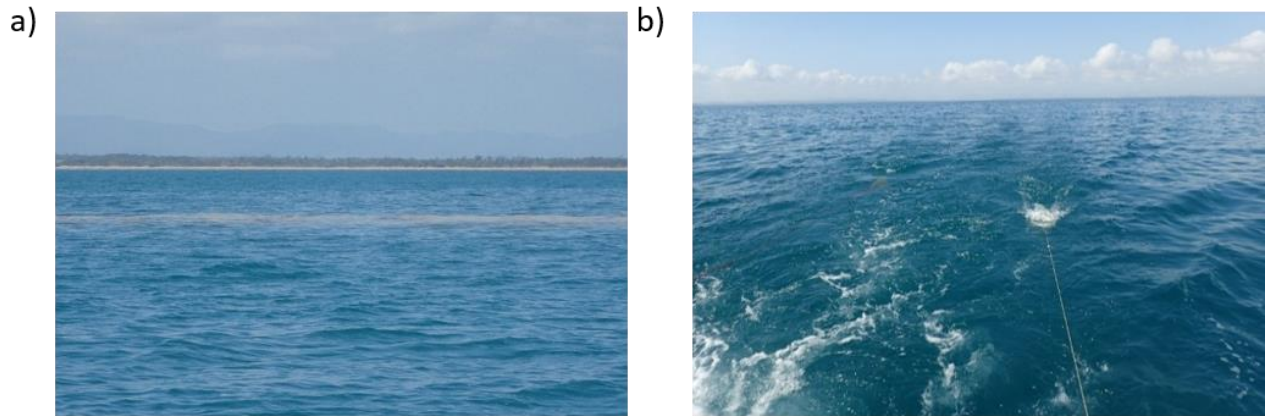
Figure 2.2   Example plankton sample. a) Trichodesmium bloom on sea surface; b) phytoplankton (60 μm) tow behind the survey vessel.

2.3   Multiparameter water quality logger

Sediment deposition, turbidity, Photosynthetically Available Radiation (PAR), water depth, Root Mean Squared (RMS) water depth and water temperature were measured at seven sites using multiparameter water quality instruments manufactured at the Marine Geophysics Laboratory, School of Engineering and Physical Sciences, James Cook University (Figure 2.3). These instruments are based on a Campbell's Scientific 1000 data logger that has been programmed to measure and store these marine physical parameters using specifically designed sensors.

2.3.1   Turbidity

The turbidity sensor provides data in Nephelometric Turbidity Unit's equivalent (NTUe) and can be calibrated to Suspended Sediment Concentration (SSC) in mg L^{-1} (Larcombe et al., 1995). The sensor is located on the side of the logger, pointing parallel light-emitting diodes (LED) and transmitted through a fibre optic bundle. The backscatter probe takes 250 samples in an eight second period to attain an accurate turbidity value. The logger is programmed to take these measurements at 10 minute intervals. The sensor interface is cleaned by a mechanical wiper at a two hour interval allowing for long deployment periods where bio-fouling would otherwise seriously affect readings.

It must be noted the international turbidity standard ISO7027 defines NTU only for 90 degree scatter, however, the Marine Geophysics Laboratory instruments obtain an NTUe value using 180 degree backscatter as it allows for much more effective cleaning. Because particle size influences the angular scattering functions of incident light (Ludwig and Hanes 1990; Conner and De Visser 1992; Wolanski et al., 1994; Bunt et al., 1999), instruments using different scattering angles can provide different measurements of turbidity (in NTU). This has to be acknowledged if later comparison between instruments collecting NTUe and NTU are to be made. To enhance the data, all sites were calibrated to provide a measure of SSC (mg L^{-1}) and enable for the accurate comparison between 90 degree backscatter and 180 degree backscatter measurements.

2.3.2   Sediment deposition

Deposition is recorded in Accumulated Suspended Sediment Deposition (ASSD) (mg cm^{-2}). The sensor is wiped clean of deposited sediment at a 2 hour interval to reduce bio-fouling and enable sensor sensitivity to remain high. The deposition sensor is positioned inside a small cup shape (16 mm diameter x 18 mm deep) located on the flat plate surface of the instrument facing towards the water surface. Deposited sediment produces a backscatter of light that is detected by the sensor. Deposited sediment is calculated by subtracting, from the measured data point, the value taken after the sensor was last wiped clean. This removes influence of turbidity from the value and re-zeros the deposition sensor every 2 hours.

If a major deposition event is in progress, the sensor reading will increase rapidly and will be considerably above the turbidity sensor response. Gross deposition will appear as irregular spikes in the data where the sediment is not removed by the wiper but by re-suspension due to wave or current stress. When a major net deposition event is in progress the deposited sediment will be removed by the wiper and the deposition sensor reading should fall back to a value similar to the turbidity sensor. The data will have a characteristic zigzag response as it rises, perhaps quite gently, and falls dramatically after the wipe (see Ridd et al., 2001).

Deposition data is provided as a measurement of deposited sediment in mg cm^{-2} and as a deposition rate in mg cm^{-2} d^{-1}. The deposition rate is calculated over the 2 hour interval between sensor wipes and averaged over the day for a daily deposition rate. The deposition rate is useful in deposition analysis as it describes more accurately the net deposition of sediment by smoothing spikes resulting from gross deposition events.

2.3.3   Pressure

A pressure sensor is located on the horizontal surface of the water quality logging instrument. The pressure sensor is used to determine changes in water depth due to tide and to produce a proxy for wave action. Each time a pressure measurement is made the pressure sensor takes 10 measurements over a period of 10 seconds. From these 10 measurements, average water depth (m) and Root Mean Square (RMS) water height are calculated. RMS water height, D_{rms}, is calculated as follows:

$$D_{rms} = \sqrt{\sum_{n=1}^{10} (D_n - \overline{D})^2 / n}$$

Equation 1: where D_n is the nth of the 10 readings and $\overline{D}$ is the mean water depth of the n readings.

The average water depth and RMS water depth can be used to analyse the influence that tide and water depth may have on turbidity, deposition and light levels at an instrument location. The RMS water height is a measure of short term variation in pressure at the sensor. Changes in pressure over a 10 second time period at the sensor are caused by wave energy. RMS water height can be used to analyse the link between wave re-suspension and SSC. It is important to clearly establish that RMS water height is not a measurement of wave height at the sea surface. What it does provide is a relative indication of wave shear stress at the sea floor that is directly comparable between sites of different depths. For example, where two sites both have the same surface wave height, if site one is 10 m deep and has a measurement of 0.01 RMS water height and site two is 1 m deep and has a measurement of 0.08 RMS water height. Even though the surface wave height is the same at both sites, the RMS water height is greater at the shallower site and we would expect more re-suspension due to wave shear stress at this site.

2.3.4   Water temperature

Water temperature values are obtained with a thermistor that records every 10 minutes. The sensor is installed in a bolt that protrudes from the instrument and gives sensitive temperature measurements.
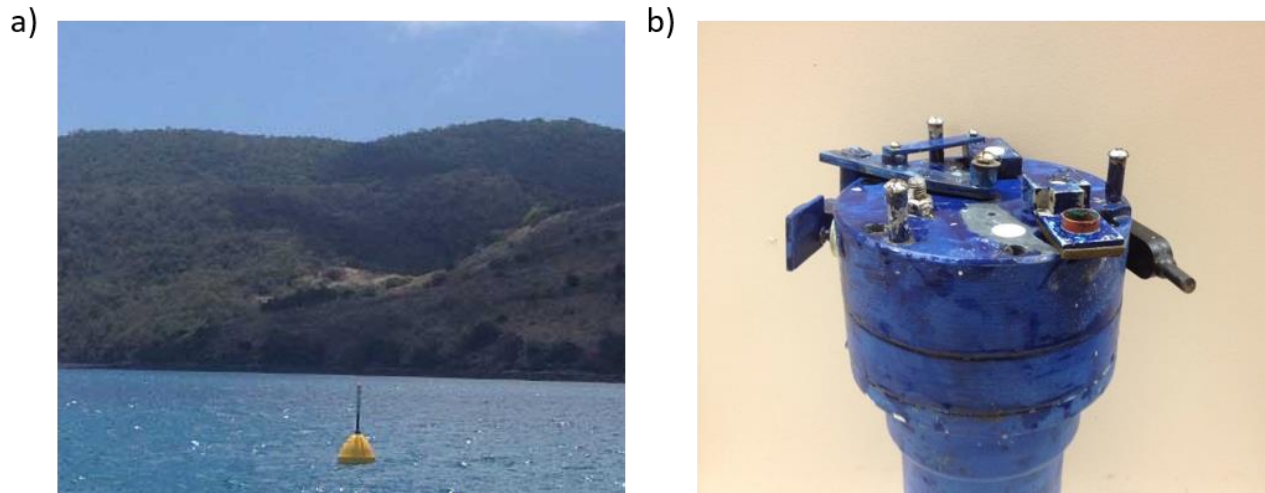
Figure 2.3   Example coastal multiparameter water quality instrument: a) site navigation beacon for safety and instrument retrieval; b) instrument showing sensors and wiping mechanisms

2.3.5   Photosynthetically Active Radiation (PAR)

A PAR sensor, positioned on the horizontal surface of the water quality logging instrument, takes a PAR measurement at ten (10) minute intervals for a one second period. To determine total daily PAR (mol m^{-2} d^{-1}) the values recorded are multiplied by 600 to provide an estimate of PAR for a 10 minute period and then summed for each day.

2.4   Marotte current meter

The Marotte HS (High Sampling Rate) is a drag-tilt current meter invented at the Marine Geophysics Laboratory (Figure 2.4). The instrument records current speed and direction with an inbuilt accelerometer and magnetometer. The current speed and direction data are smoothed over a 10-minute period. The instruments are deployed attached the nephelometer frames and data is download when the instruments are retrieved. Inclusion of this current meter has been added to the program as a way to trial new technology, gather new data and to add value to the project outcomes and deliverables.
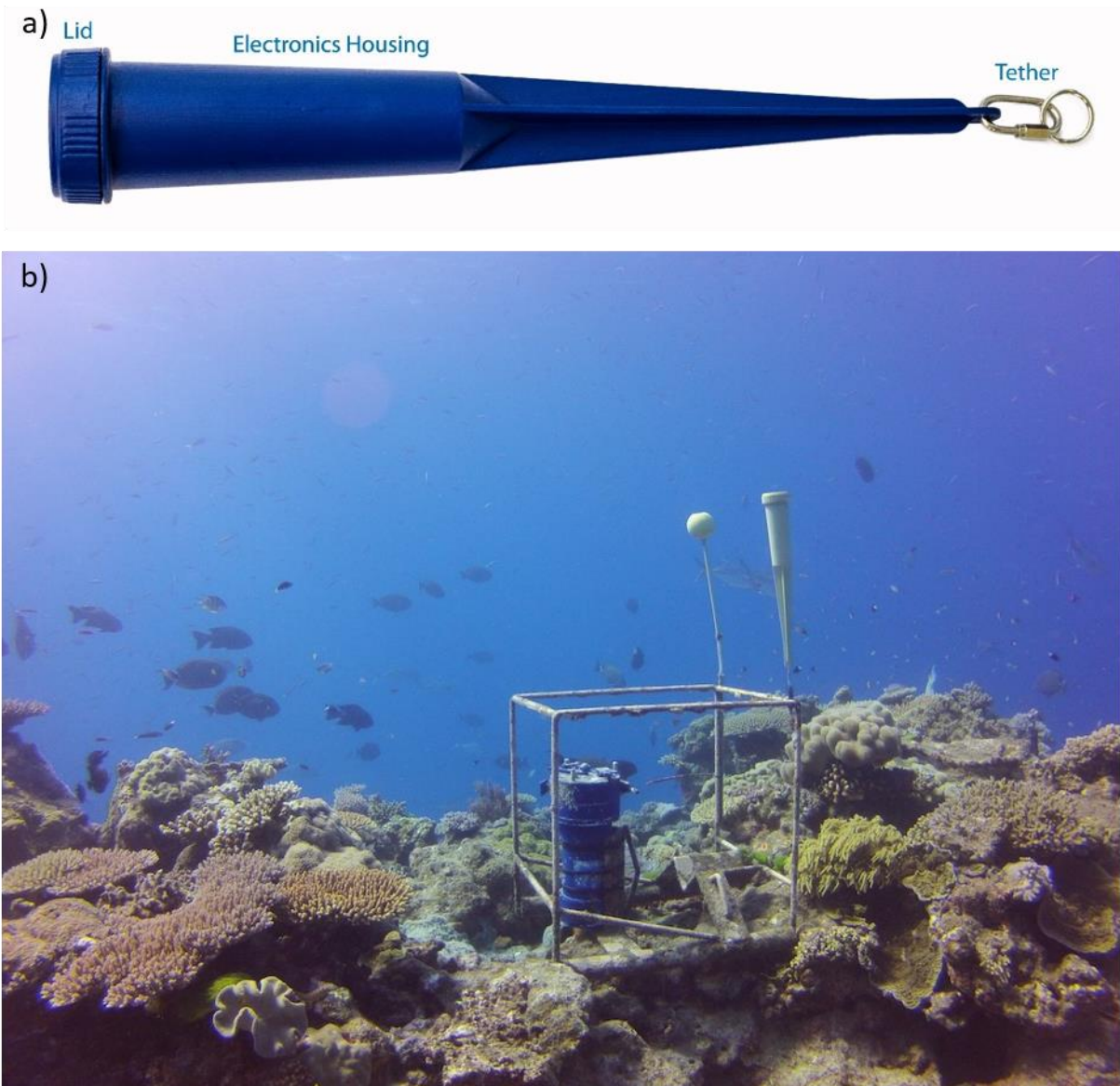
Figure 2.4   a) Basic schematic of Marotte HS current meter; and b) Marotte HS alongside Marotte tethered to a nephelometer frame at Moore Reef. Image courtesy of Eric Fisher

2.4.1   Measuring environmental controls on SSC

Stepwise regression analysis was used to investigate the environmental controls on SSC at the ambient sites, with data selected including:

(a) Ambient sites:

[1] "WQ1" "[2] "WQ2"

[3] "WQ3" [4] "WQ4"

[5] "WQ5"

(b) River Gauge Station:

[1] "Watson River"

(c) Wind Station:

[1] "Station 027045 – Weipa airport"

(d) Tide Gauge Station:

[1] "Weipa Gauge"

In this assessment, the environmental parameters with control on SSC were analysed by stepwise regression analysis followed by relative importance analysis (Grömping, 2006) using R language (R Core Team, 2015). The stepwise analysis allowed the selection of the environmental variables that explain the SSC variability in the water column. The relative importance analysis allowed these selected variables to be ranked based on their overall explanation of the SSC variability. In order to visualize the effect of each environmental parameter selected in the stepwise analysis, a partial plot analysis (Crawley, 2007) was carried out. These partial plots indicate the dependence between SSC and each selected variable when all the other variables in the model are kept constant (Crawley, 2007). The data set used in the stepwise analysis was log-transformed, if needed, in order to satisfy requirements for regression analysis. For each site, all the following variables were tested in an initial model against SSC: RMS of water depth, mean daily wind, maximum tide amplitude and river discharge. Mean daily wind was calculated from 8 daily readings decomposed into NE-SW and NW-SE components. Maximum tide amplitude was calculated as the maximum absolute difference between two consecutive maximum or minimum tide readings. Wind components were calculated as the mean value of 8 daily measurements decomposed to in two diagonals, NE-SW and NW-SE. Variables presenting autocorrelation were excluded based on a variance inflation test (Fox and Monett, 1992) > 4 and outliers were removed based on Bonferroni Outlier Test (Cook and Weisberg 1982).

3   RESULTS AND DISCUSSION

3.1   Ambient water quality

3.1.1   Spot water quality physio-chemical

For the reporting period between July 2019 and July 2018 water temperature ranged between 22 and 32 °C (Figure 3.1). There is a seasonal effect on water temperatures in the region, with the highest water temperatures observed during surveys in the summer months, and cool water temperatures observed during the winter months. These patterns are consistent throughout the water column, indicating that the water column profile is vertically well mixed. There are no guidelines for water temperature in coastal areas, however, temperature is an essential interpretative aid for ecological assessment in environments. For example, species such as fish and other animals have thermal stress point which causes discomfort and could be misconstrued as being a toxicological impact (example are the coral trout; Johansen et al. 2015). There were no observed or known impacts on aquatic species in the region during this monitoring period.

Electrical conductivity (EC) was stable across all sites, with little evidence of changing conditions through the water column (Figure 3.2). Overall EC has remained between 38 mS cm^{-1} and 55 mS cm^{-1}, generally indicating oceanic conditions. During the January 2018 to September 2019, salinity (ppt) was recorded in the field. To correct for this, we generated a relationship between water sample measured EC during trips and field salinity records, and then back calculated for EC measurements in the field. The corrected EC field data (shown in Figure 3.2) appears stable among sites and surveys. The data is presented here for completeness, but use of these data will require caution.

Dissolved oxygen saturation levels ranged 80 – 120 %, and was consistent throughout the water column, indicating that it is well-mixed (Figure 3.3). Field pH measurements were stable across sites and depths primarily ranging between 7.6 and 8.9, with the exception of the September 2018 survey showing elevated pH values (Figure 3.4).

Field turbidity measurements typically ranged between <1 to 130 NTU (Figure 3.5). Turbidity is similar among sites and relatively consistent throughout the water column (Figure 3.5). Secchi disk depth (m) is a vertical measure of the optical clarity of water column and ranged between 1 and 5 m (Figure 3.6a). The range measured is a response to localised variation in water quality, most likely a difference in tidal stage among sites during a survey – some sites may have been surveyed on an ebbing or flooding tide where water depth was lower or higher, short term localised changes in turbidity that is associated with tide (see section 3.3) or algal blooms that reduce vertical clarity. The Secchi disk depth to depth ratio (Z_{sd}:Z, Figure 3.6b) was calculated for each site and survey. This ratio corrects the Secchi disk depth for water depth. This ratio ranged between 15 and 80 % of the water column.
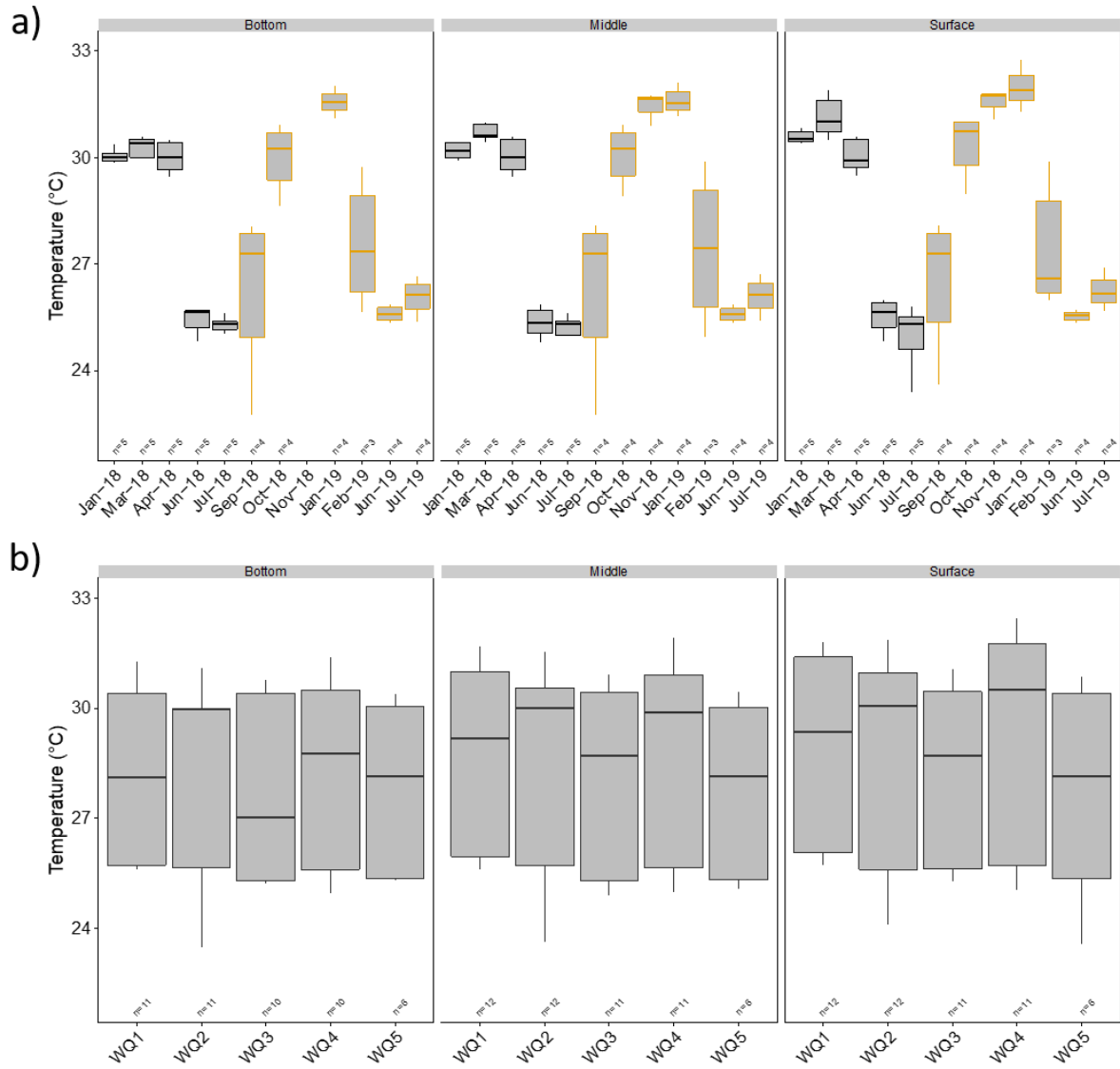
Figure 3.1 Water temperature box plots recorded: (a) the three depth horizons during each survey (sites pooled) where colour indicates monitoring period: black = January 2018 – July 2018, and orange = July 2018 – July 2019; and (b) the three depth horizons for each site (pooled across all monitoring periods 2018-2019)
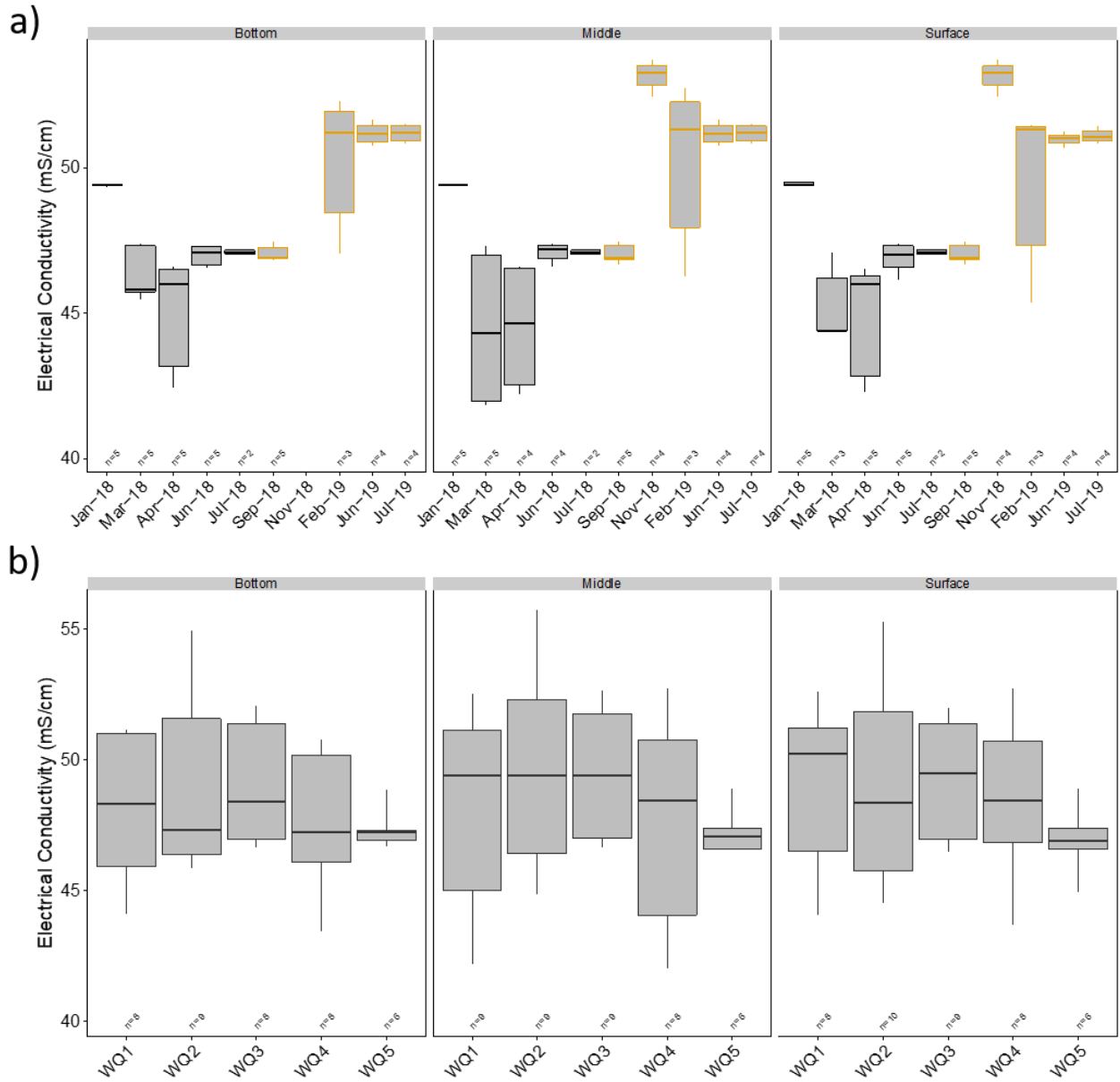
Figure 3.2   Electrical conductivity box plots recorded: (a) the three depth horizons during each survey (sites pooled) where colour indicates monitoring period: black = January 2018 – July 2018, and orange = July 2018 – July 2019; and (b) the three depth horizons for each site (pooled across all monitoring periods 2018-2019)
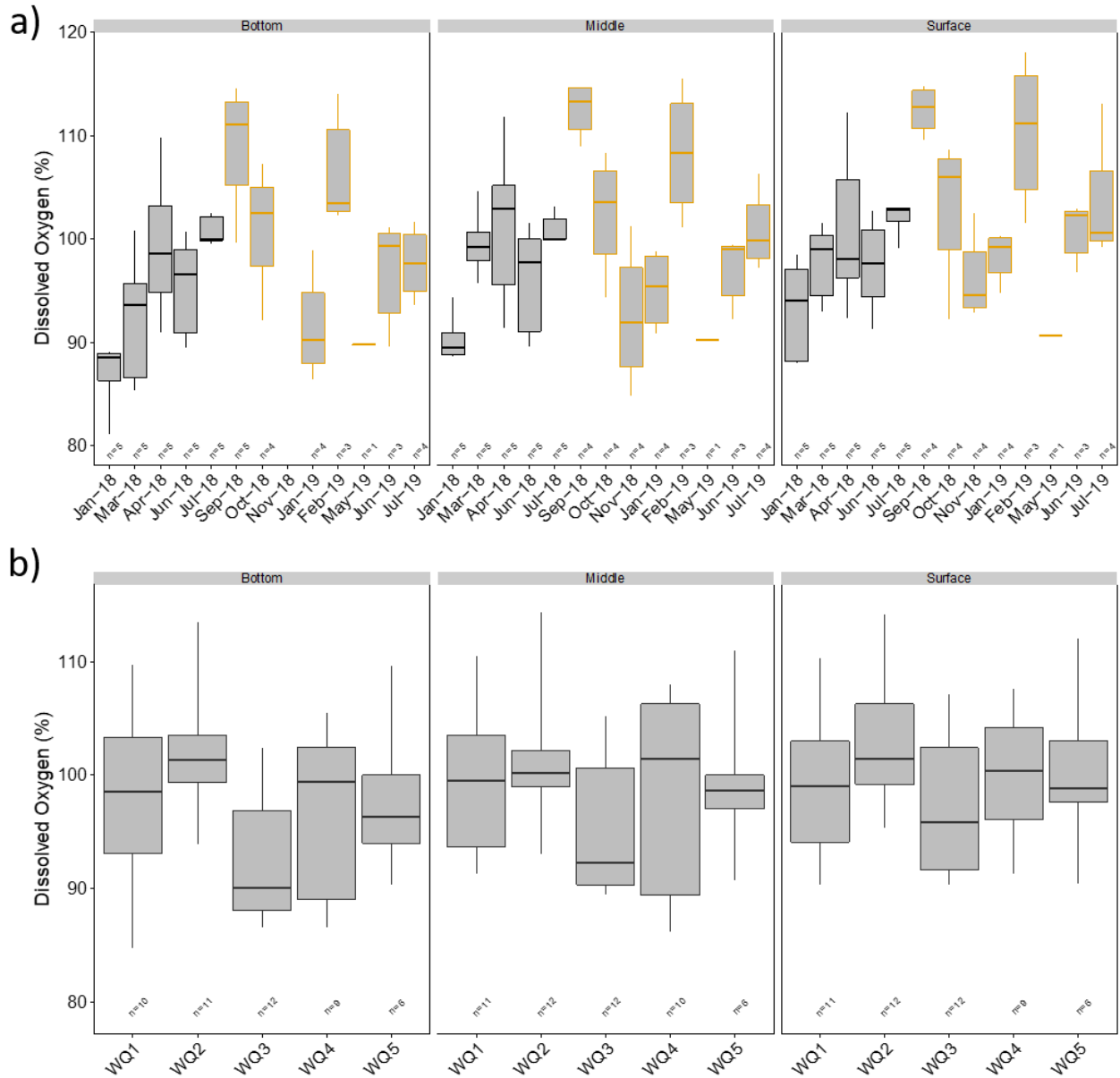
Figure 3.3   Dissolved oxygen box plots recorded: (a) the three depth horizons during each survey (sites pooled) where colour indicates monitoring period: black = January 2018 – July 2018, and orange = July 2018 – July 2019; and (b) the three depth horizons for each site (pooled across all monitoring periods 2018-2019)
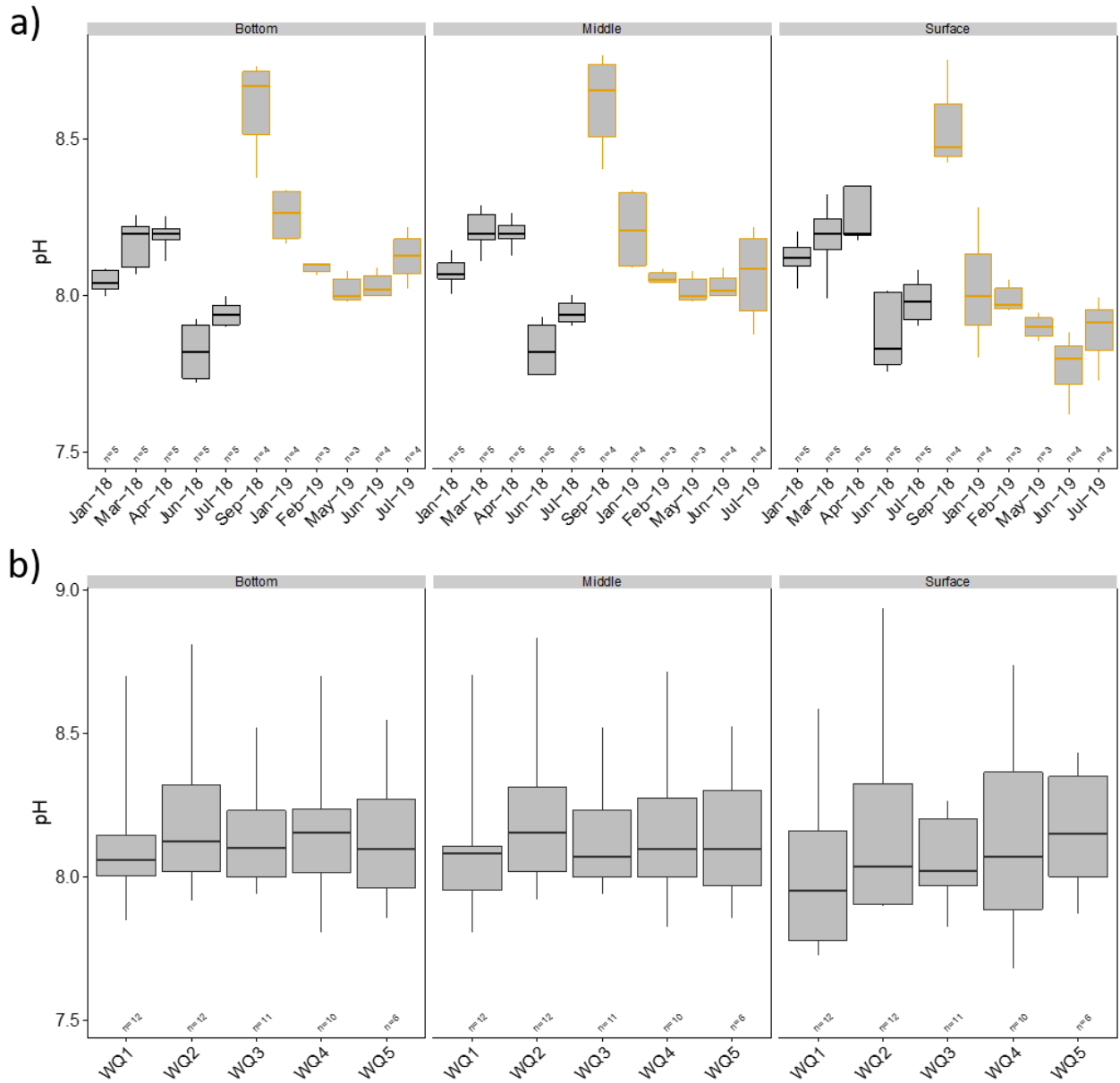
Figure 3.4   pH box plots recorded: (a) three depth horizons during each survey (sites pooled) where colour indicates monitoring period: black = January 2018 – July 2018, and orange = July 2018 – July 2019; and (b) the three depth horizons for each site (pooled across all monitoring periods 2018-2019)
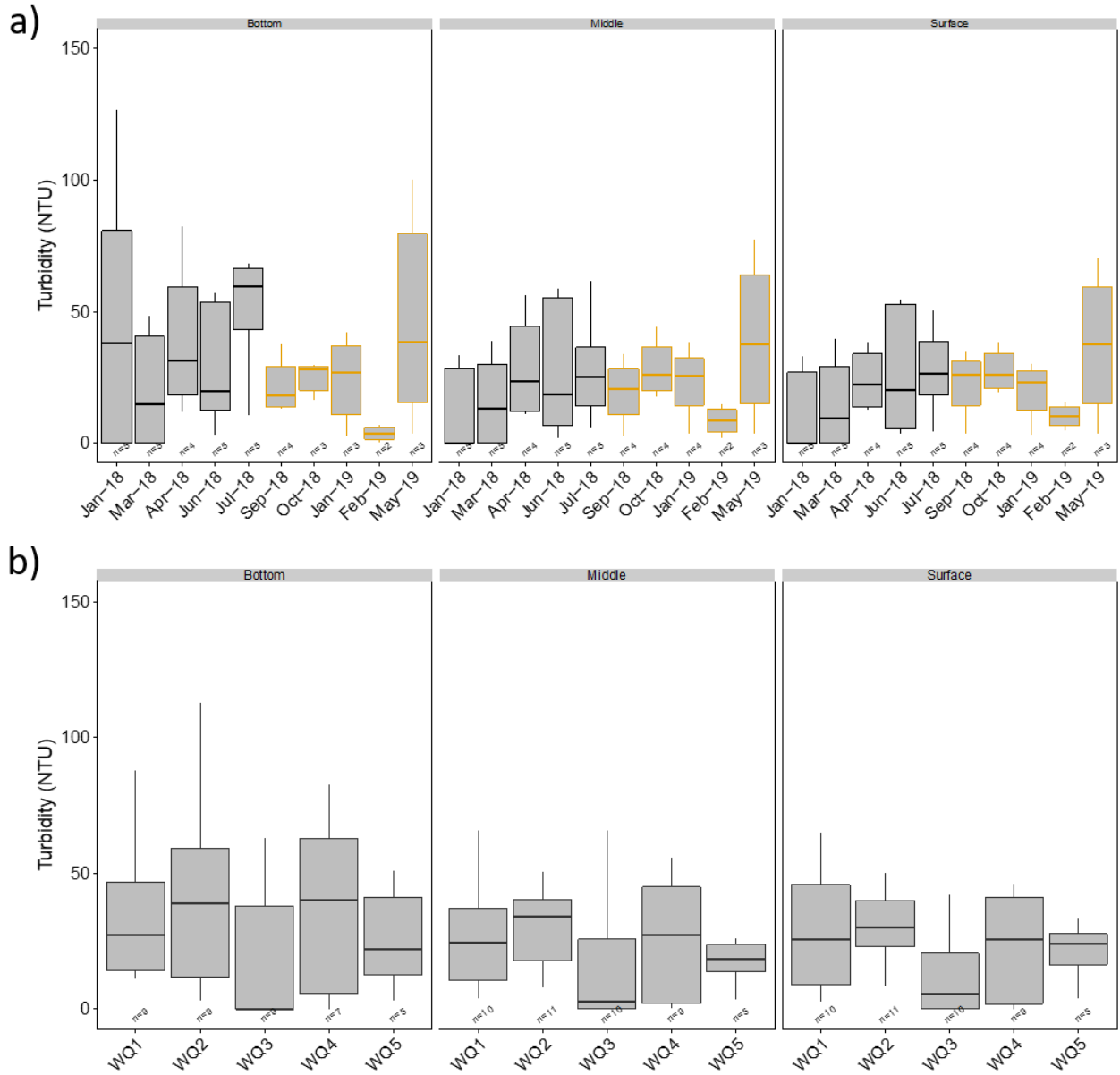
Figure 3.5   Turbidity box plots recorded: (a) the three depth horizons during each survey (sites pooled) from January 2018 to July 2019 and (b) the three depth horizons for each site (pooled across all months)
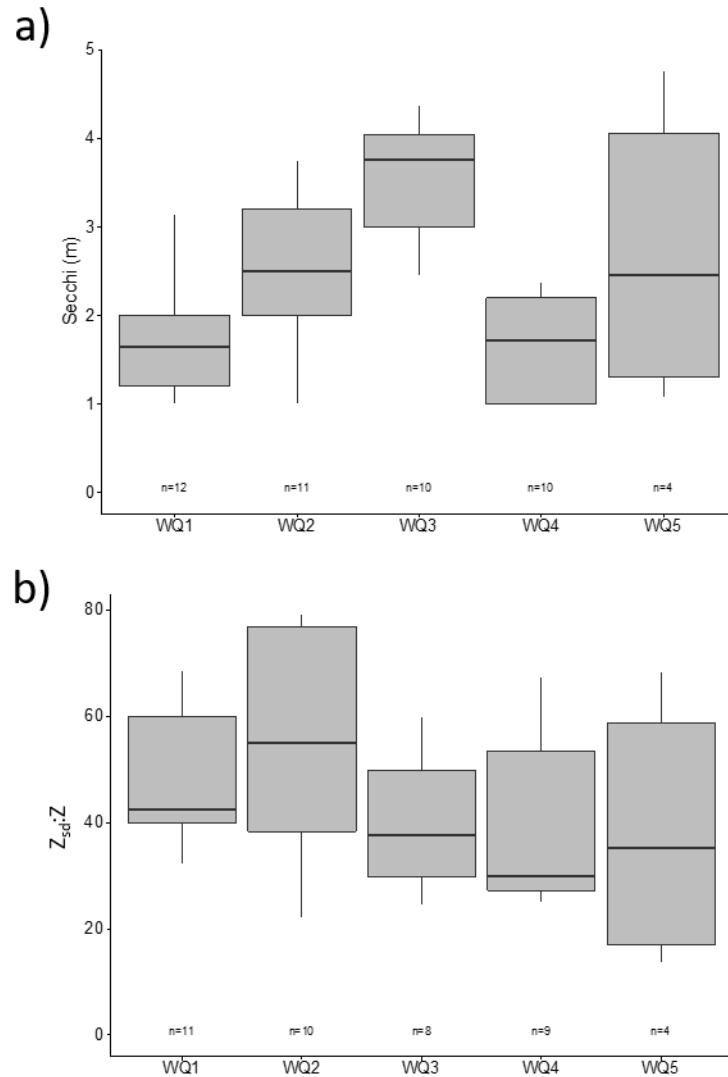
Figure 3.6   (a) Water secchi disk depth for all sites (surveys pooled); and (b) Secchi depth to depth ratio (Zsd:Z) for sites (surveys pooled)

3.1.2   Nutrients and chlorophyll-*a*

Particulate nitrogen (PN) and phosphorus (PP) concentrations were compared to the Water Quality Guidelines for the Great Barrier Marine Park Authority (GBRMPA, 2010) and the Queensland Water Quality Guidelines (DEHP, 2013). (Note that Weipa is not within the Great Barrier Reef World Heritage Area (GBRWHA), but GBRMPA guidelines are used to provide context when comparing to NQBP's other east-coast Ports that are located adjacent to the GBRWHA). Particulate nitrogen concentrations have exceeded the guideline in all surveys thus far (Figure 3.7a). Despite high concentrations during certain months, PN is generally similar across all sites (Figure 3.7b).

High concentrations of PN might be associated with a range of different factors, such as the contribution from local land use activities, whereby despite low rainfall, there would be still some base flow from rivers and local rainfall that is known to contribute to nutrient loadings to coastal regions along the east coast of Queensland (Brodie et al. 2012; Kroon et al. 2012; Schaffelke et al. 2012; Logan et al. 2014). It is also possible that township municipal waste treatment at Weipa could contribute to high PN concentrations, or that concentrations could be naturally high due to adjacent soil conditions. Other sources of nutrients might be via remobilisation of coastal sediments, and release of available nutrients adsorbed to coastal sediments

(Devlin et al. 2012). Elevated nutrients might also be related to reprocessing of nutrients with algal blooms, where there has been an obvious trichodesmium (a marine cyanobacteria; Capone et al. 1997) bloom across the region during most surveys, but most notably during late spring and early summer. Although surveys thus far have recorded PN concentrations that exceed the GBRMPA guidelines, additional data from multiple years is required to make inferences regarding the natural variability in concentrations at the Port of Weipa. This will help to inform local guidelines that are specific to the Port of Weipa and encompass natural variability in water quality conditions.

Particulate phosphorus concentrations exceeded guidelines in all surveys and at all sites (Figure 3.8). Although particulate phosphorus concentrations are above GBRMPA guidelines, continued monitoring will determine baseline natural variability in PP at Weipa and help to inform local guidelines.

Chlorophyll-*a* concentrations were elevated above the guidelines during all surveys and at all sites (Figure 3.9). Relationships between nutrient levels (i.e. PN, PP, Chl-*a*, and Phaeophytin-*a*) across all sites and sampling periods were positive but weak, with correlation coefficients (r) ranging between 0.17 − 0.58 (Figure 3.10).
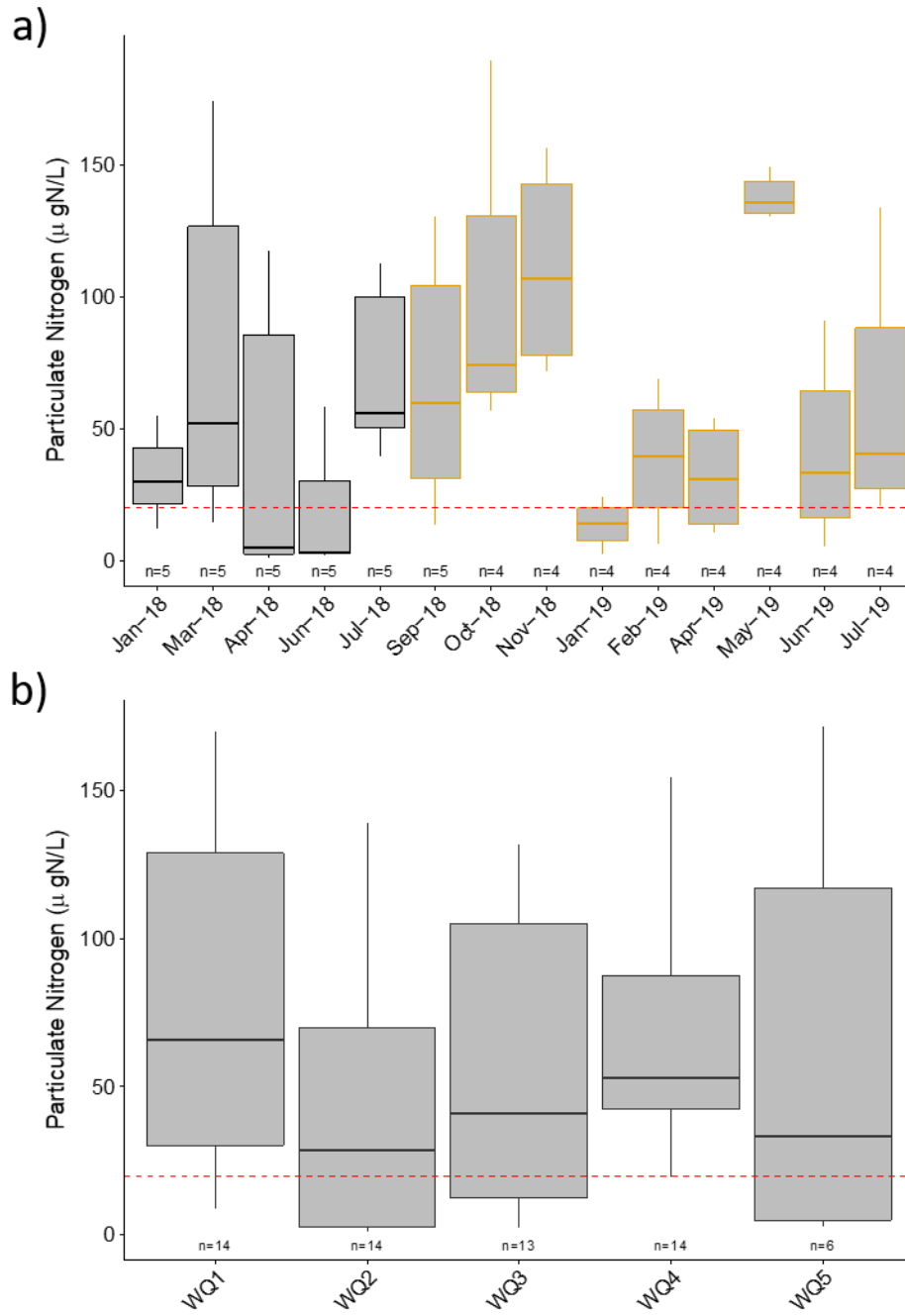
Figure 3.7   Particulate nitrogen box plots: (a) during each survey (sites pooled) from January 2018 to July 2019 and (b) at each site pooled across all monitoring periods
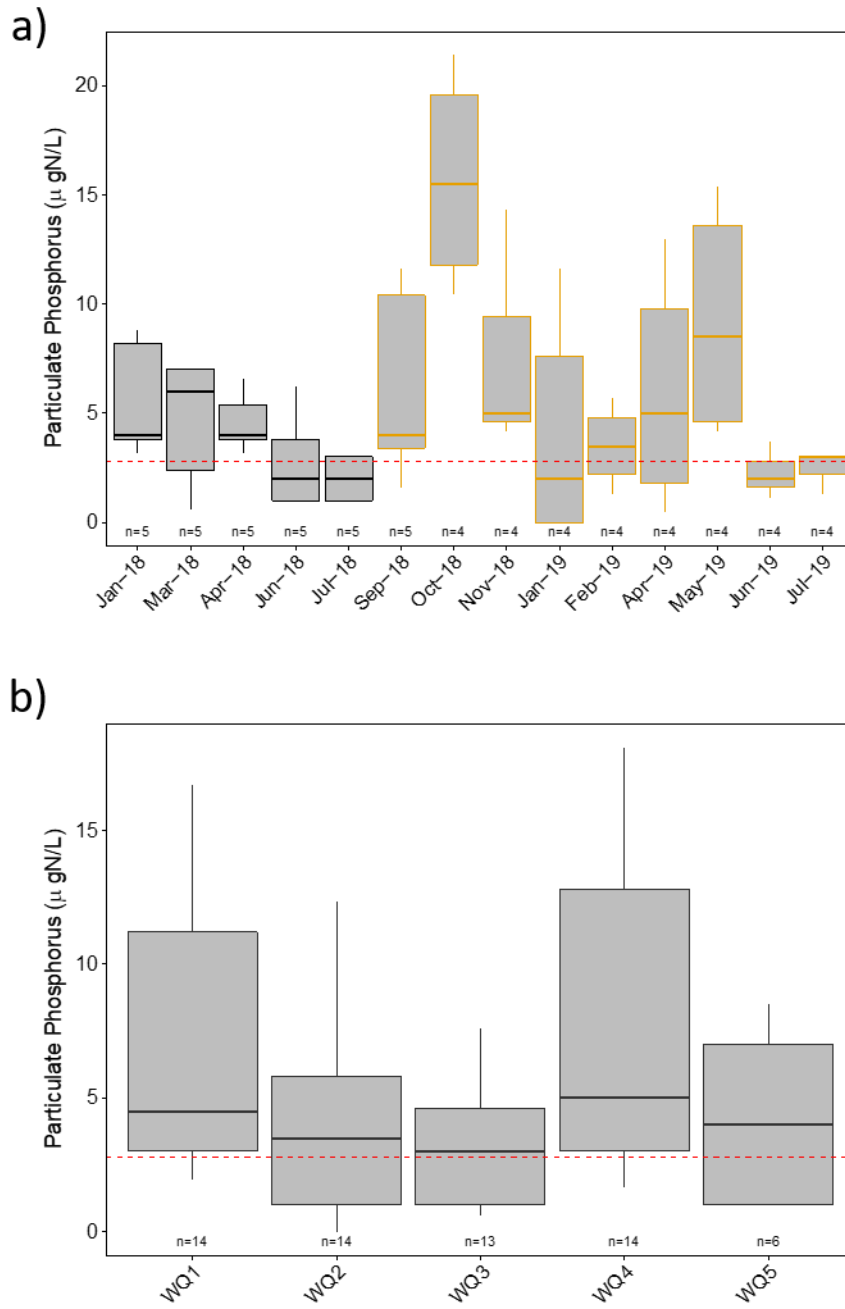
Figure 3.8 Particulate phosphorus box plots: (a) during each survey (sites pooled) from January 2018 to July 2019 and (b) at each site pooled across all monitoring periods
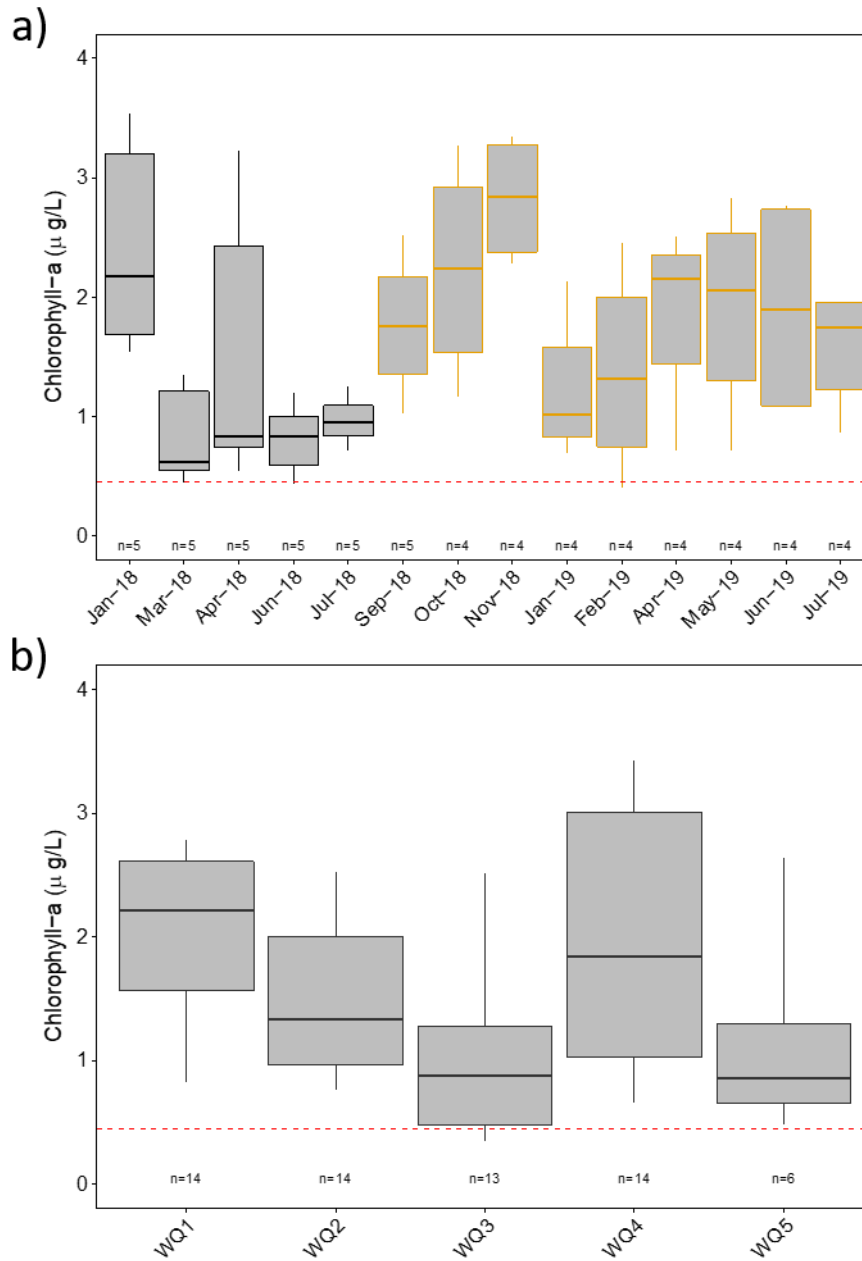
Figure 3.9 Chlorophyll-*a* box plots: (a) during each survey (sites pooled) from January 2018 to July 2019 and (b) at each site pooled across all monitoring periods
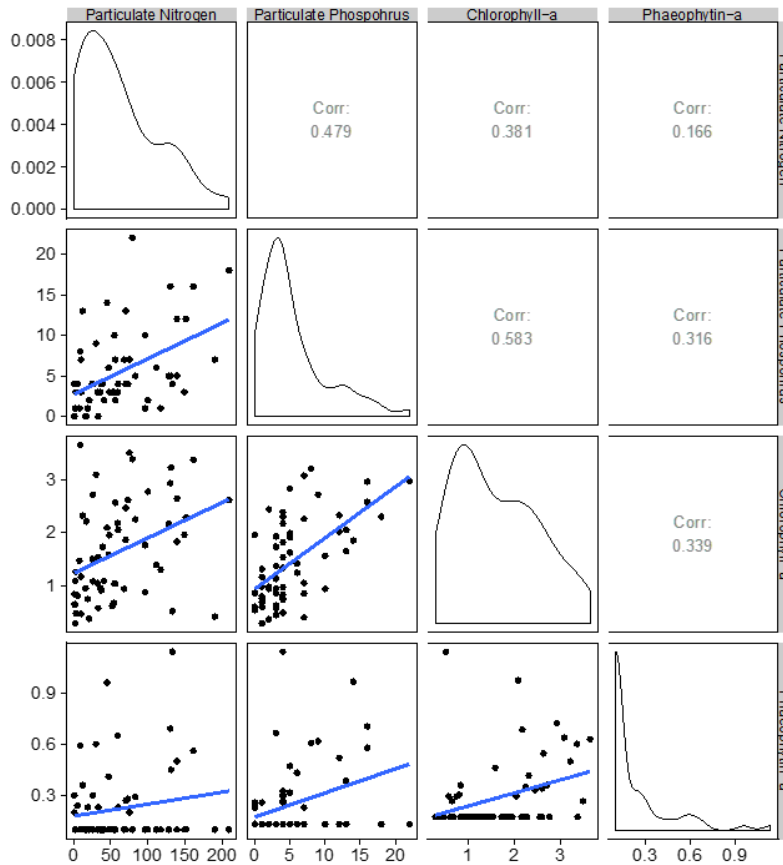
Figure 3.10   Scatterplot of nutrient relationships at pooled across all sites and surveys. Lines of best fit with 95 % confidence intervals are displayed in blue, and correlation coefficients are shown in corresponding plots. Density plots generally show log-normal distribution of the data, and therefore non-parametric spearman correlation was used.

3.1.3   Ultra-trace water heavy metals

Ultra-trace heavy metal concentrations were compared to the ANZECC and ARMCANZ 2000 water quality guidelines (ANZECC, 2000). Most of the filterable metals were not detected above the Limit of Reporting (LOR), except for Zinc following significant rainfall in the wet season months (Table 3.1). No ANZECC guideline exists has been established for arsenic. Arsenic is released into the environment naturally by weathering of arsenic-containing rocks and volcanic activity. It can be in the form of As (III) or As (V), which can be toxic to marine aquatic life. A low reliability marine guideline trigger value of 4.5 µg L^{-1} for As (V) and 2.3 µg L^{-1} for As (III) has been derived (ANZECC, 2000), however, these trigger guidelines are only an indicative interim working level. Measured As concentrations at Weipa sites were below these interim guidelines.

Table 3.1   Summary statistics for metals data recorded at all sites during the program. Values are pooled across sites. Values are compared to the ANZECC 95% protection guideline values (2000). (-) sample not collected

		Arsenic	Cadmium	Copper	Lead	Nickel	Silver	Zinc	Mercury
	Unit	ug/L	ug/L	ug/L	ug/L	ug/L	ug/L	ug/L	mg/L
	LOR	-	0.2	1	0.2	0.5	0.1	5	0.001
	ANZECC	-	5.5	1.3	4.4	70	1.4	15	0.4
Apr-18	Mean	1.5	<0.2	<1	<0.2	<0.5	<0.1	5.6	<0.0001
	Min	1.3	<0.2	<1	<0.2	<0.5	<0.1	<5	<0.0001
	Max	1.6	<0.2	1	<0.2	<0.5	<0.1	10	<0.0001
Sep-18	Mean	1.7	<0.2	<1	<0.2	<0.5	<0.1	<5	<0.0001
	Min	1.5	<0.2	<1	<0.2	<0.5	<0.1	<5	<0.0001
	Max	1.8	<0.2	1	<0.2	<0.5	<0.1	<5	<0.0001
Jan-19	Mean	1.2	<0.2	<1	<0.2	<0.5	<0.1	6.1	<0.0001
	Min	1	<0.2	<1	<0.2	<0.5	<0.1	<5	<0.0001
	Max	1.4	<0.2	1	<0.2	<0.5	0.1	17	<0.0001

3.1.4   Water pesticides and herbicides

The major pesticide and herbicide concentrations were not detected above the limit of reporting (Table 3.2). Where possible, these concentrations were compared to the water quality improvement guidelines for the Great Barrier Reef Marine Park (GBRMPA, 2010) to provide context for comparisons to NQBP's other east-coast Ports, and all detected concentrations were well below the 95 % protection values. The Mackay-Whitsunday Water Quality Improvement Plan's water quality objectives (2014), however, use a region wide guideline of 0.01 µg L^{-1} (LOD unchanged since 2008).

Table 3.2   Summary (average) statistics for pesticides/herbicides recorded at all sites during the program (all values are µg L^{-1}). Values are pooled across sites for each survey and compared to the Water Quality Guidelines for the Great Barrier Reef Marine Park (GBRMPA, 2010) 95 % protection level.

Survey	Atrazine µg L^{-1}	Ametryn µg L^{-1}	Diuron µg L^{-1}	Hexazinone µg L^{-1}	Tebutryn µg L^{-1}
Guideline trigger value	1.4	1.0	1.6	1.2	-
April 2018	0.00014	0.0001	0.0017	0.0001	0.0001
September 2018	0.00010	0.0001	0.0007	0.0001	0.0001
January 2019	0.00033	0.0001	0.0083	0.0006	0.0001

3.1.5   Ordination of data

Spot water quality measurements have been collected at all sites for water temperature, electrical conductivity, dissolved oxygen (%), pH, turbidity, and light attenuation. In addition to these spot measurements, Secchi depth has also been recorded, as a measure of the optical clarity of the water column. Field in-situ measurements have been recorded at three depth horizons; surface (0.25 m), middle, and the bottom horizon (1 m above substrate). These measurements continue to assist in characterising water quality conditions within the water column, among sites and surveys.

Principal components analysis (PCA) was used to explore relationships between physiochemical and nutrient data collected at the water surface at each site during each month of sampling. Results show that 54.1 % of the variability among sites and sampling months was explained by physiochemical and nutrient variables (Figure 3.11). There were some seasonal differences among sites, with higher particulate nitrogen and particulate phosphorus concentrations in wet season months.
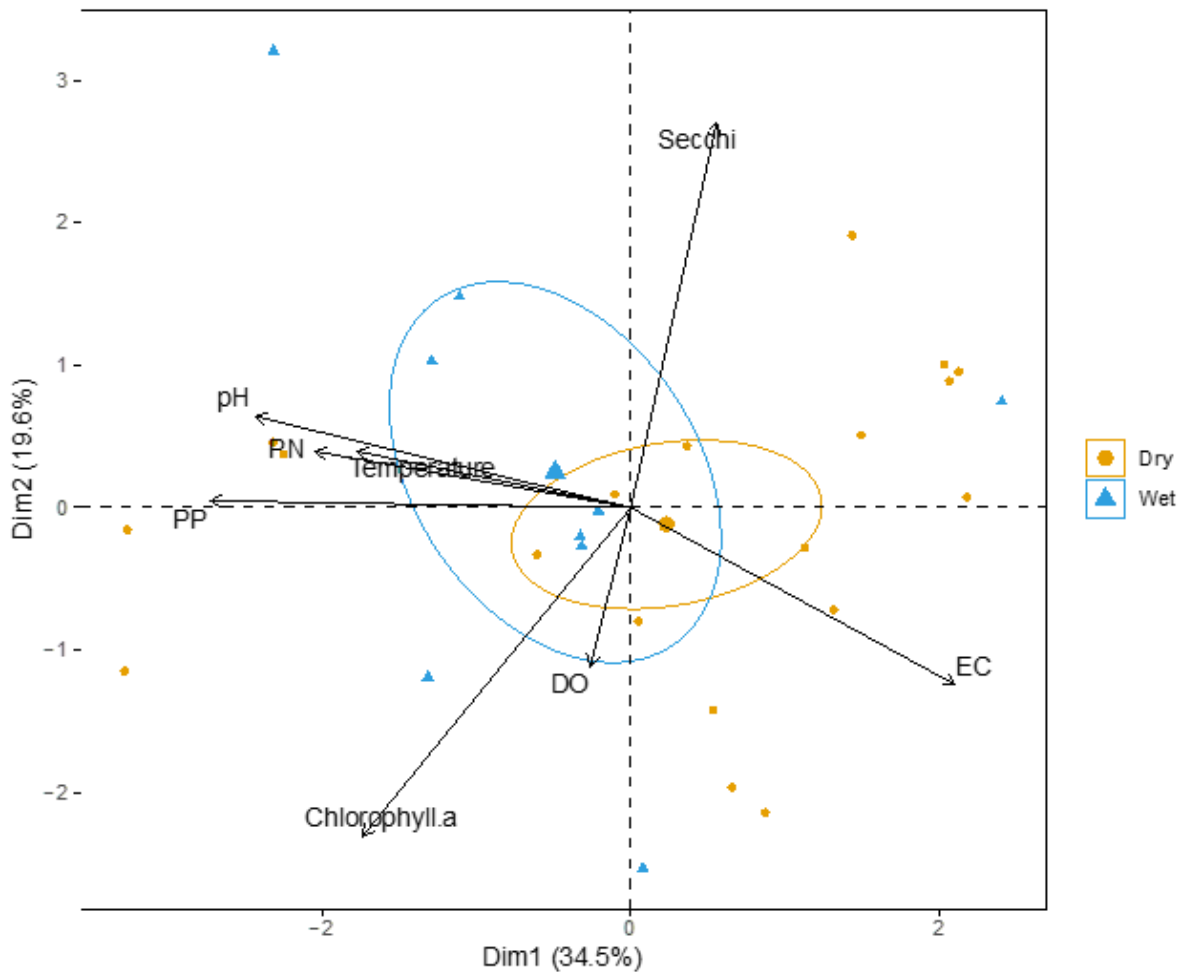
Figure 3.11   Principal components analysis (PCA) exploring relationships between nutrients and physiochemical parameters (black vectors) and monitoring sites. The 95 % confidence interval ellipses show overall differences between sites grouped by season. Vector labels are abbreviated as follows: PP = Particulate Phosphorus, PN = Particulate Nitrogen, EC = Electrical Conductivity, and DO = Dissolved Oxygen. Total variance explained by Dimension 1 and Dimension 2 = 54.1 %

3.2   Plankton communities

3.2.1   Diversity and abundance

A total of 58 phytoplankton species have been identified, comprising cyanobacteria, diatoms, flagellates and green algae taxa. Several species were recorded at all sites, including *Azpeita* spp, *Bacteriastrum* spp, *Rhizosolenia* spp, *Chaetoceros* spp, *Chlamydomonas* spp, *Dinophysis caudata*, *Guinardia* spp, *Odontella* spp, *Rhizosolenia* spp, and *Thalassionema* spp. In March 2018, WQ2 had the highest phytoplankton species richness (27 species), while the lowest species richness was recorded at during May 2019 at WQ2, WQ3, and WQ4 (Figure 3.12a). WQ1 showed peaks in phytoplankton abundance in April 2018 and again in May 2019 (Figure 3.12b).

A total of 24 different species of zooplankton were recorded during all surveys. WQ4 had the highest species richness (15 species) in September 2018, and the lowest diversity was recorded in January 2018 at WQ1 (1 species) (Figure 3.13a). The total abundance of zooplankton peaked at multiple sites in March 2018 (WQ2, WQ3, and WQ5), again in November 2018 at WQ4, and in May 2019 at WQ3 (Figure 3.13b).
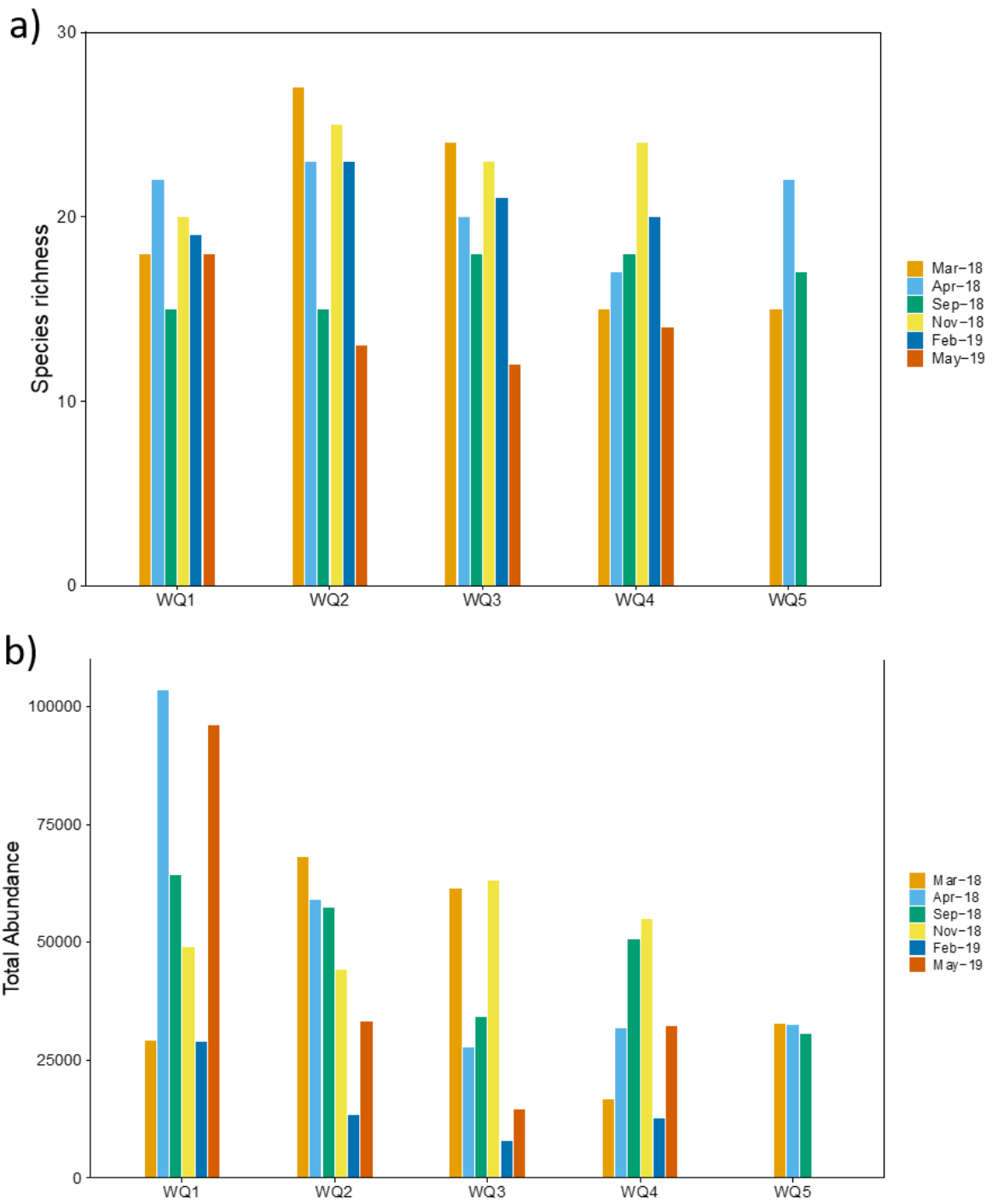
Figure 3.12   a) Species richness of phytoplankton; and b) total abundance of phytoplankton at each site during each survey period. Note that WQ5 was decommissioned following September 2018.
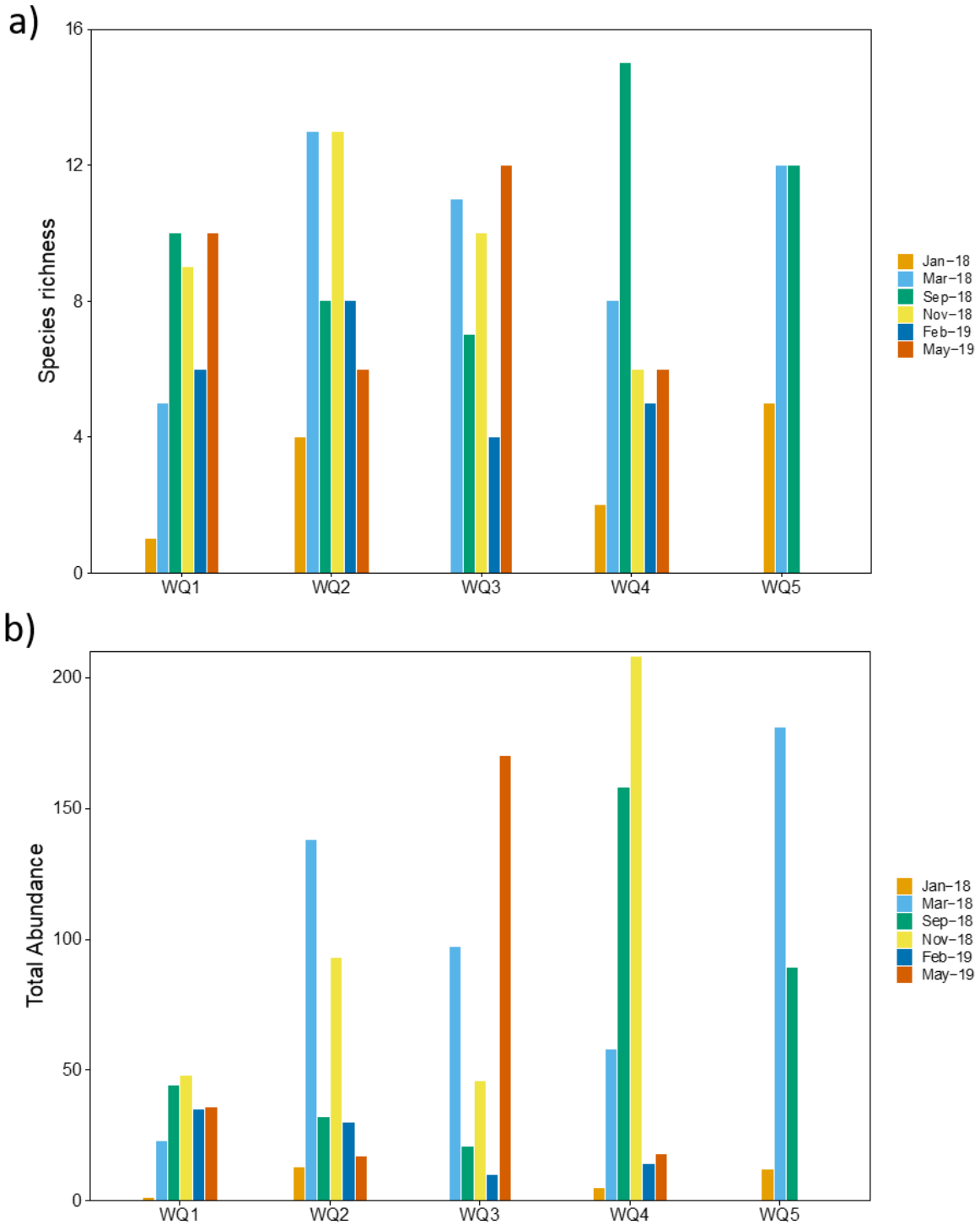
Figure 3.13   a) Species richness of zooplankton and b) total abundance of zooplankton at each site during each survey. Note that WQ5 was decommissioned following September 2018.

3.2.2 Plankton ordinations

Exploratory statistical analysis of the plankton using non-dimensional scaling (nMDS) revealed differences in species composition of phytoplankton (Figure 3.14) and zooplankton communities (Figure 3.15) between surveys. Overall, phytoplankton communities were showed little similarity in species composition between

surveys (with the exception of surveys in March 2018 and May 2019) (Figure 3.14). Zooplankton communities showed higher similarity in species composition in comparison to phytoplankton, particularly in surveys from the current monitoring period (September/November 2018 and February/May 2019).
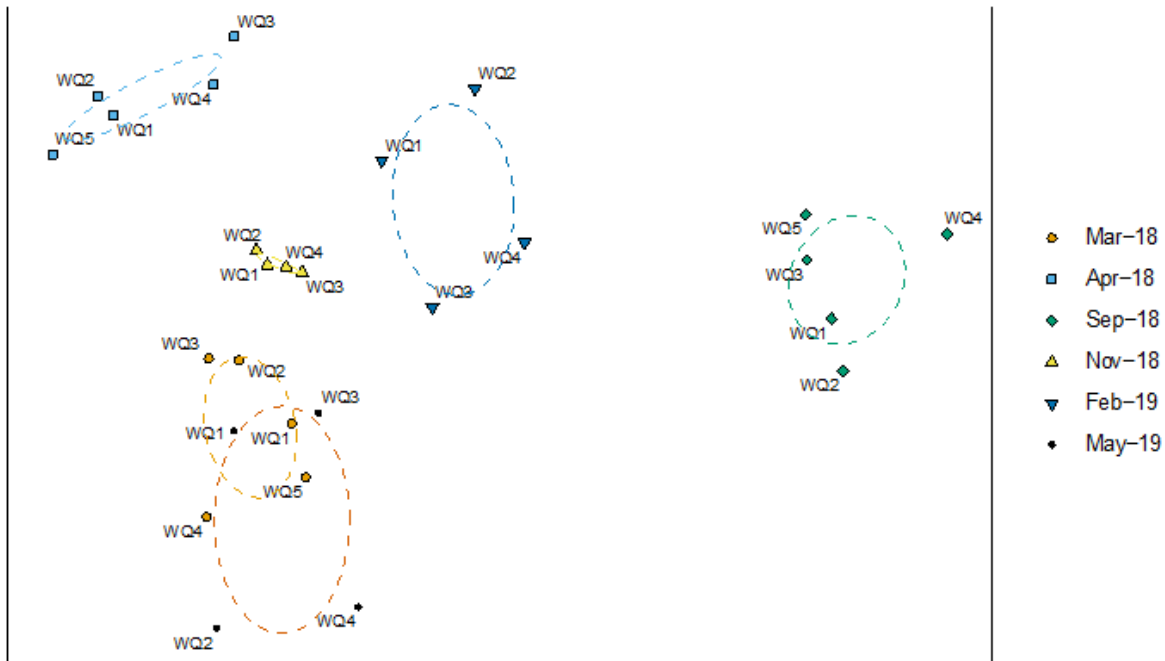
Figure 3.14   Non-dimensional ordination plot for phytoplankton collected during six survey periods throughout 2019. Dashed lines represent 95 % confidence interval ellipses for each survey period and colours correspond to survey periods as follows: light orange = March 2018, light blue = April 2018, green = September 2018, yellow = November 2018, dark blue = February 2019, dark orange = May 2019. Data has been squared root transformed on the Bray Curtis distance matrix (stress = 0.15, Clarke and Gorley 2006)
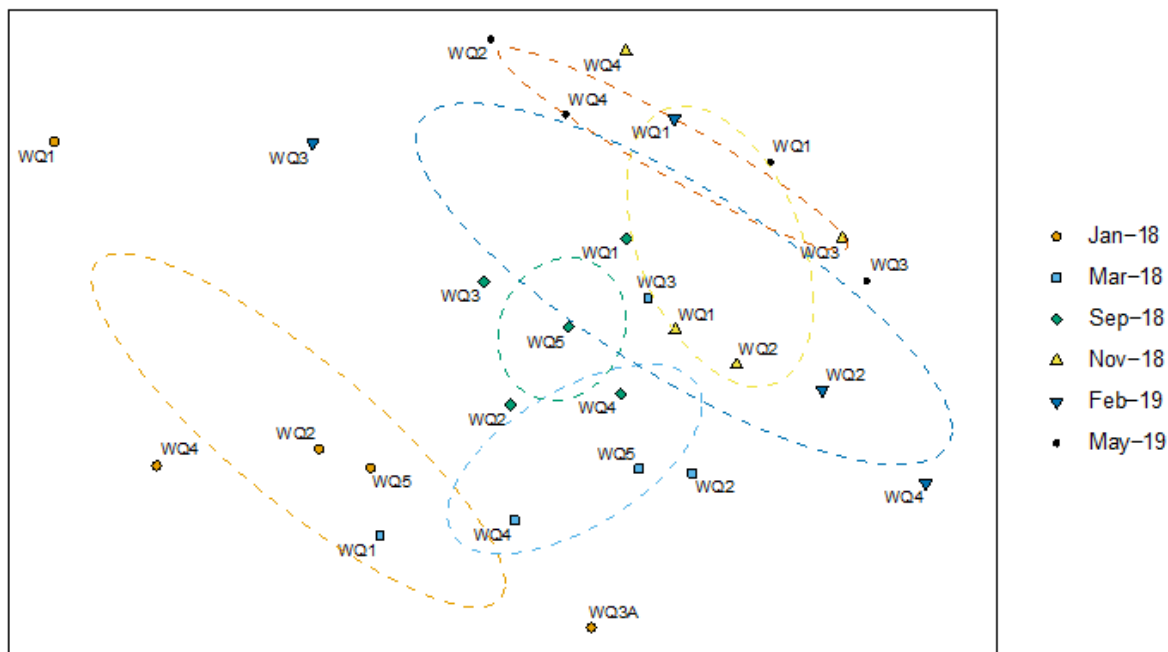
Figure 3.15   Non-dimensional ordination plot for zooplankton collected during two survey periods in 2019. Dashed lines represent 95 % confidence interval ellipses for each survey period and colours correspond to survey periods as follows: light orange = March 2018, light blue = April 2018, green = September 2018, yellow = November 2018, dark blue = February 2019, dark orange = May 2019. Data has been squared root transformed on the Bray Curtis distance matrix (stress = 0.22, Clarke and Gorley 2006)

3.3   Multiparameter water quality logger

Instruments were deployed at four sites, WQ 1 to 4, from July 2018 to July 2019 (see Table 2.1). Using standard statistics, we describe observed trends and differences between sites and discuss the driving forces in these environments. In addition to data loss due to fouling, one site was lost during the deployment period (Oct-Nov 2018).

Data is presented as an annual statistical summary of root mean square water height (RMS; m), suspended sediment concentration (SSC; mg L^{-1}), sediment deposition rate (mg cm^{-2} day^{-1}), water temperature (°C), and photosynthetically active radiation (PAR; mol m^{-2} day^{-1}) for each site. The summary is depicted using box plots, whereby the central diamonds represent the mean value, the central line represents the median value, and the central box represents the range of the 25 and 75 % quartiles. The vertical bars represent the range of the 90th and 10th percentiles. Time series and monthly summaries are included in the appendices.

3.3.1   RMS water height

As mentioned in the methodology, root men square water height (RMS) is a proxy for wave energy or wave shear stress at the ocean floor (Macdonald 2015). RMS is mostly driven by weather events that increase RMS simultaneously at all sites. Variation in RMS during and in-between peak events differs among sites due to differences in water depth and exposure to wave energy.

WQ1 and WQ4, located within the Embley River, were exposed to less wind and wave energy and had lower RMS than WQ2 and WQ3, located on the coast. Median RMS at WQ1 and WQ4 were 10 % that of WQ2 and WQ3 (Figure 3.16, Table 3.3). The upper quartile and 90th percentile followed the same pattern, with values at WQ1 and WQ4 approximately 10 % that of WQ2 and WQ3.

The differences in RMS among the four sites has important implications for other water quality parameters. Similar RMS at WQ1 and WQ4 relative to WQ2 and WQ3 indicates that wave energy may explain differences in water quality between the two groups of sites but not within the two pairs of sites. For example, lower RMS would promote more sediment deposition and less sediment resuspension at WQ1 and WQ4 (in the Embley River) compared to WQ2 and WQ3 (on the coast). However, differences in water quality between WQ1 and WQ4 or between WQ2 and WQ3 could be due to different currents, depths, or benthic geologies.

The highest RMS values were observed between November and March (Appendix 1.2, Appendix 1.3).
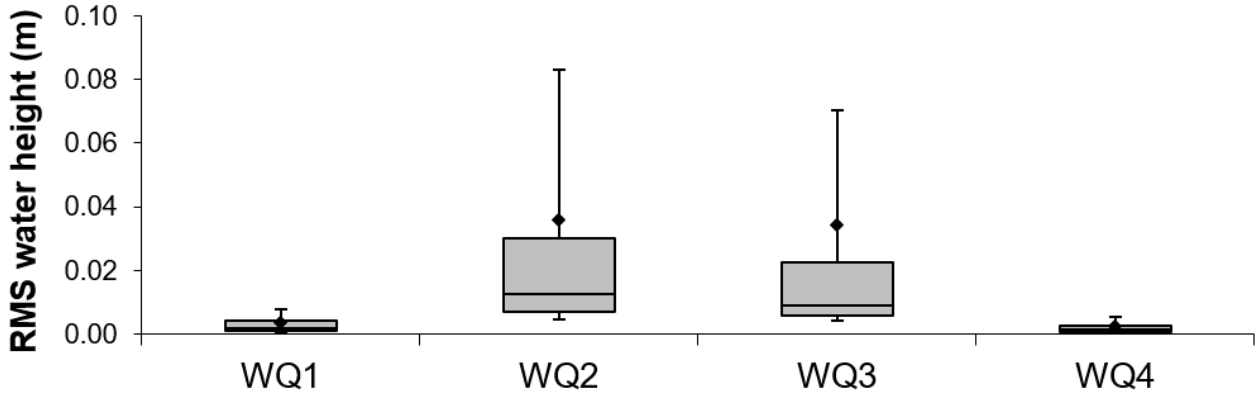
Figure 3.16 Box plot of root mean square (RMS) of water height (m) at the five sites for the monitoring period from July 2018 to July 2019. The lower whisker, lower edge of the box, central line, upper edge of the box and upper whisker represent the 10th, 25th, 50th, 75th and 90th percentiles, respectively. The diamonds represent the mean values.

Table 3.3 Summary of RMS water height (m) from July 2018 to July 2019.

Site	WQ1	WQ2	WQ3	WQ4
Mean	0.003	0.036	0.034	0.002
median	0.002	0.013	0.009	0.001
min	0.000	0.000	0.000	0.000
lower quartile	0.001	0.007	0.006	0.001
upper quartile	0.004	0.030	0.023	0.003
max	0.120	0.691	1.034	0.127
90th percentile	0.008	0.083	0.070	0.006
10th percentile	0.001	0.005	0.004	0.000
n	50694	50255	45431	50370
St. Dev	0.004	0.068	0.079	0.004
St. Error	<0.001	<0.001	<0.001	<0.001

3.3.2 NTUe/SSC

Median suspended sediment concentrations (SSC) were ≤ 17 mg L^{-1} and 75 % quartiles were less than 47 mg L^{-1} (Figure 3.17, Table 3.4). The highest SSC was observed farthest up the Embley River (WQ4), followed by outside the river mouth (WQ2), inside the river mouth (WQ1), and then far down the coast at Pera Heads

(WQ3). The relatively high means and 90th percentiles compared to their respective medians indicate that WQ2 and WQ4 experienced more extreme turbidity events than the other sites during this monitoring period.

The NTUe/SSC time series data at each site (seen in Appendix 1.2) typically follows a pattern of low background values with recurring peak events. These peak events typically occur at the same times at each site and coincide with peaks in RMS water height (Ridd et al., 2001). Differences in turbidity between sites result from variation in RMS water height, site depth, benthic geology, hydrodynamics, and proximity to river mouths.

During this reporting period, SSC levels at WQ1 were relatively constant with the highest values observed in March and May 2019 (Appendix 1.2, Appendix 1.3). SSC at WQ2 was highest in January 2018 to March 2019, coinciding with the wet season. SSC at WQ3 was highest in August 2018 and June 2019. At WQ4, the highest SSC was observed in December 2018, June 2019, and July 2019.
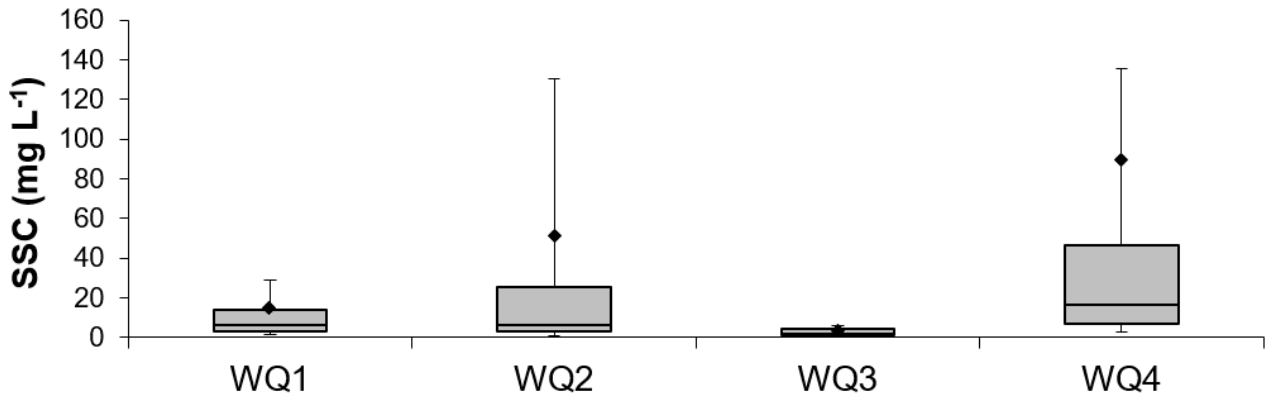
Figure 3.17   Box plot of SSC (mg L^{-1}) from July 2018 to July 2019. The lower whisker, lower edge of the box, central line, upper edge of the box and upper whisker represent the 10th, 25th, 50th, 75th and 90th percentiles, respectively. The diamond represents the mean value.

Table 3.4   Summary of SSC (mg L^{-1}) from July 2018 to July 2019.

Site	WQ1	WQ2	WQ3	WQ4
Mean	14.59	51.08	3.27	89.56
median	6.29	6.41	2.10	16.34
min	0.00	0.00	0.00	0.00
lower quartile	3.09	2.78	0.88	6.63
upper quartile	13.86	25.26	4.38	46.35
max	891.62	4817.42	79.03	7354.25
90th percentile	28.84	130.17	6.09	135.70
10th percentile	1.65	1.12	0.00	2.84
n	40910	45342	16394	40511
St. Dev	34.64	150.00	3.43	359.78
St. Error	0.17	0.70	0.03	1.79

3.3.3 Deposition

Deposition of sediment is a natural process in all coastal marine waters. Suspended sediment deposits in environments where wave energy is not sufficient to keep sediment suspended in the water column. The time series of deposition rates indicate that deposition peaks following RMS events but with a lag so that peak deposition occurs when RMS has decreased to near background levels (Appendix 1.2). An explanation for this lag is that, as waves resuspend sediment, little deposition occurs because the energy in the system keeps sediment in suspension. However, when waves decrease and there is no longer enough energy in the system to keep sediment in suspension and deposition occurs.

Management of marine habitats requires that sediment deposition be monitored for changes from ambient values. The Water Quality Guidelines for the Great Barrier Reef Marine Park (2010) set a sediment deposition trigger value at a mean annual value of 3 mg cm^{-2} day^{-1} and a daily maximum of 15 mg cm^{-2} day^{-1}. However, the Guidelines suggest that 10 mg cm^{-2} day^{-1} sedimentation is valid in areas of coarse sediment, large grainsize, or low organic content.

Deposition rates were highest at WQ4, the farthest site up the Embley River (Figure 3.18, Table 3.5). WQ3 had the second highest median deposition rate, followed by WQ1 and WQ2.

The monthly statistics indicate that deposition rates were highest within the Embley River (WQ1, WQ4) in June and July 2019 (Appendix 1.2, Appendix 1.3). Deposition rates outside the Embley River (WQ2, WQ3) were also relatively high during June and July 2019, but also during September and December 2018.

Differences in deposition rates may be more easily visualised by estimating the thickness of the sediment deposited. For example, using the relationship between density, mass and volume: median deposition value of 5 mg cm^{-2} day^{-1} is equivalent to a layer of sediment of thickness less than 35 µm, assuming a sediment density of 1.5 g cm^{-3}.
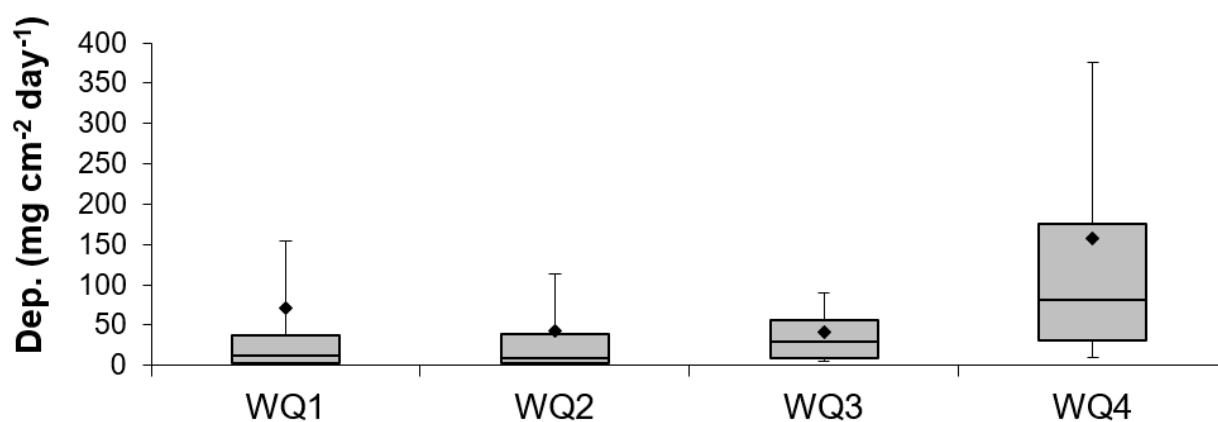
Figure 3.18 Box plot of deposition rates (mg cm^{-2} day^{-1}) from July 2018 to July 2019. The lower whisker, lower edge of the box, central line, upper edge of the box and upper whisker represent the 10th, 25th, 50th, 75th and 90th percentiles, respectively. The diamond represents the mean value.

Table 3.5 Summary of the mean daily deposition rate (mg cm^{-2} day^{-1}) statistics from July 2018 to July 2019.

Site	WQ1	WQ2	WQ3	WQ4
Mean	71.60	43.41	41.68	156.92
median	11.43	9.63	29.74	80.63
min	0.29	0.06	0.06	1.22

lower quartile	3.52	3.25	9.55	31.24
upper quartile	37.61	39.03	56.44	175.04
max	1110.29	706.17	320.26	1273.80
90th percentile	154.50	114.04	89.79	376.03
10th percentile	1.28	1.02	4.73	9.25
n	274	313	220	263
St. Dev	184.92	93.03	47.91	213.28
St. Error	11.17	5.26	3.23	13.15

3.3.4   Water temperature

Water temperatures were similar among all sites with medians of 28-29 °C and similar ranges of temperatures (Figure 3.19, Table 3.6). Water temperatures were highest in December and lowest in July (Appendix 1.2, Appendix 1.3). Water temperature is not considered to be a compliance condition for approval operations, however the temperature data presented here holds importance in future interpretation of ecological processes in the region, and across the GBR (e.g. Johansen et al., 2015).
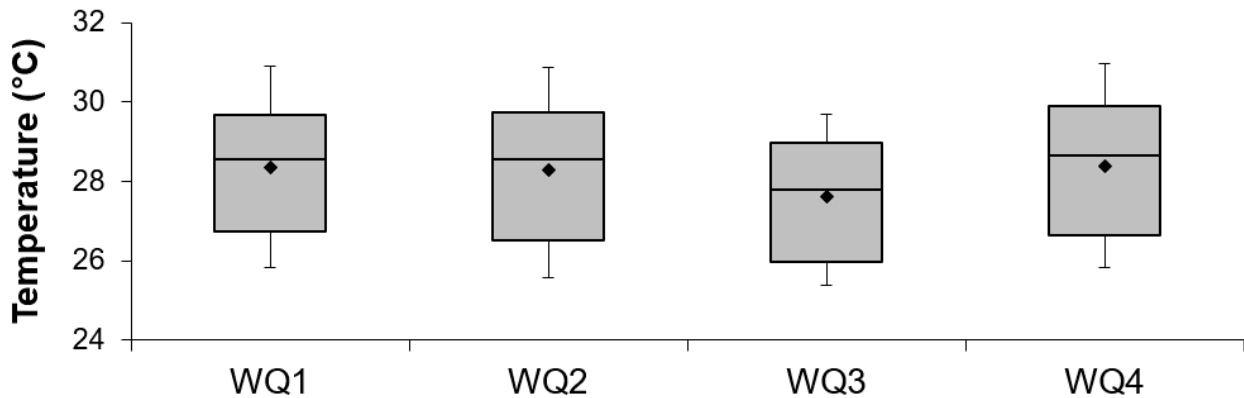
Figure 3.19   Box plot of the water temperature (°C) from July 2018 to July 2019. The lower whisker, lower edge of the box, central line, upper edge of the box and upper whisker represent the 10th, 25th, 50th, 75th and 90th percentiles, respectively. The diamond represents the mean value.

Table 3.6   Summary of water temperature (°C) from July 2018 to July 2019.

Site	WQ1	WQ2	WQ3	WQ4
Mean	28.33	28.28	27.62	28.39
median	28.55	28.57	27.79	28.66
min	24.66	24.17	24.72	23.88
lower quartile	26.72	26.50	25.96	26.63
upper quartile	29.67	29.73	28.98	29.91
max	32.47	35.95	36.04	37.55
90th percentile	30.91	30.87	29.68	30.97

10th percentile	25.84	25.57	25.37	25.82
n	50633	50202	45397	50307
St. Dev	1.84	1.92	1.67	1.91
St. Error	0.01	0.01	0.01	0.01

3.3.5   Photosynthetically active radiation (PAR)

Mean levels of benthic photosynthetically active radiation (PAR) ranged from 1.4 to 4.0 mol m^{-2} day^{-1} (Figure 3.20, Table 3.7). WQ2 had the highest median and variance in PAR. WQ4 had the lowest median PAR but also had light levels within the range observed at the other sites. WQ1 and WQ3 had similar PAR characteristics despite WQ3 being located at twice the depth as WQ1.

Benthic PAR was highly variable throughout the year, but PAR was generally highest in July-August and lowest in December-January (
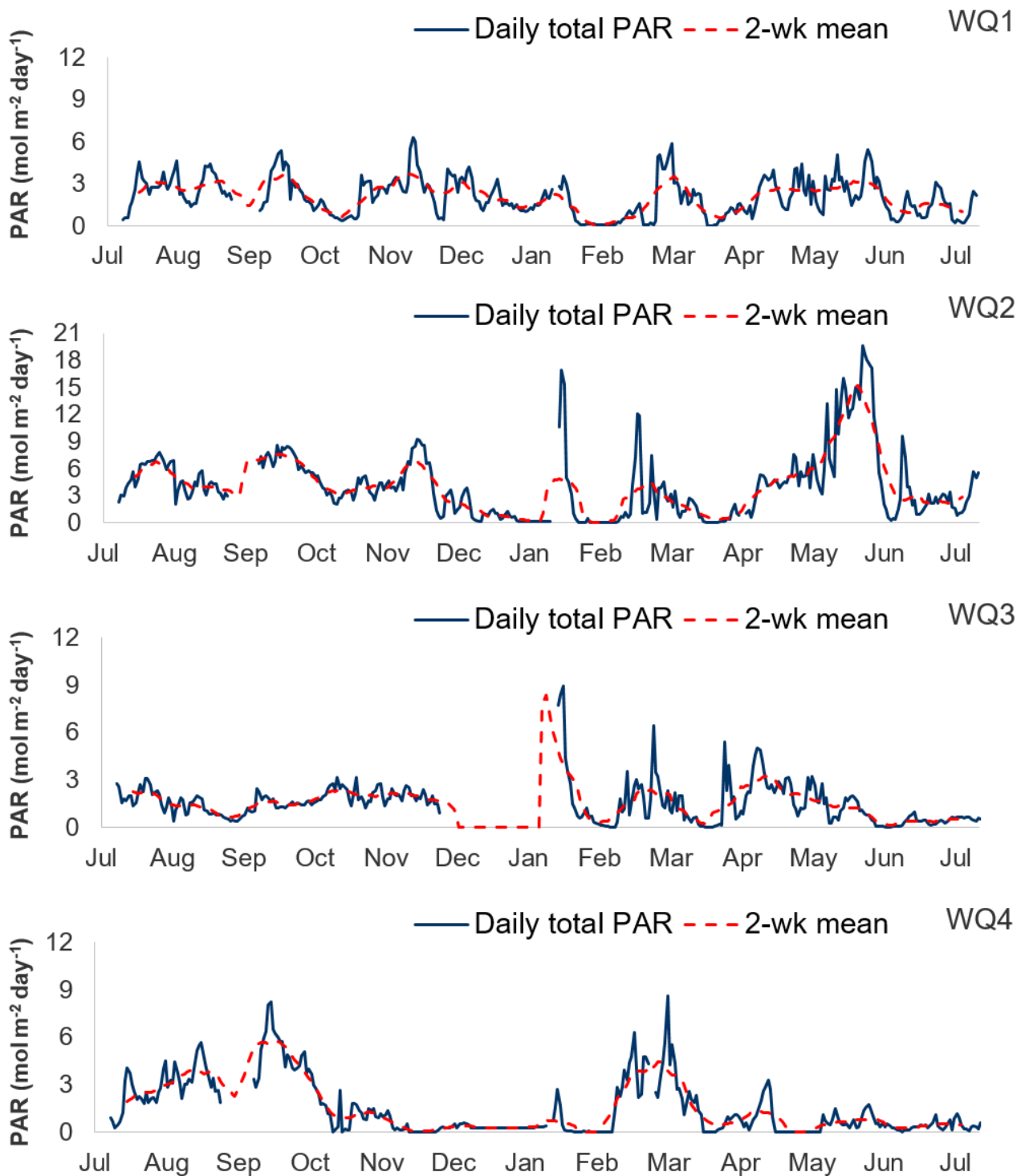
Figure 3.21, Figure 3.22). Semi-regular oscillations between low and high PAR were overridden by larger episodic events caused by storm or rainfall.
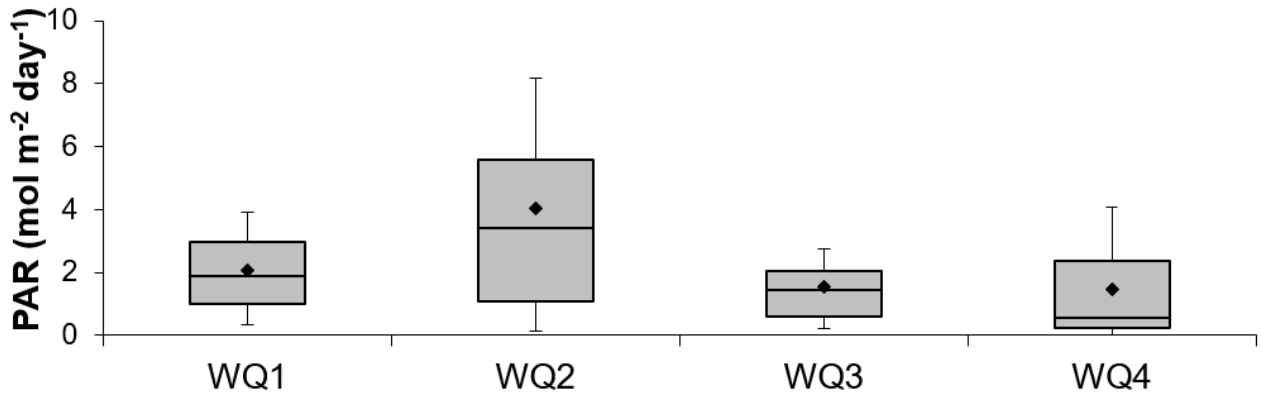
Figure 3.20   Box plot of daily PAR (mol m^{-2} day^{-1}) from July 2018 to July 2019. The lower whisker, lower edge of the box, central line, upper edge of the box and upper whisker represent the 10th, 25th, 50th, 75th and 90th percentiles, respectively. The diamond represents the mean value.

Table 3.7   Summary of daily PAR (mol m^{-2} day^{-1}) from July 2018 to July 2019.

Site	WQ1	WQ2	WQ3	WQ4
Mean	2.05	4.03	1.52	1.44
median	1.89	3.43	1.42	0.55
min	0.00	0.00	0.00	0.00
lower quartile	0.99	1.07	0.61	0.23
upper quartile	2.96	5.58	2.05	2.36
max	6.29	19.67	8.96	8.62
90th percentile	3.92	8.19	2.74	4.07
10th percentile	0.34	0.12	0.20	0.00
n	350	347	316	348
St. Dev	1.36	3.74	1.24	1.74
St. Error	0.07	0.20	0.07	0.09
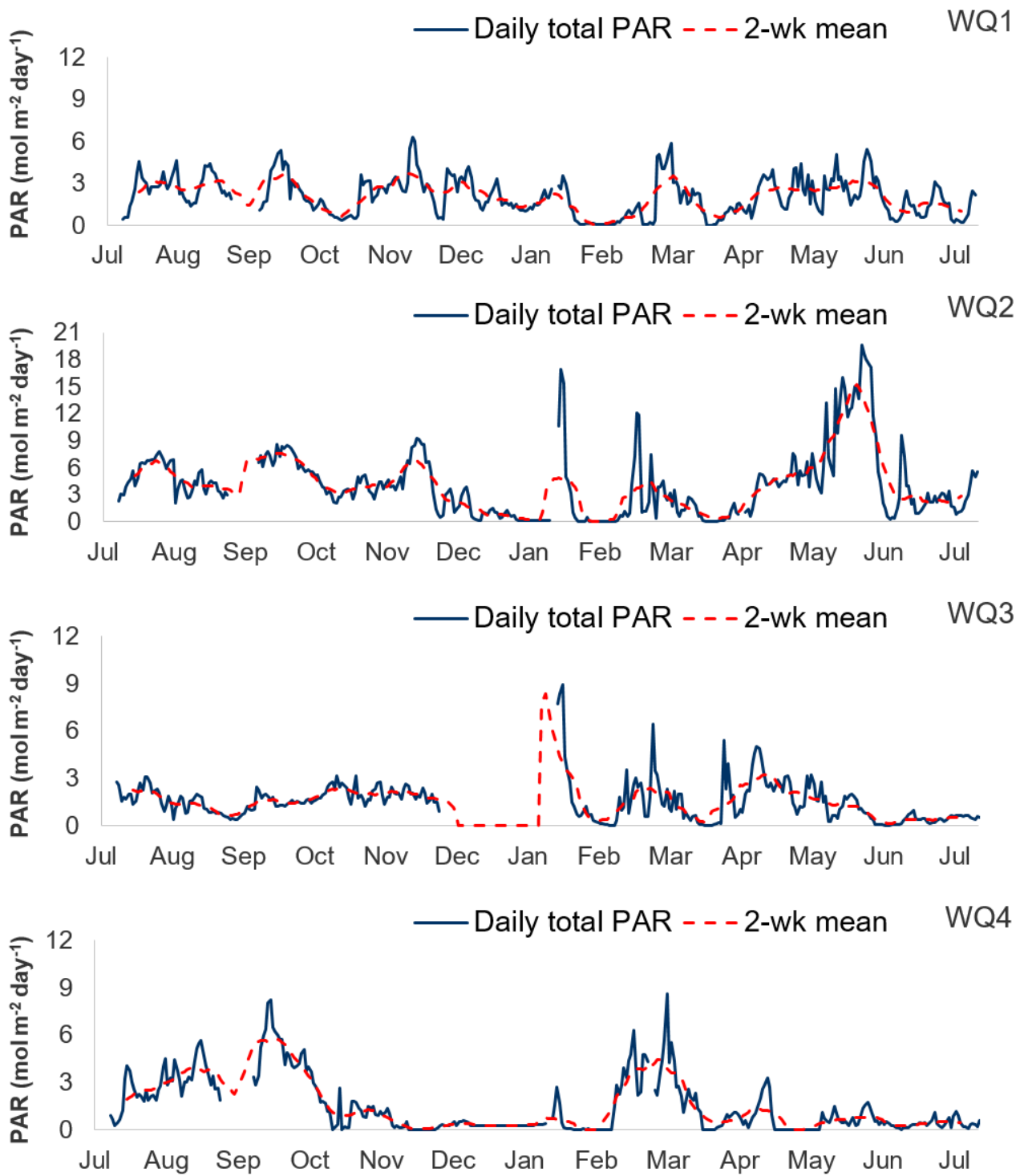
Figure 3.21   Time series of total daily PAR (mol m^{-2} day^{-1}) from July 2018 to July 2019. Daily mean PAR is plotted in blue and a 2-week moving average of daily mean PAR is plotted in red.
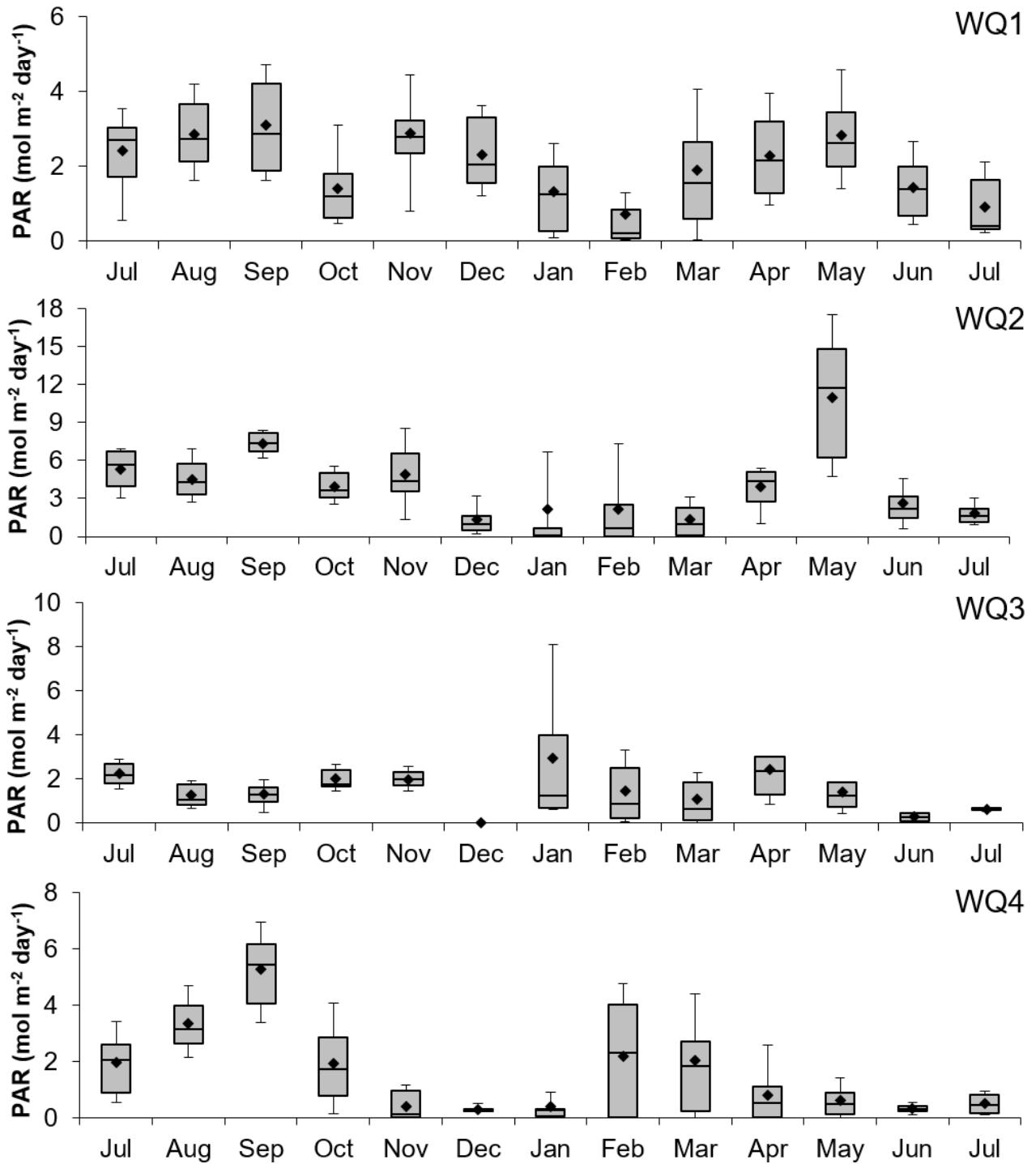
Figure 3.22 Monthly boxplots illustrating the variation in total daily PAR (mol m^{-2} day^{-1}) from July 2018 to July 2019. The lower whisker, lower edge of the box, central line, upper edge of the box and upper whisker represent the 10th, 25th, 50th, 75th and 90th percentiles, respectively. The diamond represents the mean value.

Similarities in patterns of PAR among sites

There are weak relationships between the benthic PAR at different sites (Figure 3.23). Less than 27 % of the variation in PAR at a given site could be explained by the PAR at any other site, highlighting the influence of site-specific conditions (depth, turbidity, etc.) on benthic irradiance. WQ1 and WQ2 have the strongest association (R^2 = 0.27) while WQ1 and WQ4 have the second strongest association (R^2 = 0.15). These three sites are in and around the Embley River compared to WQ3 which is 30 km to the southwest. This analysis

assists in understanding site redundancy opportunities, without missing important detail in characterising water quality in the region.
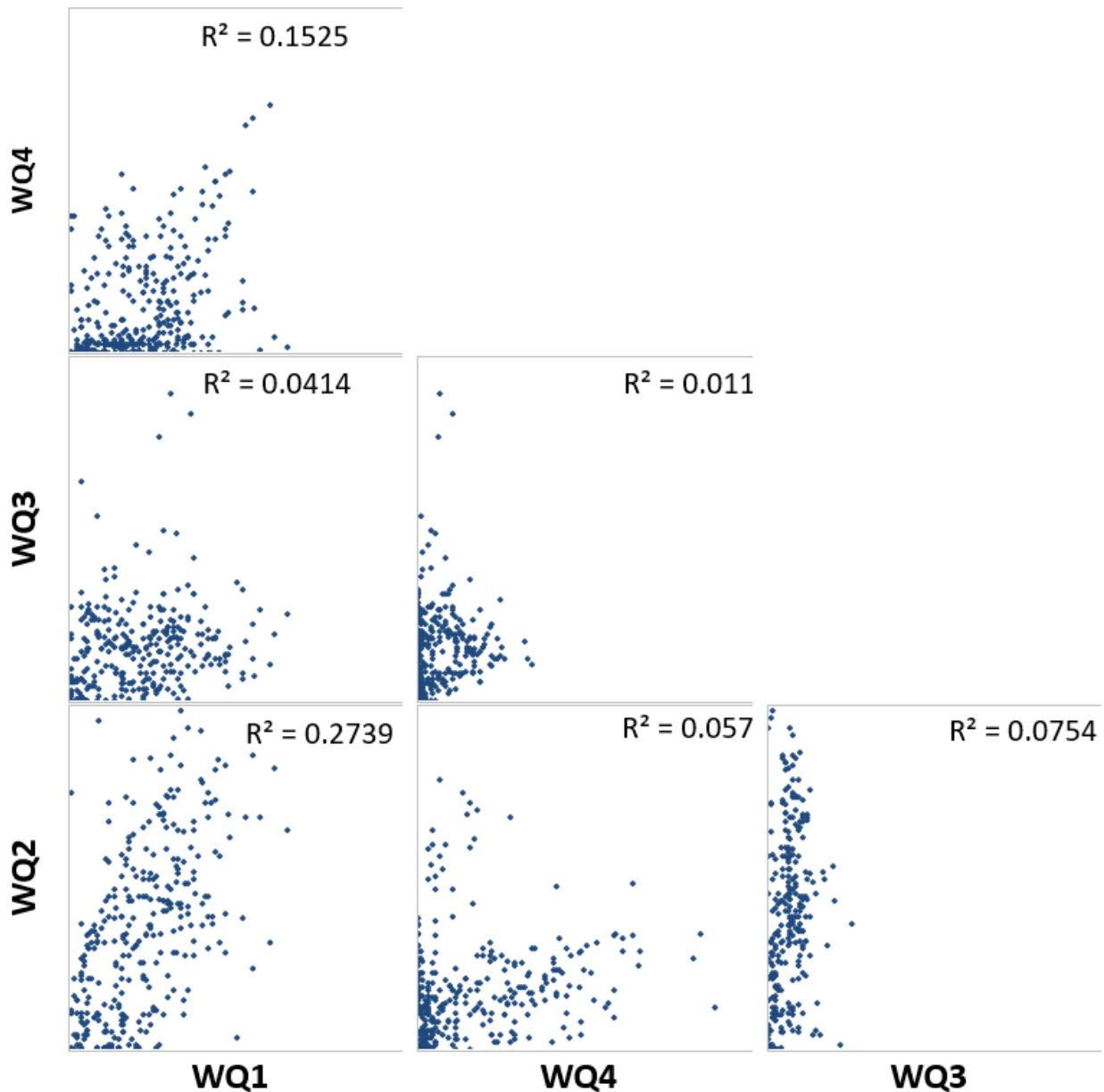
Figure 3.23   Scatterplots of PAR between sites indicating the strength of the relationships between patterns of daily PAR. R^2 values are presented for each comparison.

Relationship between light attenuation and suspended solid concentrations

In sediment-rich coastal waters, the dominant physical process that reduces PAR light intensity is scattering, which if turbidity levels are high enough, can cause underwater light to become isotropic. Investigations into the light attenuation coefficient provides an insight into the dynamic relationship between suspended solid concentrations and PAR light intensities.

Absorption and scattering describe the attenuation of light through water by interacting in a nonlinear and complex fashion within the radiative transport equations (Mobley, 1994). These equations cannot be solved analytically; however the diffuse attenuation coefficient (k_d) (averaged across the PAR waveband 400-700

52

nm) may be approximated in ocean waters by using Beer-Lambert's law (Dennison et al., 1993; Gordon, 1989; John T. O. Lewis, 1994),

$$I_z = I_{z0}e^{-k_d(z-z_0)}$$

where Iz_0 and Iz are the downward directed irradiances at an upper depth (z_0) and a lower depth (z) respectively, and k_d is the diffuse attenuation coefficient (averaged across the PAR waveband 400-700 nm) (Jerlov, 1976; J. T. O. Kirk, 1977). k_d is comprised of a component due to clear water and a component due to SSC.

Light attenuation (PAR) and suspended sediment concentration (SSC) are examined for all five sites. A general relationship is found, whereby as SSC increases, light levels decrease exponentially, as is well described by Beer-lambert's Law. An example of this relationship can be seen in Figure 3.24 where during periods of high SSC, light is attenuated and when SSC exceeds approximately 10 mg L^{-1}, light extinction occurs.
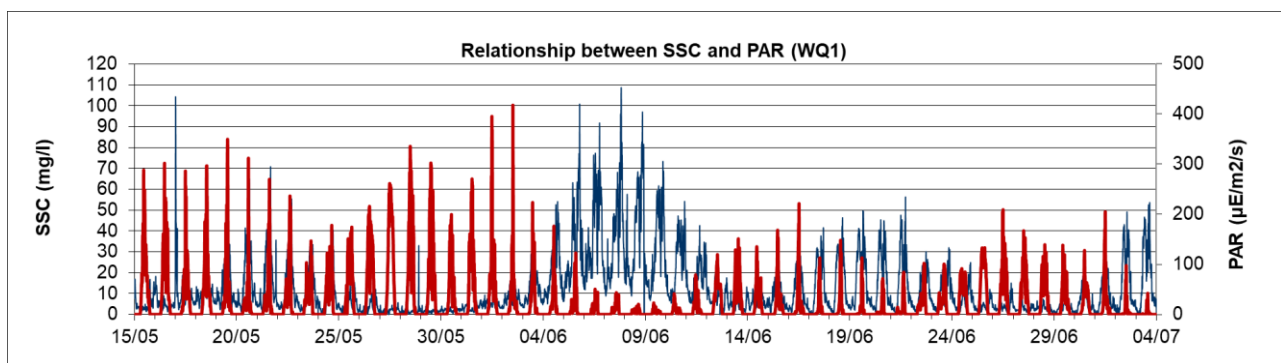
Figure 3.24 A typical example of the relationship between SSC and PAR light, showing light levels decreasing as SSC increases during May-July 2019 at WQ1

3.3.6 Seasonal variation: wet vs dry seasons

A comparison of wet and dry season water quality (2017-2019) suggests that, with some exceptions, periods of increased RMS, SSC, deposition rates, and increased PAR during the wet season.

RMS water height
Median, mean and upper quartile values were higher during wet seasons across all sites (Figure 3.25). Median RMS the wet season was double that of the dry season at most sites. The expanded upper quartiles indicate more periods of high RMS during the wet seasons. There was not a large difference in RMS between the 2018-2019 data and the cumulative 2017-2019 seasonal data.
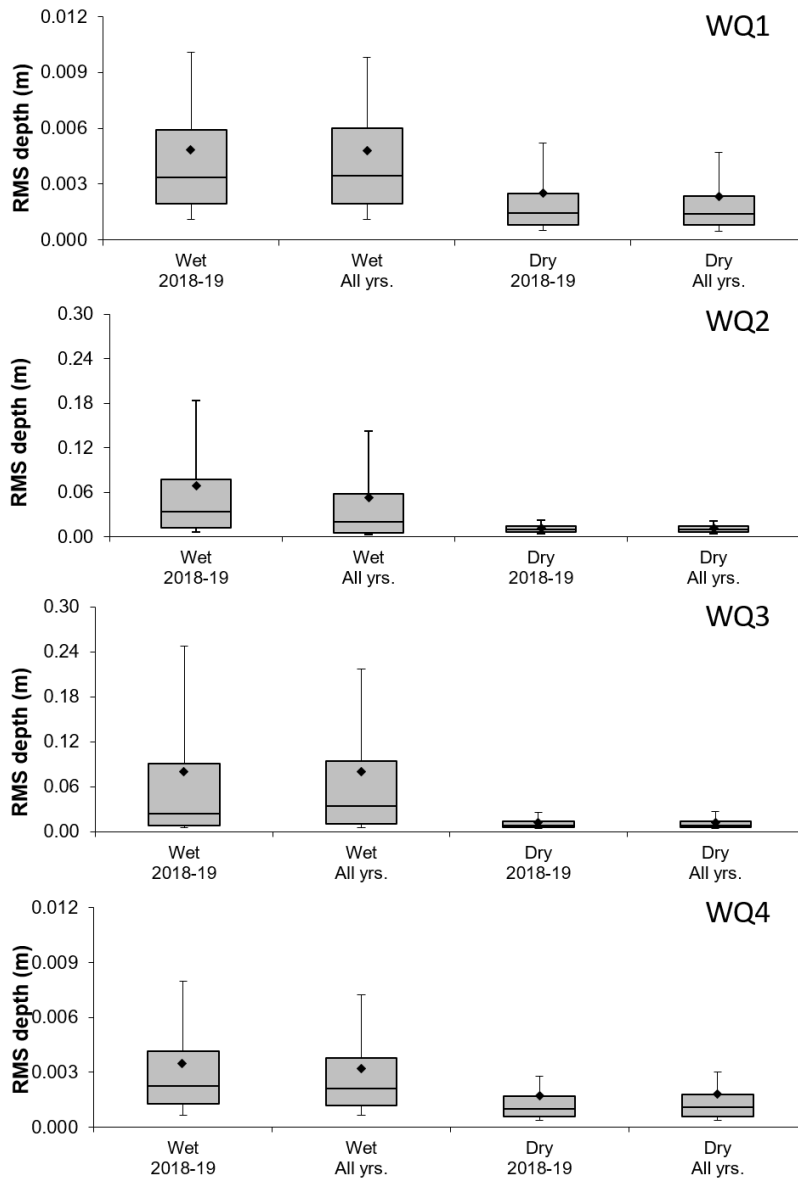
Figure 3.25   RMS box plots for WQ1-WQ4. Boxes represent the wet (1 November-31 March) and dry seasons (1 April-31 October) using either one wet season (2018-2019) or two wet seasons (2017-2019).

NTUe/SSC

Differences in suspended sediment concentration (SSC) between seasons are less straightforward than for RMS. While median SSC was somewhat similar between wet and dry seasons, the SSC upper quartiles were typically three-fold higher during the wet season, indicating more extreme turbidity events (e.g. WQ2, WQ3, WQ4; Figure 3.26). Notably, SSC at WQ1 was relatively constant throughout the deployment period (Figure 3.26, Appendix 1.3).
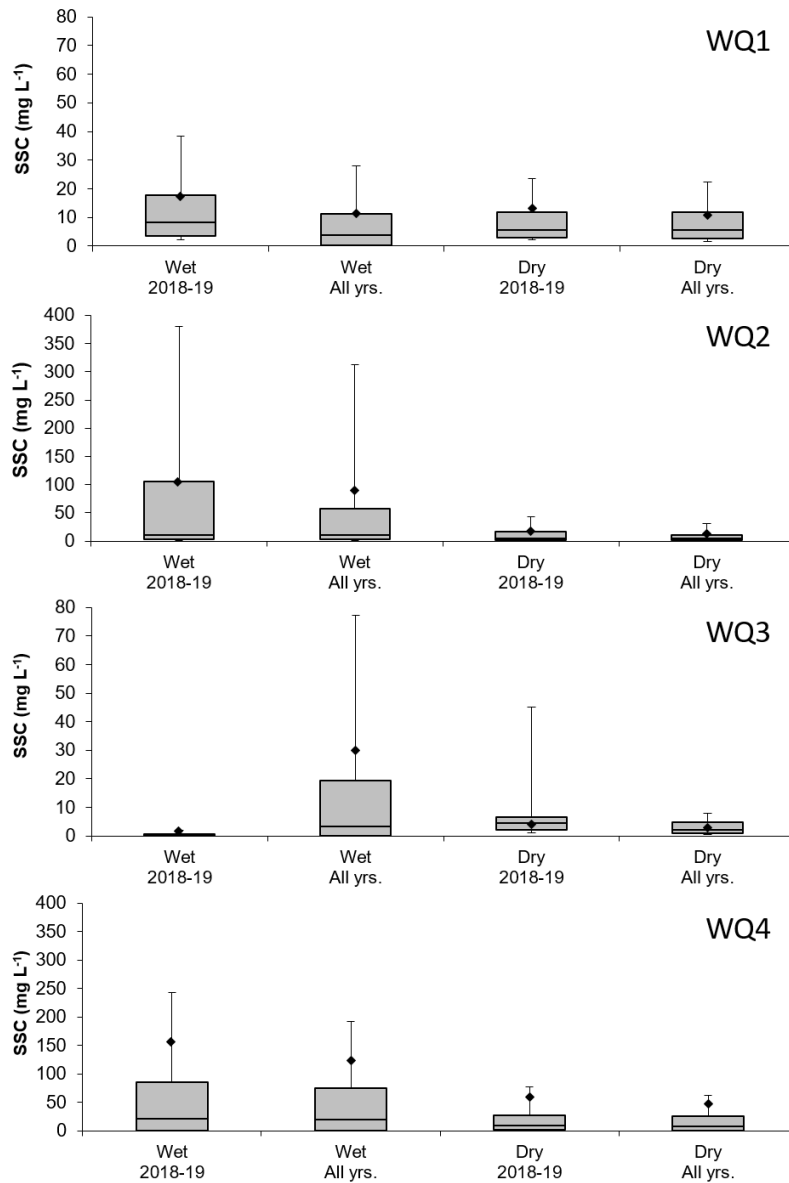
Figure 3.26   SSC box plots for WQ1-WQ4. Boxes represent the wet (1 November-31 March) and dry seasons (1 April-31 October) using either one wet season (2018-2019) or two wet seasons (2017-2019).

Deposition

Median deposition rates were largely similar between wet and dry seasons (Figure 3.27). The most apparent seasonal pattern was higher deposition rates at WQ3 during the dry season (April-October, Appendix 1.3).
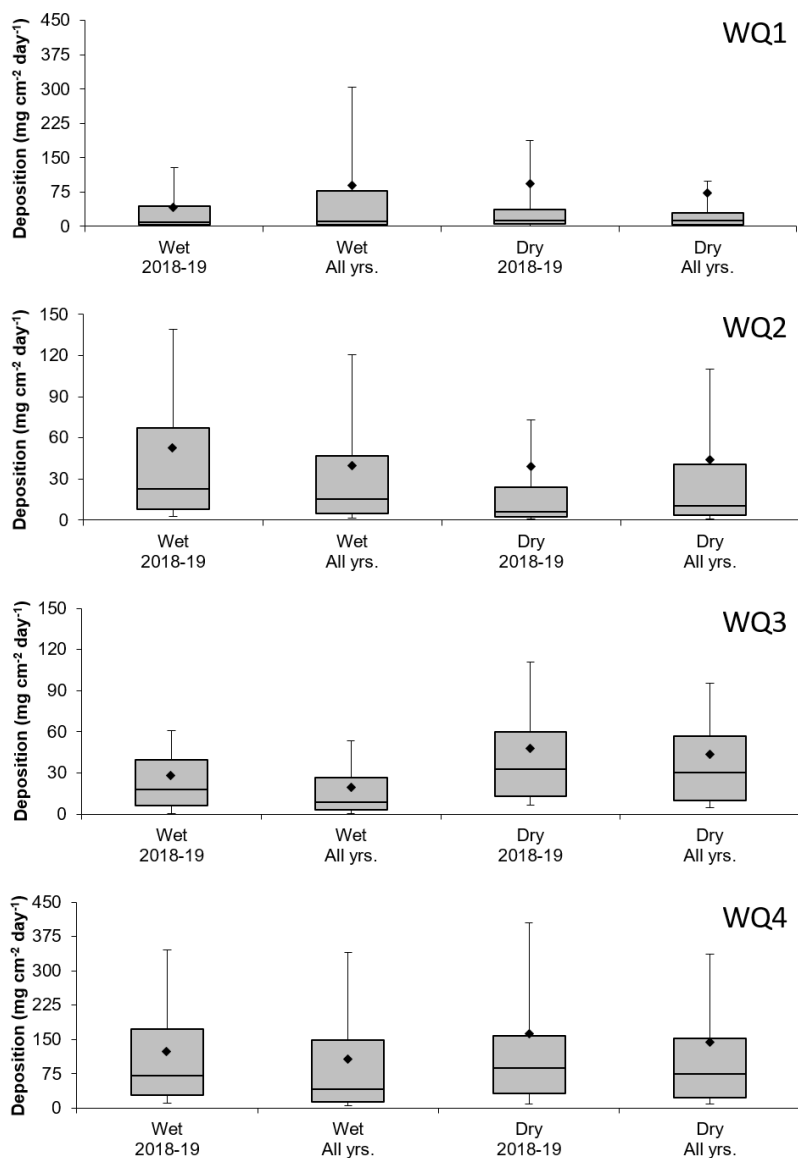
Figure 3.27   Deposition box plots for WQ1-WQ4. Boxes represent the wet (1 November-31 March) and dry seasons (1 April-31 October) using either one wet season (2018-2019) or two wet seasons (2017-2019).

Photosynthetically active radiation

Photosynthetically active radiation (PAR) could differ between seasons due to longer daylength or increased cloud cover during the wet season. The largest seasonal differences in PAR were observed at WQ4 and WQ2, whereby median PAR was 4 times higher during the dry season (Figure 3.31). WQ1 and WQ3 had largely similar PAR during both seasons. Comparison of these four sites suggest that there isn't a general pattern in PAR between seasons, especially at sites close to shore. Differences in depth, distance from the coast, and distance from river mouths may influence how PAR differs between seasons at a given location.
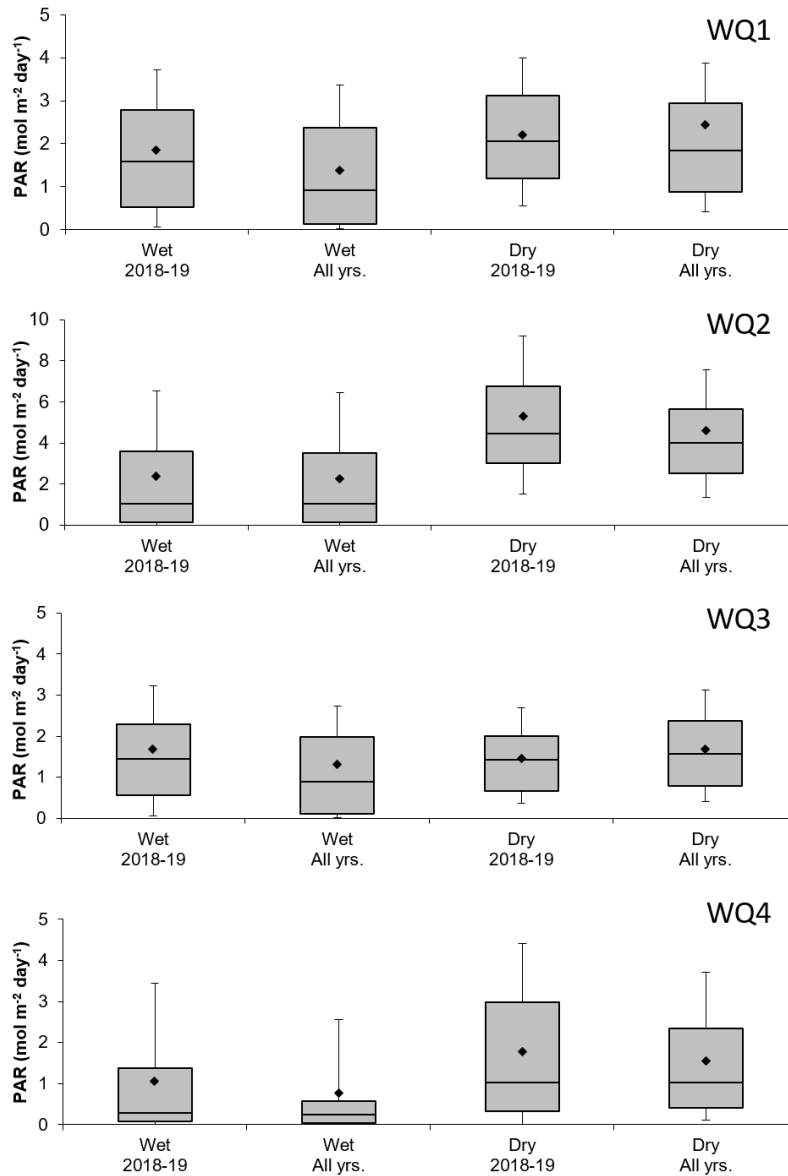
Figure 3.28 PAR box plots for WQ1-WQ4. Boxes represent the wet (1 November-31 March) and dry seasons (1 April-31 October) using either one wet season (2018-2019) or two wet seasons (2017-2019).

Water temperature

Temperatures were higher during the wet season, typically >28 °C, and lower during the dry season, typically <28 °C (Figure 3.28). Median temperatures were ~30 °C in the wet season and ~27 °C in the dry season. Notably, median temperatures during the 2018-2019 dry season at WQ3 and WQ4 were approximately 3 °C lower than the combined 2017-2018 dry seasons.
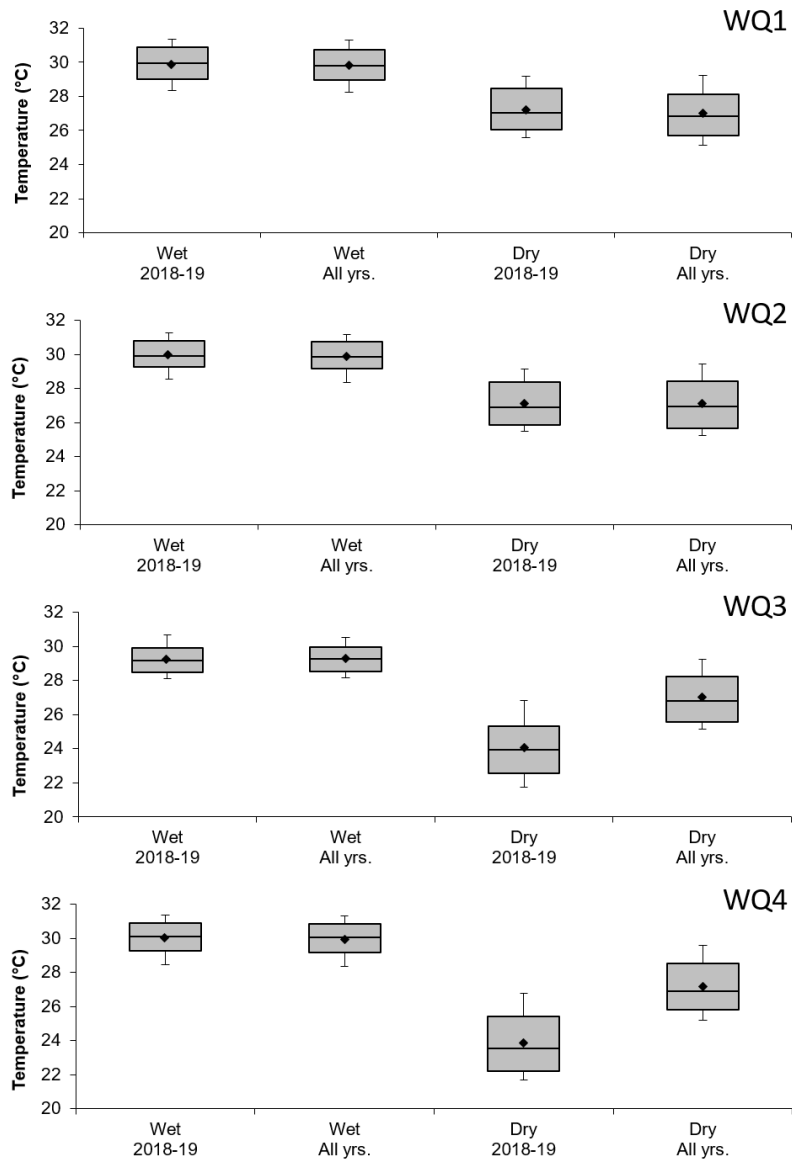
Figure 3.29   Water temperature box plots for WQ1-WQ4. Boxes represent the wet (1 November-31 March) and dry seasons (1 April-31 October) using either one wet season (2018-2019) or two wet seasons (2017-2019).

3.3.7   2019 Dredging campaign

To investigate whether dredging in 2019 affected water quality in the Port of Weipa and surrounding habitats, we compared water quality during 2019 dredging period (4 June 2019 – 13 July 2019) to the same period from 2018. This comparison assumes consistent weather patterns between 2019 and 2018, which may not be the case as wind and storm events are unpredictable. Suspended sediment concentrations, sediment deposition rates, and temperature were higher while photosynthetically available radiation was lower during the dredge period in 2019. There was no clear pattern in root mean square water depth between the two periods.

Turbidity and deposition time series
During the 2019 dredging event, there were periods of high turbidity (SSC) during low and rising tides that were often followed by a short interval of sediment deposition (Figure 3.30). The last week of dredging

exhibited a different pattern, whereby intervals increased deposition coincided with elevated turbidity (Figure 3.30; bottom panel).
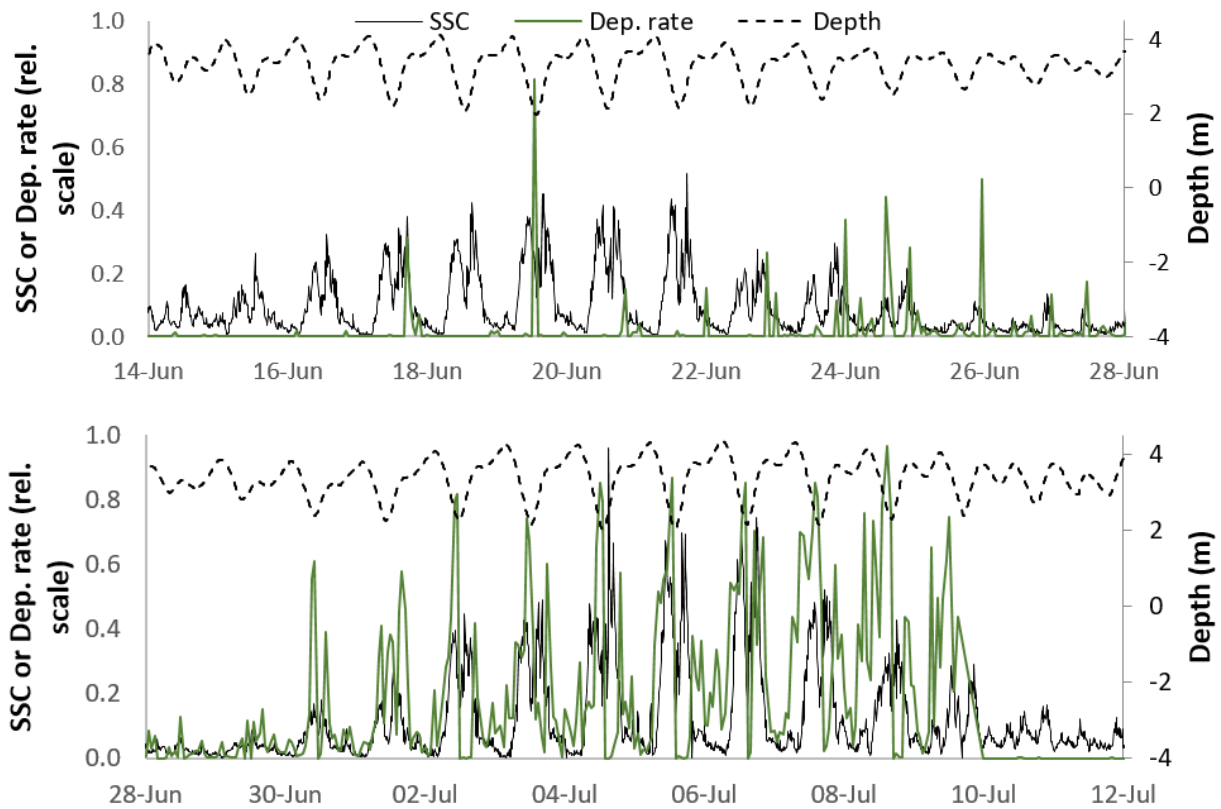
Figure 3.30   Suspended sediment concentrations (SSC) and deposition rates at WQ1 during a portion of the 2019 dredging period. SSC (solid black line) and dep. rates (green line) are displayed relative to their maximum value during the dredging period. Water depth (dashed black line) is depicted on a secondary axis to compare water quality with tide and current direction.

RMS water height
There was little difference in RMS between the 2019 dredging period and the same period from 2018 (Figure 3.31). This suggests that wind and waves did not contribute to differences in water quality between these two time periods.
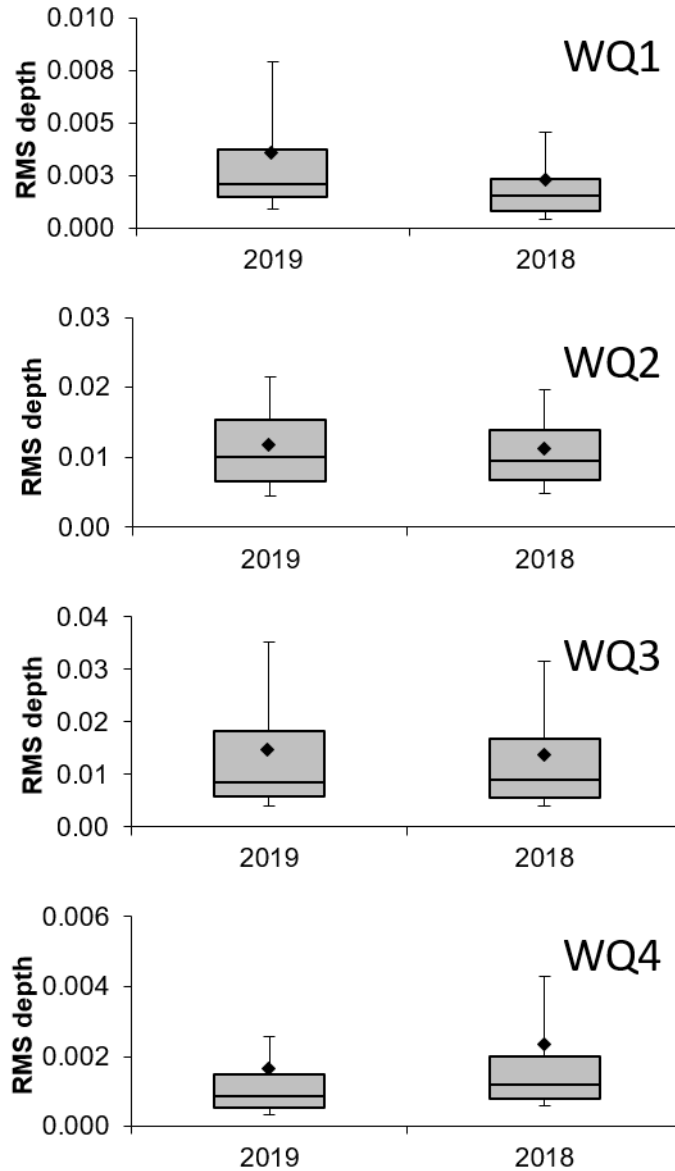
Figure 3.31   Boxplots of RMS for 4 June-13 July 2019 and 4 June-13 July 2018. The lower whisker, lower edge of the box, central line, upper edge of the box and upper whisker represent the 10th, 25th, 50th, 75th and 90th percentiles, respectively. The diamonds represent the mean values.

NTUe/SSC

Suspended sediment concentrations (SSC) were higher during the 2019 dredging compared to the same period from 2018 at all sites, particularly at WQ1, WQ2, and WQ4 (Figure 3.32). Median values were 2-3 times higher for WQ1, WQ2, and WQ3 and 3.5 times higher for WQ4. The 90th percentile, which tracks extreme events, was 6-10 times higher for the sites inside the Embley River (WQ2 and WQ4) and 2-3 times higher for the sites outside the Embley River (WQ1 and WQ3).
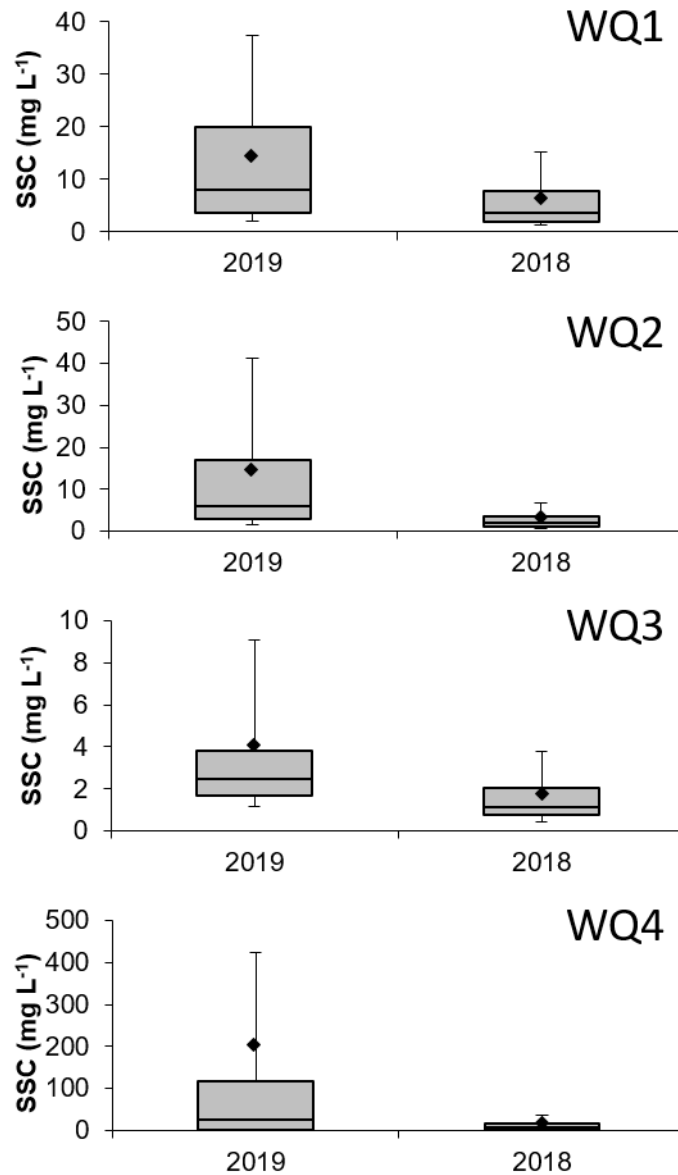
Figure 3.32   Boxplots of SSC for 4 June-13 July 2019 and 4 June-13 July 2018. The lower whisker, lower edge of the box, central line, upper edge of the box and upper whisker represent the 10th, 25th, 50th, 75th and 90th percentiles, respectively. The diamonds represent the mean values.

Deposition

Sediment deposition was higher during the 2019 dredging compared to the same period from 2018 at three of the four monitoring sites (Figure 3.33). Deposition at WQ2 was relatively similar between the 2019 and 2018 periods, but the average deposition rate increased, and the 90th percentile was more than double in 2019 compared to 2018. For the remaining three sites, the increase in deposition rates was clear, as the distribution of deposition rates was 5-10 times higher in 2019 compared to 2018. The 90th percentile, which tracks extreme events, was 17 times higher for WQ1, 3 times higher for WQ3, and 6 times higher for WQ4.
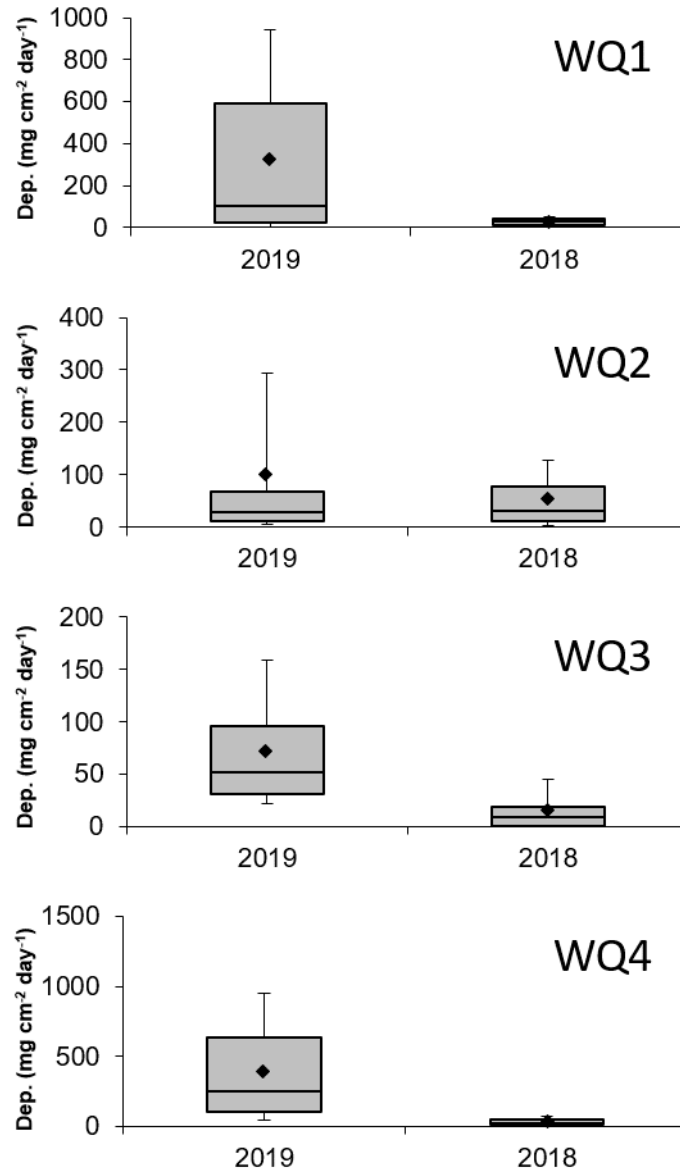
Figure 3.33   Boxplots of sediment deposition rates for 4 June-13 July 2019 and 4 June-13 July 2018. The lower whisker, lower edge of the box, central line, upper edge of the box and upper whisker represent the 10th, 25th, 50th, 75th and 90th percentiles, respectively. The diamonds represent the mean values.

Photosynthetically active radiation

Photosynthetically active radiation (PAR) was lower during the 2019 dredge period compared to the same period from 2018 across all sites (Figure 3.34). Median PAR during the dredge was 77, 46, 17, and 33 % that of the same period in 2018 at WQ1-WQ4, respectively.
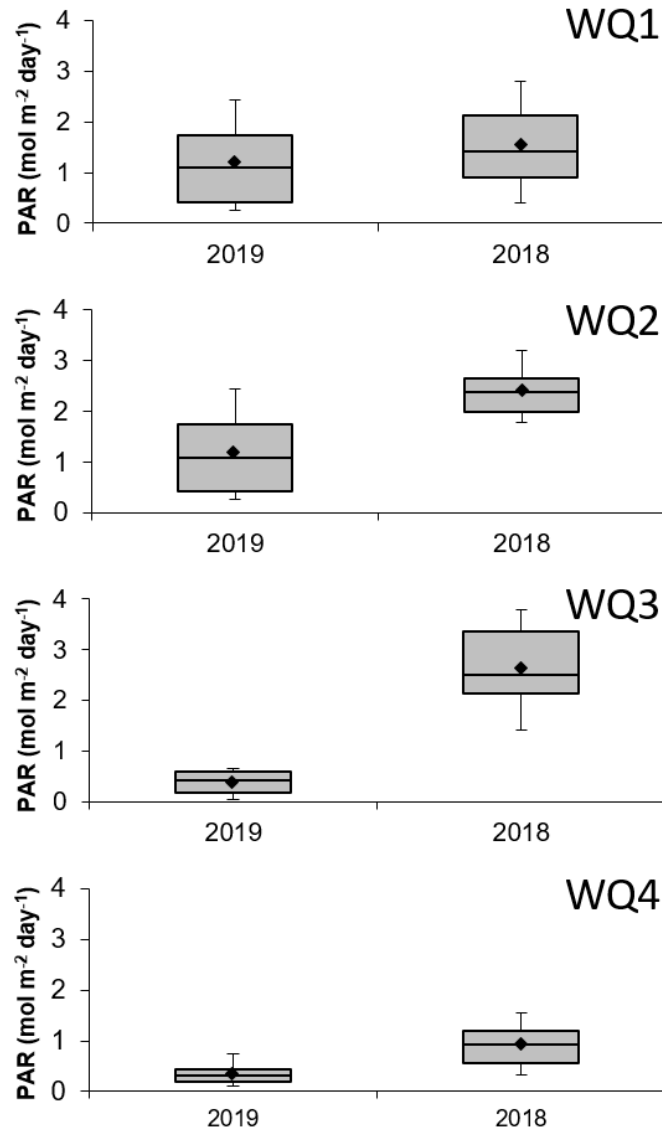
Figure 3.34   Boxplots of photosynthetically active radiation (PAR) for 4 June-13 July 2019 and 4 June-13 July 2018. The lower whisker, lower edge of the box, central line, upper edge of the box and upper whisker represent the 10th, 25th, 50th, 75th and 90th percentiles, respectively. The diamonds represent the mean values.

Water temperature

Water temperatures were higher across all sites during the 2019 dredge compared to the same period from 2018 (Figure 3.35). Median temperatures were 1-2 % higher (approx. 0.4 °C) during the dredge period in 2019.
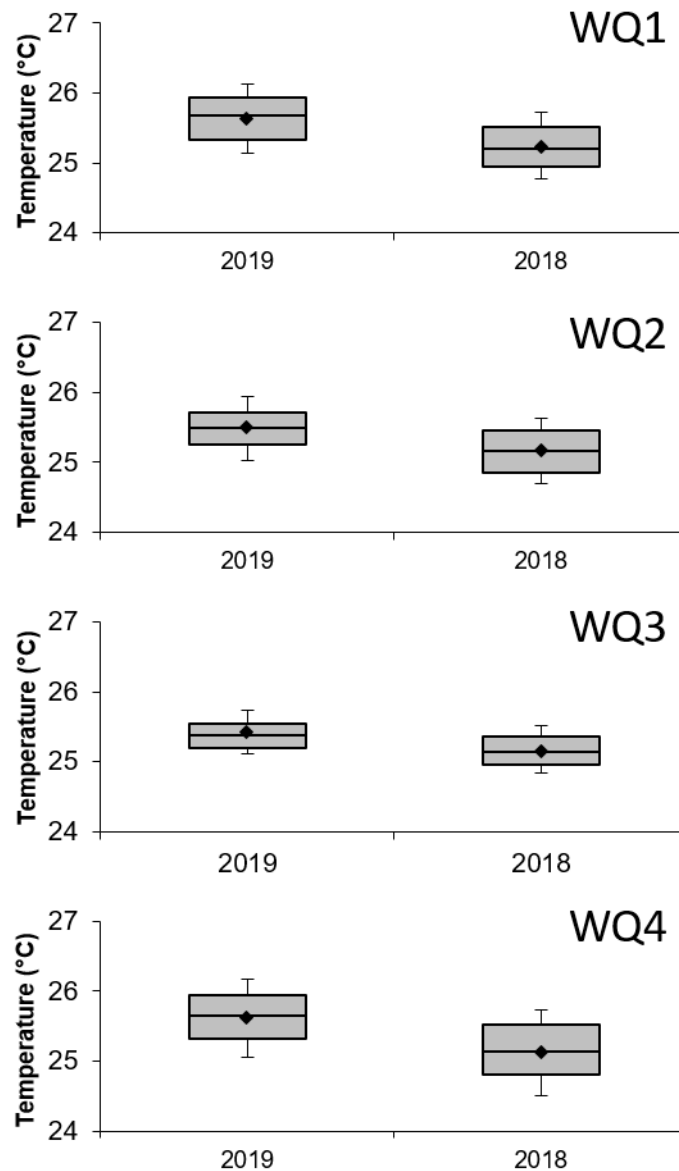
Figure 3.35   Boxplots of water temperature for 4 June-13 July 2019 and 4 June-13 July 2018. The lower whisker, lower edge of the box, central line, upper edge of the box and upper whisker represent the 10th, 25th, 50th, 75th and 90th percentiles, respectively. The diamonds represent the mean values.

3.4   Current meter

Current meter data was collected at all five sites. Marotte HS current meter instruments were deployed for the full monitoring period from July 2018 to July 2019 for WQ1-WQ4. The current meter data indicates the prominent current direction and velocity at each site. Data shows that coastal current, tidal current or a combination of both influence current direction and magnitude. The figures below display the current meter data in current rose and average current speed rose diagrams. The current rose diagrams provide a visual representation of relative prominence of current velocity and direction. The average current speed rose diagrams displays the average current speed in every direction. Presented together these diagrams highlight the prominent direction of current and the average velocity of the current in this direction. A short and long animation illustrating how the current speed and direction changes over time at each site are accessible to view via sharepoint. Links to the videos are provided in Appendix A1.4.

3.4.1   WQ1

The current at WQ1 ranges from East to West with peaks at ENE and W and average velocities ranging between 0.10 and 0.38 m s^{-1} (as shown in Figure 3.36 and Figure 3.37). This is in line with expected tidal current directions at the site.
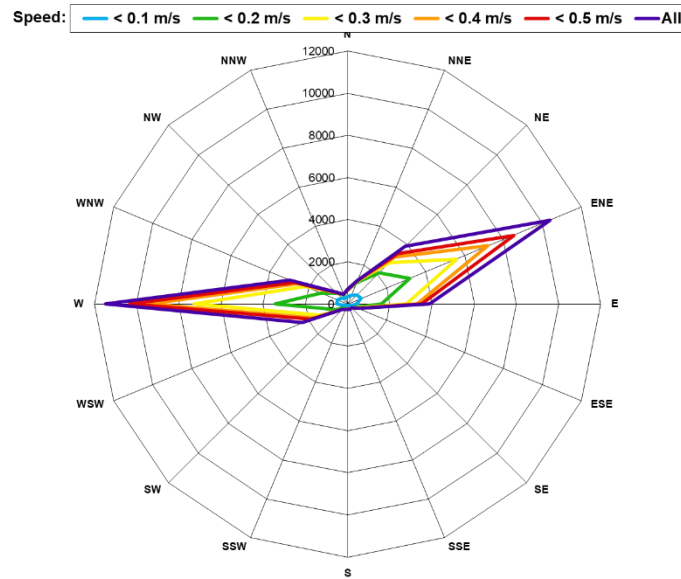
Figure 3.36   Current rose at WQ1 for the monitoring period from July 2018 to July 2019. The current rose plots the number of currents recorded in each direction within the ranges of different current speeds indicated in the legend
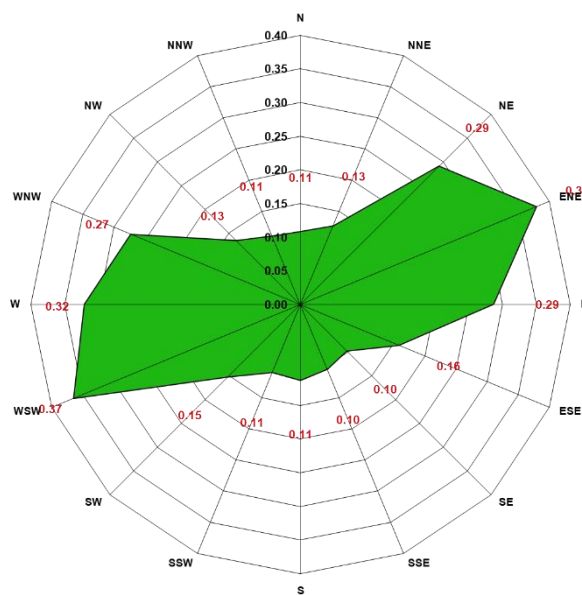
Figure 3.37   Average current speed rose at WQ1 for the monitoring period from July 2018 to July 2019. The average current speed is rose is coloured in green, while the red values indicate the average current value at each specific direction

3.4.2   WQ2

The current at WQ2 flows between SW and NE directions with average velocities between 0.06 and 0.23 m s^{-1} (as shown in Figure 3.38 and Figure 3.39). The current directions suggest that these currents are tidal.
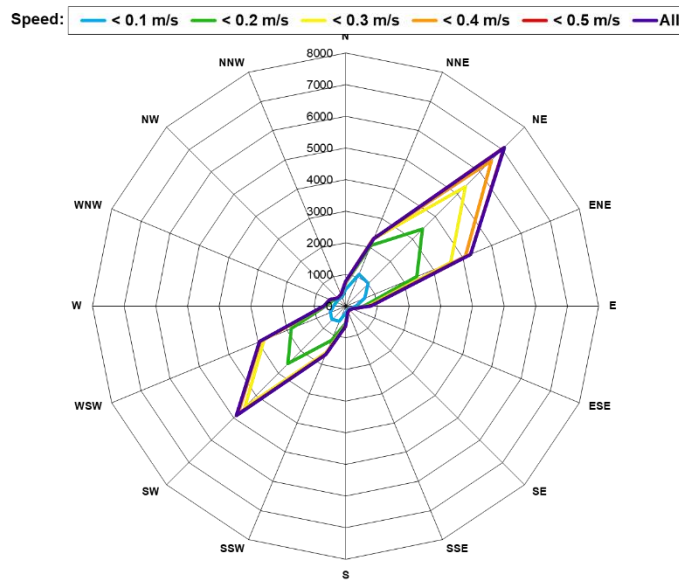
Figure 3.38   Current rose at WQ2 for the monitoring period from July 2018 to July 2019. The current rose plots the number of currents recorded in each direction within the ranges of different current speeds indicated in the legend
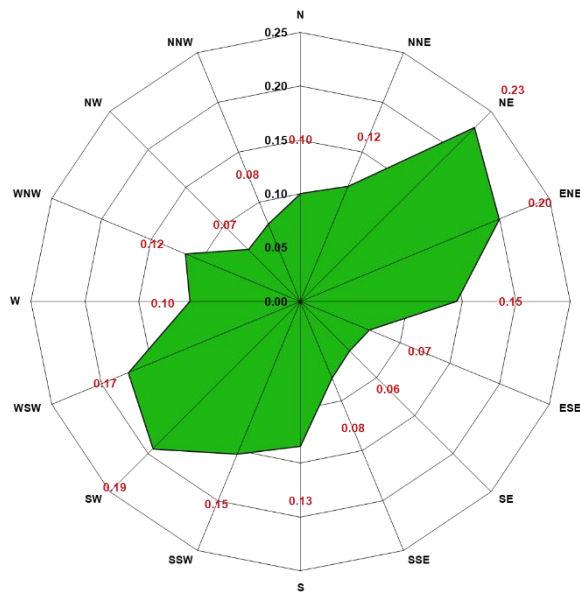
Figure 3.39   Average current speed rose at WQ2 for the monitoring period from July 2018 to July 2019. The average current speed is rose is coloured in green, while the red values indicate the average current value at each specific direction

3.4.3   WQ3

The current at WQ3 flows predominantly in the WSW direction with average current speed velocities ranging from 0.03 to 0.14 m s^{-1} (as shown in Figure 3.40 and Figure 3.41). As expected, the currents at this site flow both along the coast in both directions.
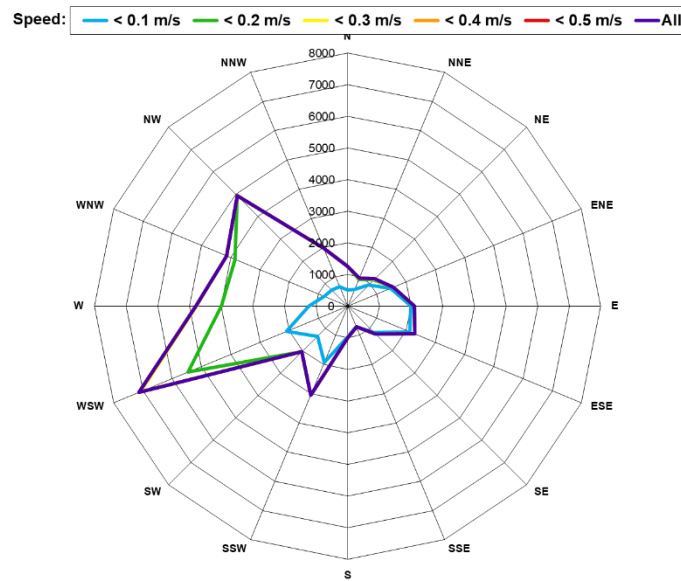
Figure 3.40 Current rose at WQ3 for the monitoring period from March 2018 to July 2018. The current rose plots the number of currents recorded in each direction within the ranges of different current speeds indicated in the legend
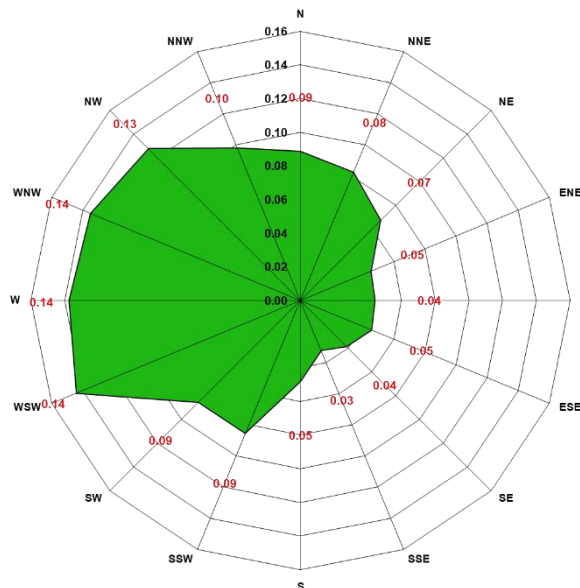
Figure 3.41 Average current speed rose at WQ3 for the monitoring period from July 2018 to July 2019. The average current speed is rose is coloured in green, while the red values indicate the average current value at each specific direction

3.4.4 WQ4

The currents that dominate the site WQ4 are in the NW and SE directions (Figure 3.42). An average current velocity of 0.06 and 0.31 m s^{-1} were recorded in these respective directions (Figure 3.43). This lines up with the direction of the river at this location.
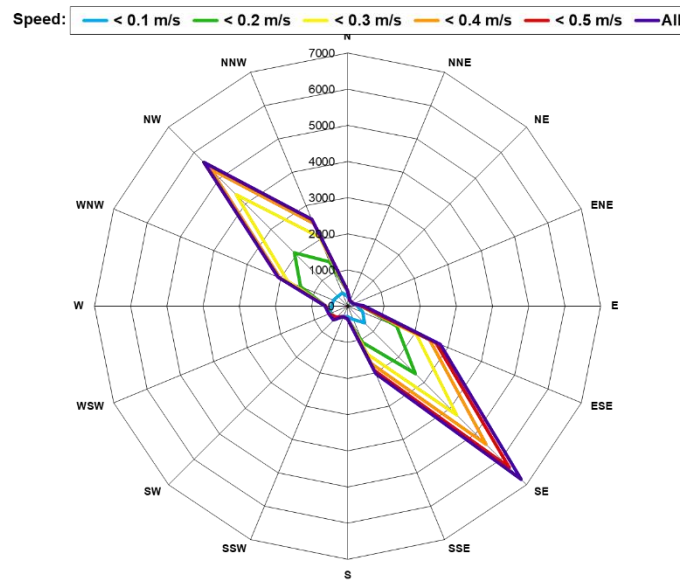
Figure 3.42   Current rose at WQ4 for the monitoring period from July 2018 to July 2019. The current rose plots the number of currents recorded in each direction within the ranges of different current speeds indicated in the legend
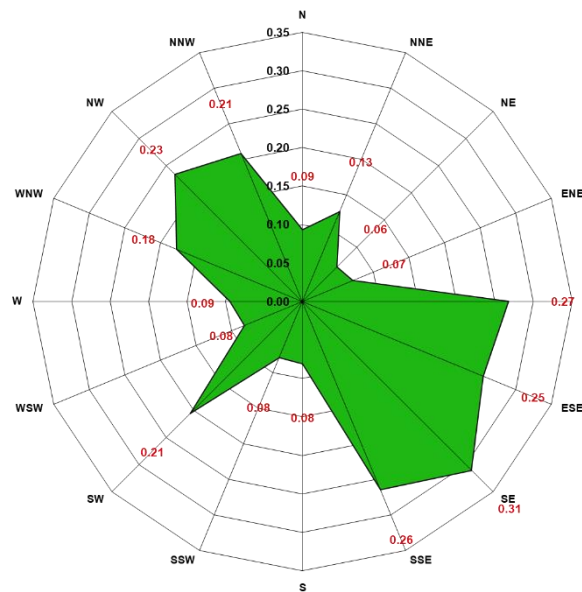
Figure 3.43   Average current speed rose at WQ4 for the monitoring period from July 2018 to July 2019. The average current speed is rose is coloured in green, while the red values indicate the average current value at each specific direction

3.5   River Plumes

An important note here is that the Watson River is located ~75km south of the Mission River system adjacent to the Port of Weipa, and therefore Watson River discharge is only a proxy of actual discharge in Mission River. Given the variable nature of rainfall and river charges, some caution is required with the final interpretation of these analysis.

3.5.1   WQ1

A stepwise regression analysis was run against the WQ1 data to identify the appropriate variable selection, excluding autocorrelation and outliers, for the multiple regression analysis. RMS of water depth, the Watson

River discharge, the NWSE wind component and tide amplitude explained 31 % of the SSC variability (Table 3.8). The relative importance analysis suggested that tidal amplitude was the most influential parameter on SSC (67 % of overall R^2), followed by Watson River discharge (15 % of overall R^2), the NWSE wind component (13 % of the overall R^2), and RMS of water depth (5 % of overall R^2; Figure 3.44). Partial effects plots (Figure 3.45) show that SSC increases with all influential environmental parameters.

Table 3.8   Statistical summary of the stepwise regression analysis to WQ1 data

	AMB1		
Predictors	*Estimates*	*CI*	*p*
(Intercept)	1.55	0.61 – 2.49	**0.001**
log(RMS)	0.16	0.02 – 0.31	**0.030**
log(Watson + 1)	0.07	0.04 – 0.10	**<0.001**
wind NWSE	0.02	0.01 – 0.03	**0.001**
Amplitude	1.13	0.89 – 1.37	**<0.001**
Observations	287		
R^2 / adjusted R^2	0.315 / 0.305		
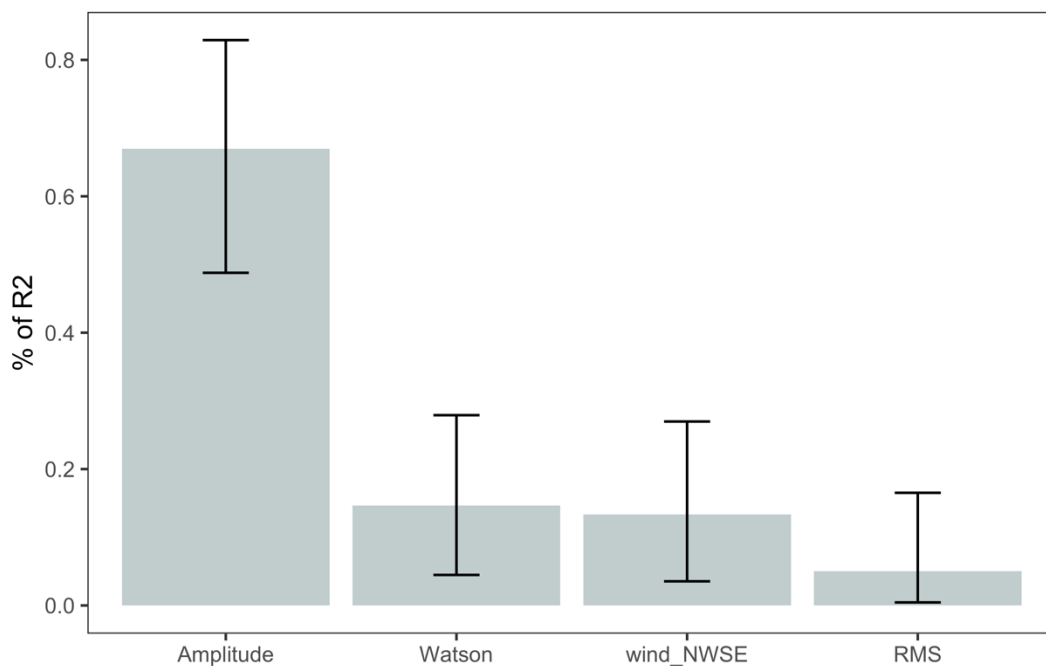
Figure 3.44   WQ1 bootstrapping relative importance analysis following a stepwise multiple regression analysis. Bars represent 95 % bootstrap confidence intervals, and % of R^2 values are normalised to sum 100 %.
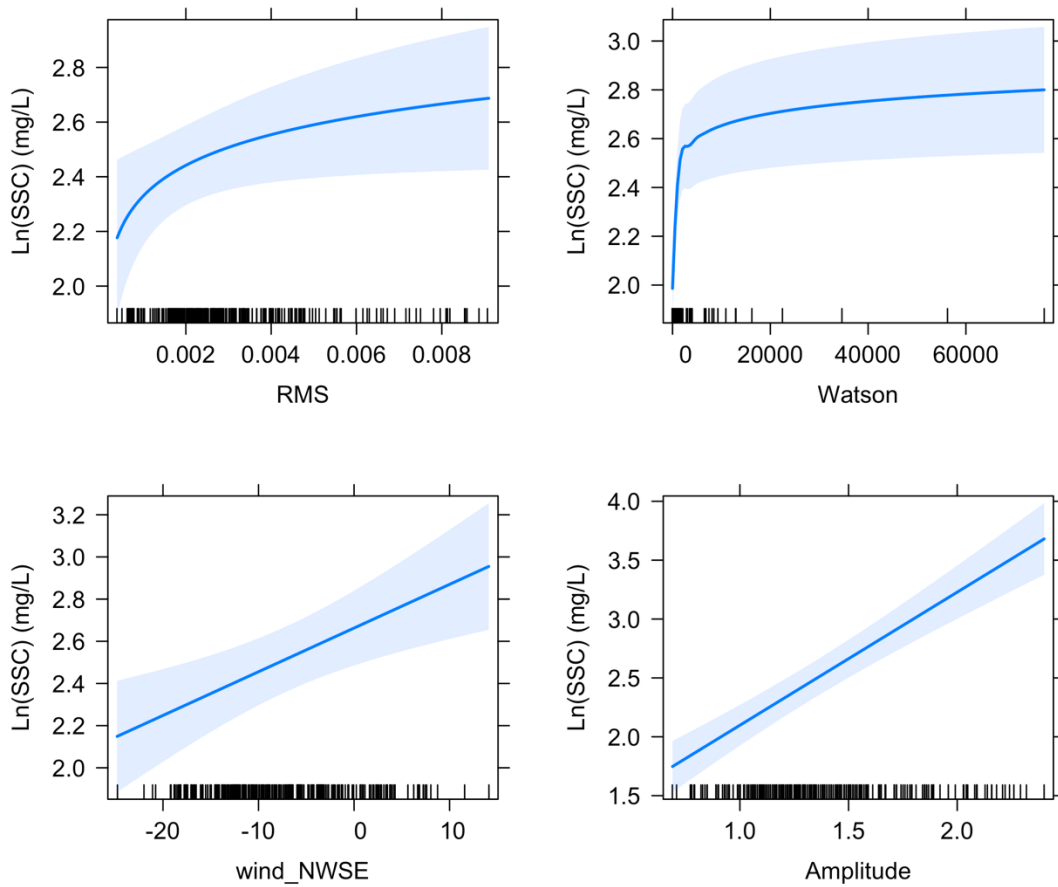
Figure 3.45   Partial effect plots for WQ1 parameters affecting the concentration of suspended solids in the water column. Grey area indicates 95 % CI and rug on x-axis stand for data density.

3.5.2   **WQ2**

A stepwise regression analysis was run against the WQ2 data to identify the appropriate variable selection, excluding autocorrelation and outliers, for the multiple regression analysis. RMS of water depth, Watson River discharge, the NESW wind component, and tidal amplitude explained 66 % of the SSC variability (Table 3.9). The relative importance analysis suggested that Watson River discharge was the most influential parameter on SSC (42 % of overall R^2), followed by RMS of water depth (39 % of overall R^2), the NESW wind component (12 % of overall R^2), and tidal amplitude (6 % of overall R^2) (Figure 3.46). Results of the partial effects plots followed expected trends for SSC in relation to each environmental parameter selected in the model (Figure 3.47).

Table 3.9   Statistical summary of the stepwise regression analysis to WQ2 data

Predictors	Estimates	CI	p
AMB2			
(Intercept)	3.43	2.73 – 4.13	**<0.001**
log(RMS)	0.65	0.52 – 0.77	**<0.001**
log(Watson + 1)	0.21	0.18 – 0.24	**<0.001**
wind NESW	-0.03	-0.05 – -0.01	**0.014**
Amplitude	0.77	0.50 – 1.04	**<0.001**
Observations	317		
R^2 / adjusted R^2	0.658 / 0.654		
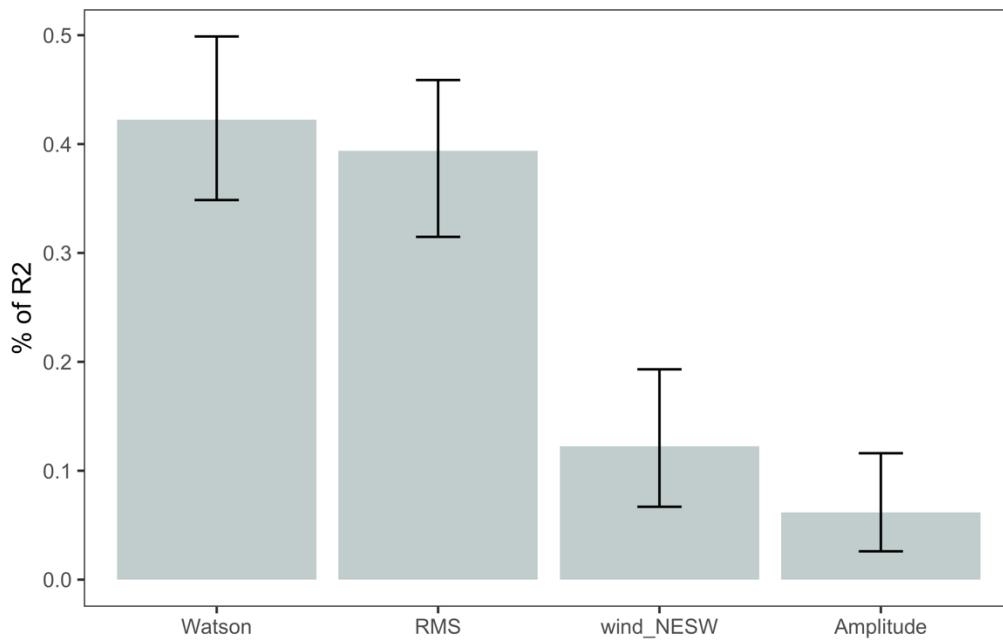
Figure 3.46   WQ2 bootstrapping relative importance analysis following a stepwise multiple regression analysis. Bars represent 95% bootstrap confidence intervals, and % of r squared values are normalised to sum 100 %
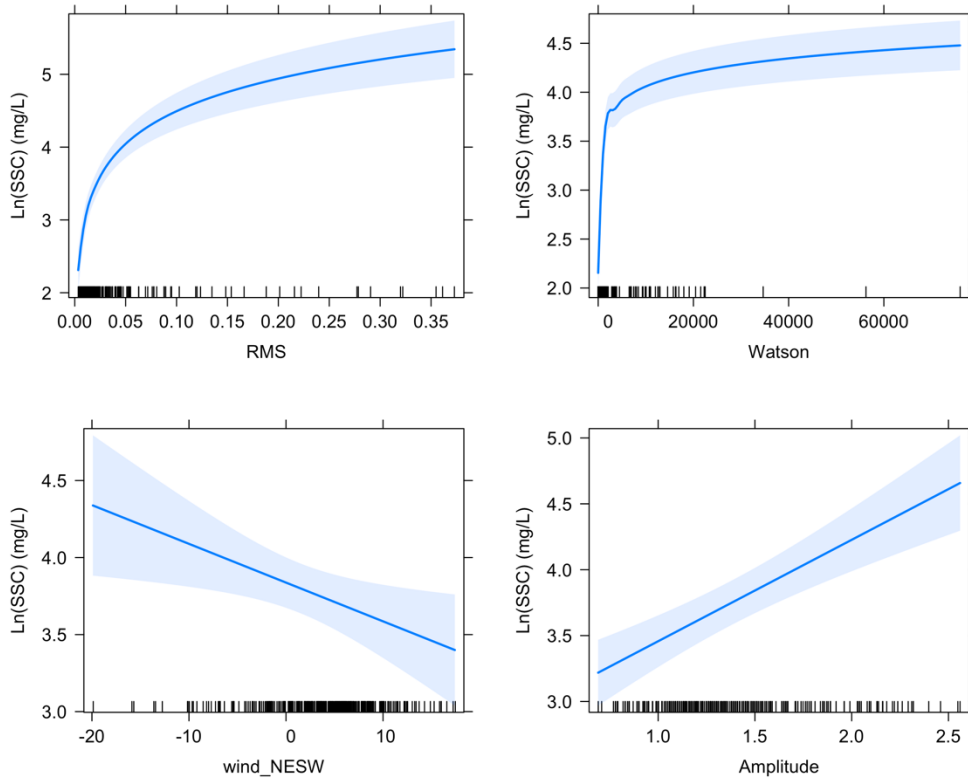
Figure 3.47   Partial effect plots for WQ2 parameters affecting the concentration of suspended solids in the water column. Grey area indicates 95% CI and rug on x-axis stand for data density

3.5.3   WQ3

A stepwise regression analysis was run against the WQ3 data to identify the appropriate variable selection, excluding autocorrelation and outliers, for the multiple regression analysis. RMS of water depth and Watson River discharge were the environmental parameters that were significantly related to SSC, explaining 37 % of the SSC variability (Table 3.10). The relative importance analysis suggested that RMS of water depth is the most influential parameter on SSC (63 % of overall R^2), followed by Watson River discharge (37 % of overall R^2) (Figure 3.48). The partial effects plot shows that SSC increases in relation to increasing RMS of water depth, but has a negative relationship with Watson River discharge (Figure 3.49).

Table 3.10   Statistical summary of the stepwise regression analysis to WQ3 data

	WQ3		
Predictors	*Estimates*	*CI*	*p*
(Intercept)	3.89	3.25 – 4.53	**<0.001**
log(RMS)	0.62	0.48 – 0.76	**<0.001**
log(Watson + 1)	-0.13	-0.16 – -0.09	**<0.001**
Observations	217		
R^2 / adjusted R^2	0.370 / 0.364		
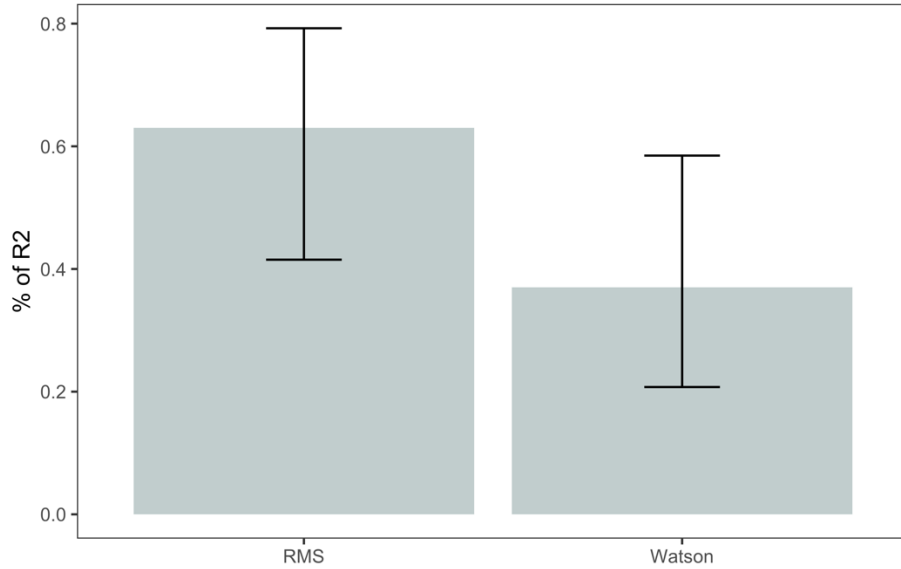
Figure 3.48   WQ3 bootstrapping relative importance analysis following a stepwise multiple regression analysis. Bars represent 95 % bootstrap confidence intervals, and % of R^2 values are normalized to sum 100 %.
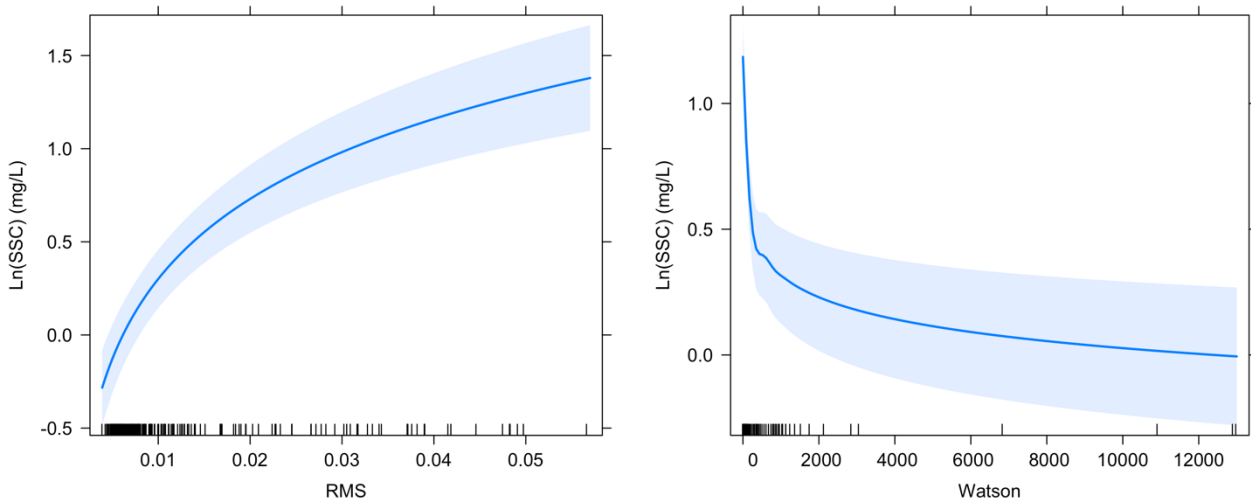
Figure 3.49   Partial effect plots for WQ3 parameters affecting the concentration of suspended solids in the water column. Grey area indicates 95 % CI and rug on x-axis stand for data density

3.5.4   WQ4

A stepwise regression analysis was run against the WQ4 data to identify the appropriate variable selection, excluding autocorrelation and outliers, for the multiple regression analysis. Watson River discharge, the NESW wind component and tidal amplitude together explained 16 % of SSC variability (Table 3.11). The relative importance analysis suggested that tidal amplitude is the most influential parameter on SSC (56 % of overall R^2), followed by the NESW wind component (26 % of overall R^2), and Watson River discharge (17 % of overall R^2) (Figure 3.50). Results of the partial effects plots followed expected trends for SSC in relation to each environmental parameter selected in the model (Figure 3.51). An increase in SSC was observed with increases in Watson River discharge and tidal amplitude, while stronger the winds coming from the east (i.e. positive values for wind NESW) were related to lower SSC values.

Table 3.11   Statistical summary of the stepwise regression analysis to WQ4 data

	AMB4		
Predictors	*Estimates*	*CI*	*p*
(Intercept)	2.01	1.40 – 2.63	**<0.001**
log(Watson + 1)	0.09	0.04 – 0.13	**0.001**
wind NESW	-0.05	-0.08 – -0.03	**<0.001**
Amplitude	1.14	0.75 – 1.54	**<0.001**
Observations	285		
R^2 / adjusted R^2	0.166 / 0.157		
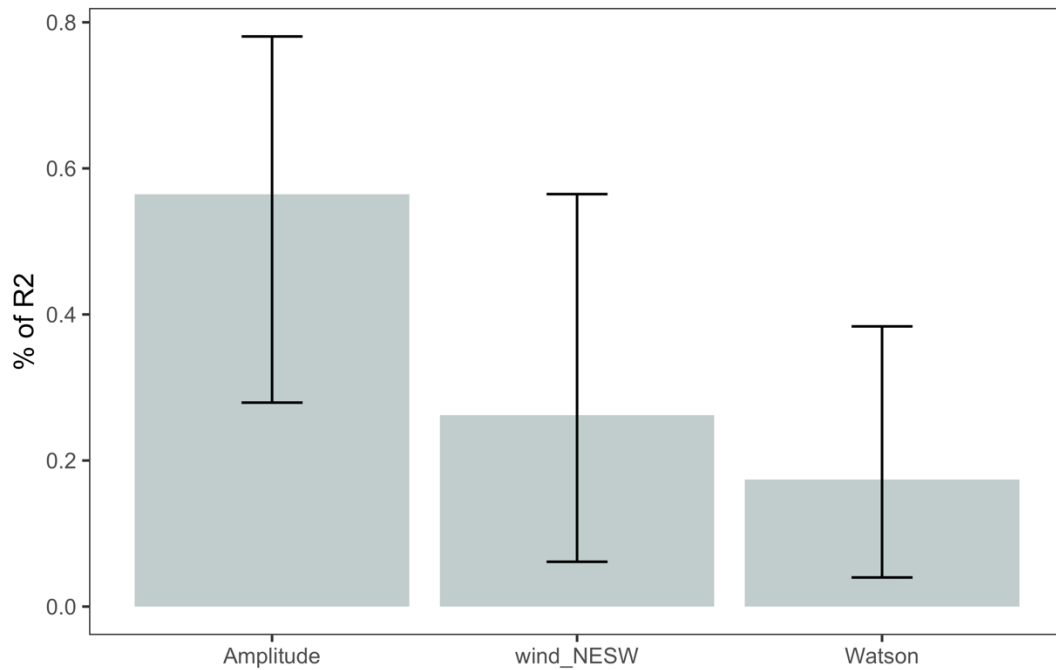
Figure 3.50   WQ4 bootstrapping relative importance analysis following a stepwise multiple regression analysis. Bars represent 95 % bootstrap confidence intervals, and % of R^2 values are normalized to sum 100 %.
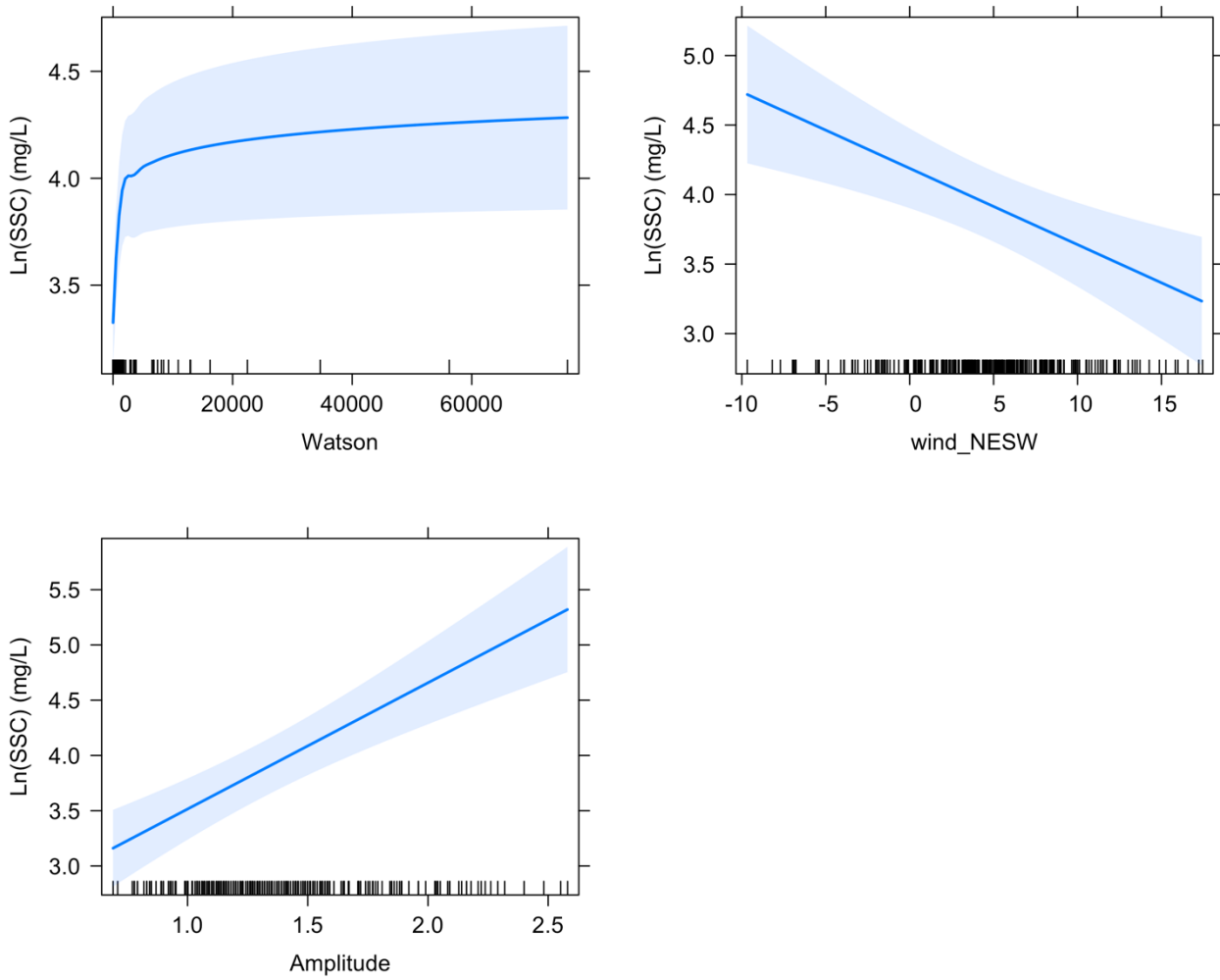
Figure 3.51   Partial effect plots for WQ4 parameters affecting the concentration of suspended solids in the water column. Grey area indicates 95 % CI and rug on x-axis stand for data density.

4 CONCLUSIONS AND RECOMMENDATIONS

4.1 Conclusions

4.1.1 Climatic conditions

1. The 2018-2019 wet season was in the order of the 80th percentile for rainfall in the region. An important factor to consider when interpreting data during this monitoring period. Comparison of these data with future years will be important to characterise ambient water quality conditions. It is important to capture monitoring data over a range of climatic conditions.
2. The daily average wind speed and direction recorded at Weipa airport for the reporting period (2018-2019) was predominantly from the south east and east and rarely reached speeds greater than 24 km h^{-1}

4.1.2 Ambient water quality

1. There is a seasonal pattern for water temperature emerging, with highest water temperatures experienced during summer months, while winter months experience cooler conditions. This pattern will continue to be monitored in future reporting years.
2. The water column is well mixed, with depth profiles for dissolved oxygen, temperature, electrical conductivity and pH showing only minor gradients of change.
3. Turbidity values are generally higher at depth, contributing to a difference in water clarity between the surface and bottom water horizons. Higher turbidity values at the bottom water horizon is probably related to RMS wave height, currents, and sediment resuspension processes. The elevated turbidity in the bottom horizon becomes an important consideration when examining sensitive receptor habitats, such as seagrass which are sensitive to water clarity changes. Measuring bottom horizon turbidity is a very relevant component of this program; surface measurements for turbidity, or indeed suspended solid concentrations, might not be an entirely relevant measure when the objective is to protect and enhance benthic habitats.
4. Particulate nitrogen (PN) and phosphorus (PP) concentrations exceed guideline values during all 2018-2019 surveys and at all sites.
5. Chlorophyll-*a* concentrations exceed guideline values during all 2018-2019 surveys and at all sites.
6. Phytoplankton and zooplankton communities had a very different species composition between surveys completed so far, which could reflect local seasonal conditions – this pattern will be further explored as more data becomes available for the region.
7. Trace metals were generally well below guideline values throughout the reporting year. Zinc was detected across all sites in April 2018 and Zinc concentrations at WP_AMB4 exceeded guideline values in January 2019.
8. The major pesticide and herbicide concentrations were not detected above the limit of reporting

4.1.3 Sediment deposition and turbidity

3. Continuous sediment deposition and turbidity logging data supports the pattern found more broadly in North Queensland coastal marine environments, that during dry periods with minimal rainfall, elevated turbidity along the coastline is driven by the re-suspension of sediment and this has been most notable here given the links drawn between RMS water depth and NTUe/SSC. Large peaks in NTUe/SSC and RMS water depth were recorded over periods longer than a week.
4. Sediment deposition rates around Weipa were much higher than measured across other north Queensland coastal marine sites investigated during the same period.

4.1.4 Photosynthetically active radiation (PAR)

3. Fine-scale patterns of PAR are primarily driven by tidal cycles with fortnightly increases in PAR coinciding with neap tides and lower tidal flows. Larger episodic events which lead to extended periods of low light conditions are driven by a combination of strong winds leading to increases in wave height and resuspension of particles (Orpin and Ridd 2012), and rainfall events resulting from storms leading to increased catchment flows and an input of suspended solids (Fabricius et al., 2013).

4. Patterns of light were similar among all the coastal sites. Light penetration in water is affected in an exponential relationship with depth as photons are absorbed and scattered by particulate matter (Kirk 1985; Davis-Colley and Smith 2001). Therefore variation in depth at each location means benthic PAR is not directly comparable among sites as a measure of water quality. Generally, however, shallow inshore sites reached higher levels of benthic PAR and were more variable than deeper water coastal sites and sites of closer proximity to one another were more similar than distant sites.

5. While turbidity is the main indicator of water quality used in monitoring of dredge activity and benthic light is significantly correlated with suspended solid concentrations (Erftemeijer and Lewis 2006; Erftemeijer et al., 2012), the relationship between these two parameters is not always strong (Sofonia and Unsworth 2010). At many of the sites where both turbidity and benthic light were measured, the concentration of suspended solids in the water column explained less than half of the variation in PAR. As PAR is more biologically relevant to the health of photosynthetic benthic habitats such as seagrass, algae and corals it is becoming more useful as a management response tool when used in conjunction with known thresholds for healthy growth for these habitats (e.g., Chartrand et al., 2012). For this reason, it is important to include photosynthetically active radiation (PAR) in the suite of water quality variables when capturing local baseline conditions of ambient water quality.

4.2 Recommendations

2. Given this monitoring program commenced in January 2018, and is now only into its 2nd full year of operation it is recommended that the current program remain for the 2019/20 period.

4.2.1 Data base repository

An electronic version of the ambient marine water quality database has been made available to NQBP via the NQBP Ambient Environmental Monitoring Sharepoint website. It currently comprises MS-Excel Workbooks containing raw data files including results for water chemistry (in-situ field measurements, nutrients, filterable metals, pesticides/herbicides) collected as during the quarterly sampling, and all the continuous high frequency logger data files for sediment deposition, PAR, turbidity, water temperature, and RMS recorded during the period January and July 2019. This data base continues to be maintained by TropWATER personal, with back up copy archived on the James Cook University network with restricted access.

5   REFERENCES

ANZECC and ARMCANZ (2000) Australian Water Quality Guidelines for Fresh and Marine Waters. Australia and New Zealand Environment Conservation Council and Agriculture and Resource Management Council of Australia and New Zealand, Canberra.

APHA (2005) Standard Methods for the examination of water and waste water. 21st Edition. American Public Health Association. Washington, D.C.

Brodie, J. E., Kroon, F. J., Schaffelke, B., Wolanski, E. C., Lewis, S. E., Devlin, M. J., Bohnet, I. C, Bainbridge, Z. T., Waterhouse, J., Davis, A. M. (2012) Terrestrial pollutant runoff to the Great Barrier Reef: an update of issues, priorities and management responses. Marine Pollution Bulletin, 65, 81-100.

Bunt, J., Larcombe, P., Jago, C. F. (1999) Quantifiying the response of optical backscatter devices and transmissiometers to variations in suspended particulate matter (SPM). Continental Shelf Research 19: 1199-1220

Capone, D. G., Zehr, J. P., Paerl, H. W., Bergman, B., Carpenter, E. J. (1997). Trichodesmium, a globally significant marine cyanobacterium. Science, 276, 1221-1229.

Conner, C. S., De Visser, A. M. (1992) A laboratory investigation of particle size effects on an optical backscatterance sensor. Marine Geology 108:151-159

Cook, R. D., Weisberg, S. (1982) Residuals and Influence in Regression. Chapman and Hall.

Crawley, M.J. (2007) The R Book. John Wiley and Sons, Ltd.

DEHP (2013) Queensland Water Quality Guidelines, Version 3, Department of Environment and Heritage Protection. Brisbane

Dennison, W. C., Orth, R. J., Moore, K. A., Stevenson, J. C., Carter, V., Kollar, S., . . . Batiuk, R. A. (1993). Assessing Water Quality with Submersed Aquatic Vegetation. Bioscience, 43(2), 86-94.

Devlin, M. J., McKinna, L. W., Alvarez-Romero, J. G., Petus, C., Abott, B., Harkness, P., Brodie, J. (2012) Mapping the pollutants in surface riverine flood plume waters in the Great Barrier Reef, Australia. Marine Pollution Bulletin, 65, 224-235. doi: 10.1016/j.marpolbul.2012.03.001

Erftemeijer, P. L. A., B. Riegl, B. W. Hoeksema, Todd, P. A. (2012) Environmental impacts of dredging and other sediment disturbances on corals: A review. Marine Pollution Bulletin 64, 1737-1765.

Erftemeijer, P. L. A., Lewis, R. R. R. (2006) Environmental impacts of dredging on seagrasses: a review. Marine Pollution Bulletin 52, 1553-1572.

Fabricius, K. E., G. De'ath, C. Humphrey, I. Zagorskis, Schaffelke, B. (2013) Intra-annual variation in turbidity in response to terrestrial runoff on near-shore coral reefs of the Great Barrier Reef. Estuarine, Coastal and Shelf Science 116, 57-65.

Fox, J., Monette, G. (1992) Generalized collinearity diagnostics. JASA, 87, 178–183.

GBRMPA (2010) Water quality guidelines for the Great Barrier Reef Marine Park 2010 current edition. Great Barrier Reef Marine Park Authority.

Gordon, H. R. (1989). Can the Lambert-Beer law be applied to the diffuse attenuation coefficient of ocean water? Limnology and Oceanography, 34(8), 1389-1409. doi:10.4319/lo.1989.34.8.1389

Grömping, G. (2006) Relative Importance for Linear Regression in R: The Package relaimpo. Journal of Statistical Software, 17, 1-27.

Jerlov, N. G. (1976). Marine optics. Amsterdam: Elsevier Scientific Pub. Co.

Johansen, J. L., Pratchett, M. S., Messmer, V., Coker, D. J., Tobin, A. J., Hoey, A. S. (2015) Large predatory coral trout species unlikely to meet increasing energetic demands in a warming ocean. Scientific Reports, 5.

Kirk, J. T. O. (1985) Effects of suspendiods (turbidity) on penetration of solar rediation in aquatic ecosystems. Hydrobiologia, 125, 195-208.

Kirk, J. T. O. (1994). Light and photosynthesis in aquatic ecosystems. Cambridge [England]: Cambridge University Press.

Kirk, J. T. O. (1977). Attenuation of Light in Natural Waters. Aust. J. Mar. Freshwater Res.,, 28, 497-508.

Kroon, F. J., Kuhnert, P. M., Henderson, B. L., Wilkinson, S. N., Kinsey-Henderson, A., Abbott, B., Brodie. J. E., Turner, R. D. (2012) River loads of suspended solids, nitrogen, phosphorus and herbicides delivered to the Great Barrier Reef lagoon. Marine Pollution Bulletin, 65, 167-181.

Larcombe P, Ridd PV, Prytz A, Wilson, B. (1995) Factors controlling suspended sediment ion inner-shelf coral reefs, Townsville, Australia. Coral Reefs 14:163-171

Logan, M., Fabricius, K., Weeks, S., Rodriguez, A., Lewis, S., Brodie, J. (2014) Tracking GBR water clarity over time and demonstrating the effects of river discharge events. Progress Report: Southern and Northern NRM Regions. Report to the National Environmental Research Program. Reef and Rainforest Research Centre Limited, Cairns (53pp.).

Ludwig, K. A., Hanes, D. M. (1990) A laboratory explanation of optical backscatterance suspended solids sensors exposed to sand-mud mixtures. Mar Geol 94:173-179

Macdonald, R.K. (2015). Turbidity and Light Attenuation in Coastal Waters of the Great Barrier Reef (Doctoral dissertation). Retrieved from https://researchonline.jcu.edu.au/46029/

Mobley, C. D. (1994). Light and Water: Radiative Transfer in Natural Waters: Academic Press.

Orpin, A. R., Ridd, P. V. (2012) Exposure of inshore corals to suspended sediments due to wave-resuspension and river plumes in the central Great Barrier Reef: A reappraisal. Continental Shelf Research 47, 55-67.

R Core Team (2015) R: A language and environment for statistical computing. R Foundation for Statistical Computing, Vienna, Austria. URL http://www.R-project.org/.

Schaffelke, B., Carleton, J., Skuza, M., Zagorskis, I., Furnas, M. J. (2012) Water quality in the inshore Great Barrier Reef lagoon: Implications for long-term monitoring and management. Marine Pollution Bulletin, 65(4), 249-260.

Sofonia, J. J., Unsworth, R. K. F. (2010) Development of water quality thresholds during dredging for the protection of benthic primary producer habitats. Journal of Environmental Monitoring 12:159-163.

Standards Australia (1998) Water Quality – Sampling. Part 1: Guidance on the design of sampling programs, sampling techniques and the preservation and handling of samples. AS/NZS 5667.1:1998. Standards Australia, Homebush.

Taylor, H.A., Rasheed, M.A., Carter, A.B. (2015) Port of Weipa long-term seagrass monitoring 2000 – 2014. Centre for Tropical Water & Aquatic Ecosystem Research (TropWATER) Publication 15/02, 41 pp.

Thomas, S., Ridd, P. V., Renagi, O. (2003) Laboratory investigation on the effect of particle size, water flow and bottom surface roughness upon the response of an upward- pointing optical backscatter sensor to sediment accumulation. Continental Shelf Research. 23, 1545-1557.

TropWATER (2015) Assessment of the contamination risk posed by sampling consumables to the detection and monitoring of filterable metals in water samples. Internal report. Centre for Tropical Water and Aquatic Ecosystem Research, James Cook University.

Wolanski, E., Delesalle, B., Gibbs, R. (1994) Carbonate mud in Mataiva Atoll, French Polynesia: Suspension and export. Marine Pollution Bulletin 29:36-41.

A1   APPENDIX

A1.1   Calibration procedures

A1.1.1 Turbidity/Deposition Calibration

The turbidity and deposition sensors on each instrument are calibrated to a set of plastic optical standards that give consistent NTU return values. This enables the calculation of raw data values into NTU values. The NTU values can then be converted into SSC and ASSD values through the SSC calibration process. Deposition sensors are calibrated to give measurements in units of mg/cm2 using the methodology outlined in Ridd et al (2000) and Thomas et al (2003). Instruments are calibrated every six months or after every deployment. Sediment samples are taken at each deployment site and used to determine sediment calibration coefficients used to account for variations in grain size and shape that can alter the implied SSC value.

A1.1.2 SSC Calibration

An instrument is placed in a large container (50 l) with black sides and the output is read on a computer attached to the logger. Saltwater is used to fill the container. Sediment from the study site is added to a small container of salt water and agitated. The water-sediment slurry is then added to the large container which is stirred with a small submerged pump. A water sample is taken and analysed for total suspended sediment (TSS) using standard laboratory techniques in the ACTFR laboratory at JCU which is accredited for these measurements. Approximately 6 different concentrations of sediment are used for each site. TSS is then plotted against the NTU reading from the logger for each of the different sediment concentrations. A linear correlation between NTU and SSC is then calculated. The correlations typically have an r2 value equal to or greater than 0.9.

A1.1.3 Light Calibration

The light sensors on each logger are calibrated every six months or after every deployment. The light sensor is calibrated against a LICOR U250A submersible sensor that was calibrated in the factory within the last 12 months. The results of the logger light sensor and LICOR U250A are compared and a calibration coefficient is used to ensure accurate reporting of PAR data. An in-field comparison between the logger light sensor and LICOR U250A is made on deployment of the instruments to ensure accurate reporting of the data. In field calibration of the nephelometer light sensor against the LICOR U250A at varying depth has been carried out to account for changes in sensitivity changes at depth.

A1.1.4 Pressure Sensor Calibration

All pressure sensors are calibrated against a pressure gauge and the pressure is converted into depth in metres.

A1.2   Time Series

A1.2.1   WQ1
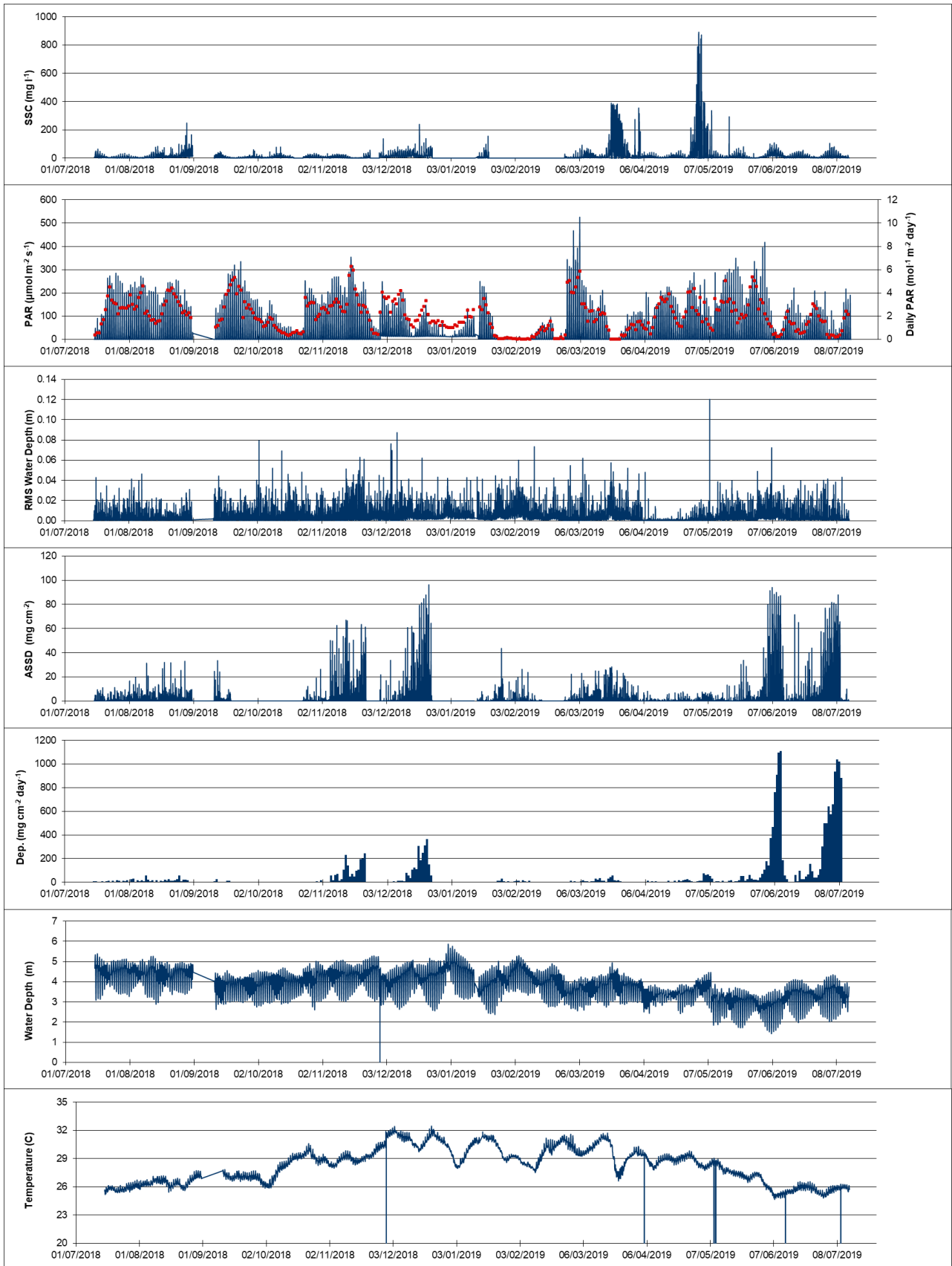
A1.2.2 WQ2
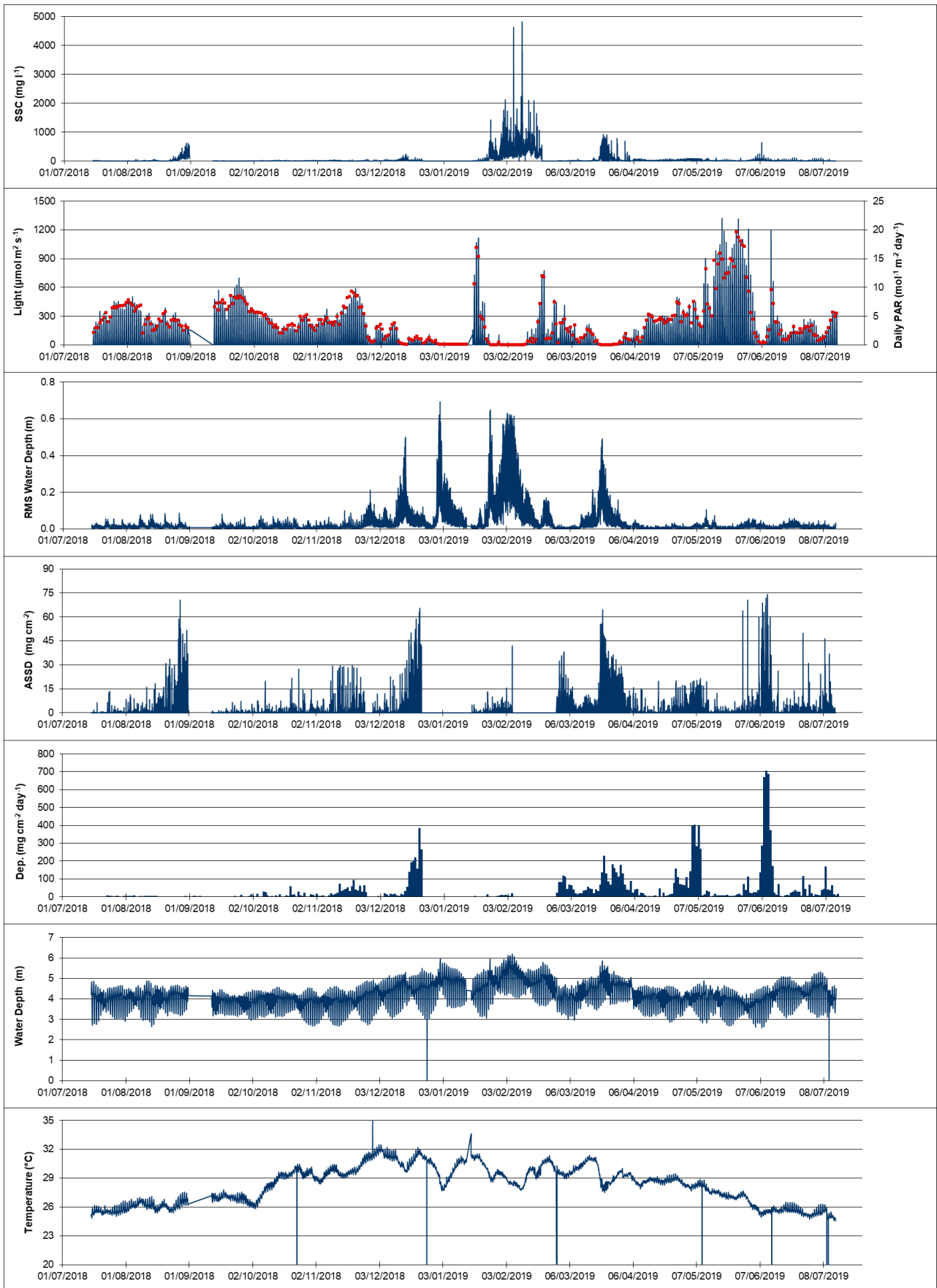
A1.2.3   WQ3
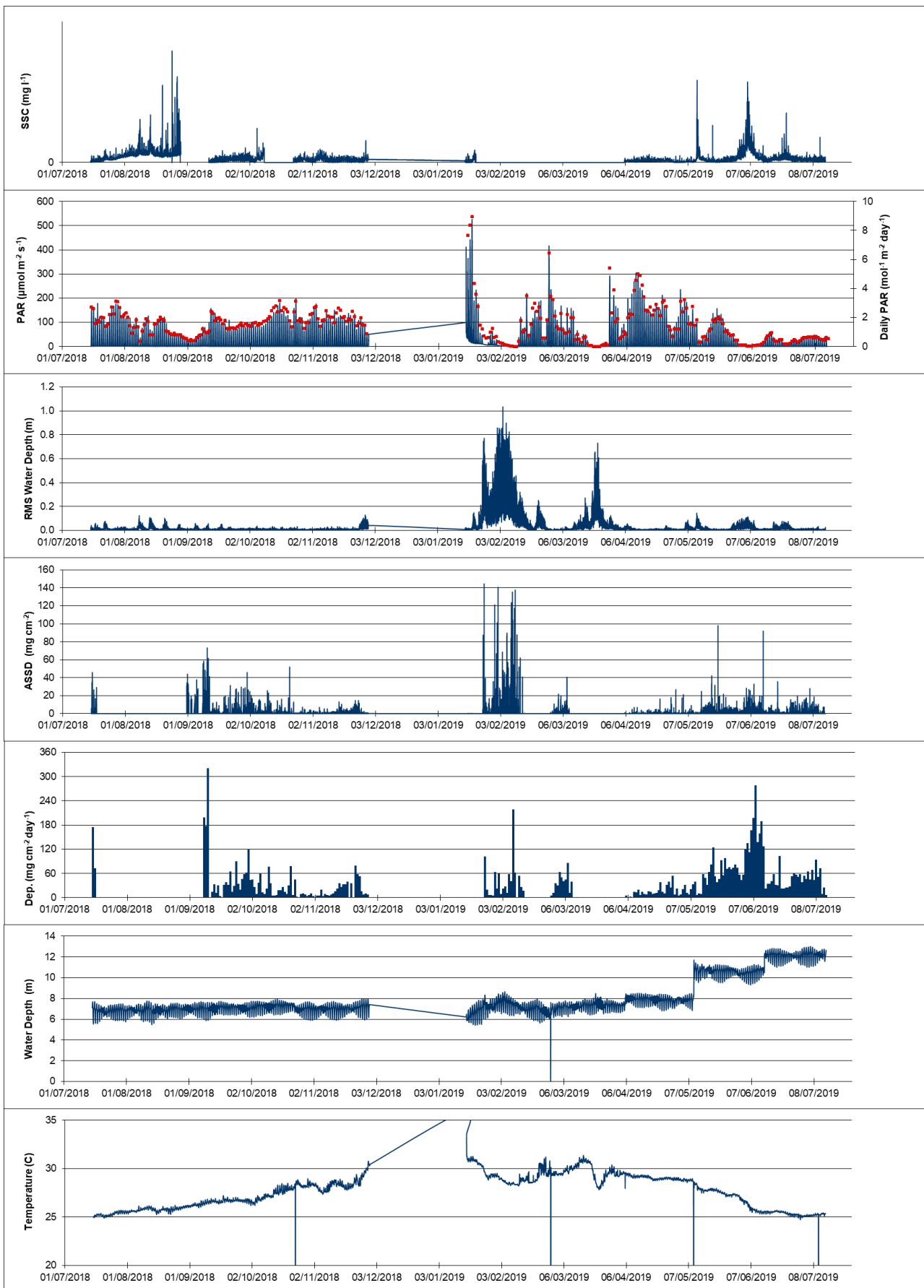
A1.2.4 WQ4
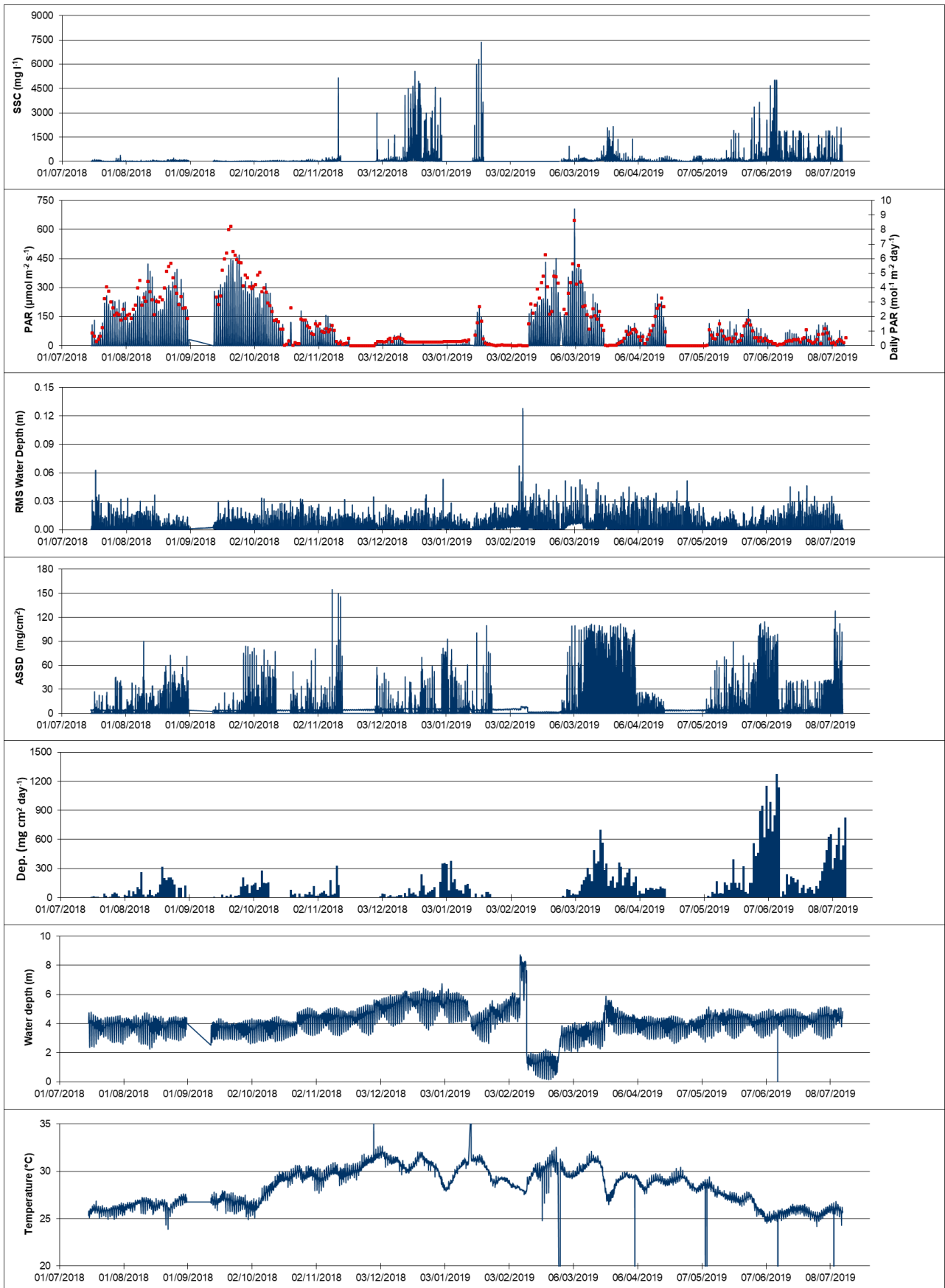
A1.3 Monthly statistics

A1.3.1 WQ1

SSC	07/2018	08/2018	09/2018	10/2018	11/2018	12/2018	01/2019	02/2019	03/2019	04/2019	05/2019	06/2019	07/2019
Mean	7.00	12.23	5.23	7.55	6.62	21.21	10.78	3.98	25.84	10.72	29.77	13.96	14.13
median	4.36	7.72	3.11	5.58	4.35	14.53	5.01	2.59	7.26	5.16	5.18	7.87	7.29
min	0.52	0.00	0.10	1.07	0.00	3.06	0.00	0.14	0.00	0.48	0.00	0.00	0.01
lower	2.45	3.39	1.70	3.52	1.58	9.79	2.39	1.48	3.53	3.19	2.74	3.77	3.94
upper	8.28	16.00	6.82	9.80	9.23	28.19	12.64	4.70	22.74	9.58	14.17	18.84	19.46
max	64.11	246.51	59.14	78.71	56.77	239.57	155.97	29.12	389.70	355.24	891.62	108.65	104.52
90th percentile	15.56	27.77	12.12	15.71	16.35	43.83	31.86	8.27	64.83	18.67	51.17	34.76	38.62
10th percentile	1.55	1.81	0.99	2.27	0.45	7.41	0.83	0.91	1.75	2.15	1.60	2.10	2.23
n	2436	4354	2907	3815	3569	3365	783	329	4419	4291	4390	4311	1865
St. Dev	7.58	13.96	5.70	5.91	7.09	17.51	14.46	4.20	50.45	22.41	81.27	15.12	15.34
St. Error	0.15	0.21	0.11	0.10	0.12	0.30	0.52	0.23	0.76	0.34	1.23	0.23	0.36

Dep. (mg cm^{-2} day^{-1})	07/2018	08/2018	09/2018	10/2018	11/2018	12/2018	01/2019	02/2019	03/2019	04/2019	05/2019	06/2019	07/2019
Mean	8.37	18.52	8.66	3.71	79.43	95.45	5.81	5.55	13.28	6.12	24.39	220.84	519.48
median	8.95	17.40	5.79	3.48	58.88	56.35	3.07	3.29	9.37	2.46	17.20	81.07	575.72
min	1.17	3.38	2.72	1.63	0.73	0.47	0.39	0.31	0.64	0.46	0.65	0.98	0.29
lower	4.36	9.36	3.54	2.00	14.98	8.98	0.83	1.64	3.84	1.34	7.49	38.14	1.67
upper	11.98	21.99	10.74	4.16	106.91	138.33	7.37	9.96	16.41	9.98	34.85	185.31	882.08

max	17.73	59.04	25.58	8.87	246.14	363.98	32.07	17.51	56.91	24.62	74.86	1110.29	1039.84
90th percentile	14.42	28.73	16.12	5.73	197.67	293.38	11.66	12.38	31.15	15.04	61.16	776.73	1003.79
10th percentile	1.38	5.93	3.26	1.66	1.45	2.61	0.56	1.09	1.94	1.18	4.13	6.87	0.59
n	17	28	8	8	22	23	16	17	31	30	31	30	13
St. Dev	5.19	13.47	7.64	2.34	77.60	113.50	8.01	5.18	13.57	6.45	22.10	321.77	402.27
St. Error	1.26	2.55	2.70	0.83	16.54	23.67	2.00	1.26	2.44	1.18	3.97	58.75	111.57

RMS	07/2018	08/2018	09/2018	10/2018	11/2018	12/2018	01/2019	02/2019	03/2019	04/2019	05/2019	06/2019	07/2019
Mean	0.0018	0.0019	0.0022	0.0025	0.0043	0.0048	0.0057	0.0057	0.0039	0.0010	0.0031	0.0046	0.0022
median	0.0011	0.0013	0.0015	0.0015	0.0025	0.0036	0.0044	0.0039	0.0026	0.0007	0.0018	0.0026	0.0015
min	0.0000	0.0000	0.0000	0.0000	0.0000	0.0000	0.0007	0.0000	0.0000	0.0000	0.0000	0.0003	0.0000
lower	0.0008	0.0009	0.0008	0.0008	0.0014	0.0026	0.0026	0.0020	0.0014	0.0005	0.0011	0.0018	0.0009
upper	0.0017	0.0019	0.0024	0.0026	0.0052	0.0055	0.0071	0.0075	0.0045	0.0009	0.0034	0.0054	0.0022
max	0.0428	0.0463	0.0443	0.0794	0.0628	0.0873	0.0446	0.0734	0.0619	0.0480	0.1203	0.0724	0.0430
90th percentile	0.0030	0.0033	0.0040	0.0050	0.0097	0.0084	0.0107	0.0129	0.0080	0.0015	0.0071	0.0104	0.0033
10th percentile	0.0006	0.0007	0.0005	0.0005	0.0008	0.0016	0.0020	0.0011	0.0008	0.0003	0.0007	0.0013	0.0006
n	2448	4383	2913	4460	4241	4464	4262	4026	4464	4314	4457	4316	1869
St. Dev	0.0027	0.0026	0.0029	0.0039	0.0054	0.0044	0.0047	0.0056	0.0047	0.0017	0.0043	0.0048	0.0034
St. Error	0.0001	0.0000	0.0001	0.0001	0.0001	0.0001	0.0001	0.0001	0.0001	0.0000	0.0001	0.0001	0.0001

Temperature	07/2018	08/2018	09/2018	10/2018	11/2018	12/2018	01/2019	02/2019	03/2019	04/2019	05/2019	06/2019	07/2019
Mean	25.85	26.51	27.04	28.44	29.25	31.00	29.88	29.57	29.67	28.99	27.71	25.67	25.72
median	25.84	26.47	27.05	28.80	29.11	31.04	29.80	29.67	29.75	28.98	27.59	25.66	25.82

min	25.18	25.43	25.97	25.86	27.98	29.27	27.96	27.51	26.62	27.79	26.45	24.66	24.81
lower	25.65	26.20	26.86	27.97	28.72	30.50	29.00	28.53	29.14	28.73	27.26	25.32	25.50
upper	26.02	26.79	27.22	29.21	29.61	31.49	30.88	30.53	30.49	29.33	28.20	25.99	25.95
max	26.74	27.73	27.85	30.61	31.87	32.47	31.85	31.60	31.73	30.31	29.05	27.03	26.29
90th percentile	26.22	27.09	27.42	29.53	30.38	31.83	31.27	30.93	31.08	29.48	28.52	26.24	26.09
10th percentile	25.50	26.02	26.66	26.32	28.34	30.17	28.53	28.09	27.79	28.37	27.03	25.13	25.21
n	2448	4383	2913	4452	4241	4464	4262	4026	4464	4305	4430	4307	1861
St. Dev	0.27	0.42	0.31	1.12	0.77	0.64	1.04	1.09	1.14	0.43	0.56	0.44	0.33
St. Error	0.01	0.01	0.01	0.02	0.01	0.01	0.02	0.02	0.02	0.01	0.01	0.01	0.01

PAR	07/2018	08/2018	09/2018	10/2018	11/2018	12/2018	01/2019	02/2019	03/2019	04/2019	05/2019	06/2019	07/2019
Mean	2.40	2.84	3.10	1.41	2.87	2.29	1.33	0.71	1.90	2.27	2.84	1.43	0.91
median	2.71	2.73	2.88	1.19	2.78	2.05	1.25	0.19	1.56	2.15	2.62	1.37	0.41
min	0.40	1.37	1.08	0.34	0.43	1.07	0.07	0.02	0.00	0.49	0.79	0.23	0.16
lower	1.71	2.13	1.86	0.61	2.35	1.54	0.25	0.06	0.60	1.26	1.98	0.67	0.32
upper	3.04	3.65	4.22	1.80	3.21	3.31	1.99	0.83	2.66	3.20	3.45	1.99	1.63
max	4.50	4.60	5.34	3.63	6.29	4.19	3.52	5.07	5.86	4.39	5.37	3.16	2.44
90th percentile	3.52	4.20	4.72	3.09	4.44	3.63	2.61	1.30	4.06	3.94	4.57	2.67	2.11
10th percentile	0.55	1.63	1.62	0.46	0.79	1.21	0.09	0.02	0.02	0.97	1.41	0.43	0.21
n	17	30	20	31	30	31	29	28	31	30	31	30	12
St. Dev	1.15	0.96	1.33	0.95	1.41	0.97	1.02	1.28	1.61	1.14	1.21	0.86	0.84
St. Error	0.28	0.17	0.30	0.17	0.26	0.17	0.19	0.24	0.29	0.21	0.22	0.16	0.24
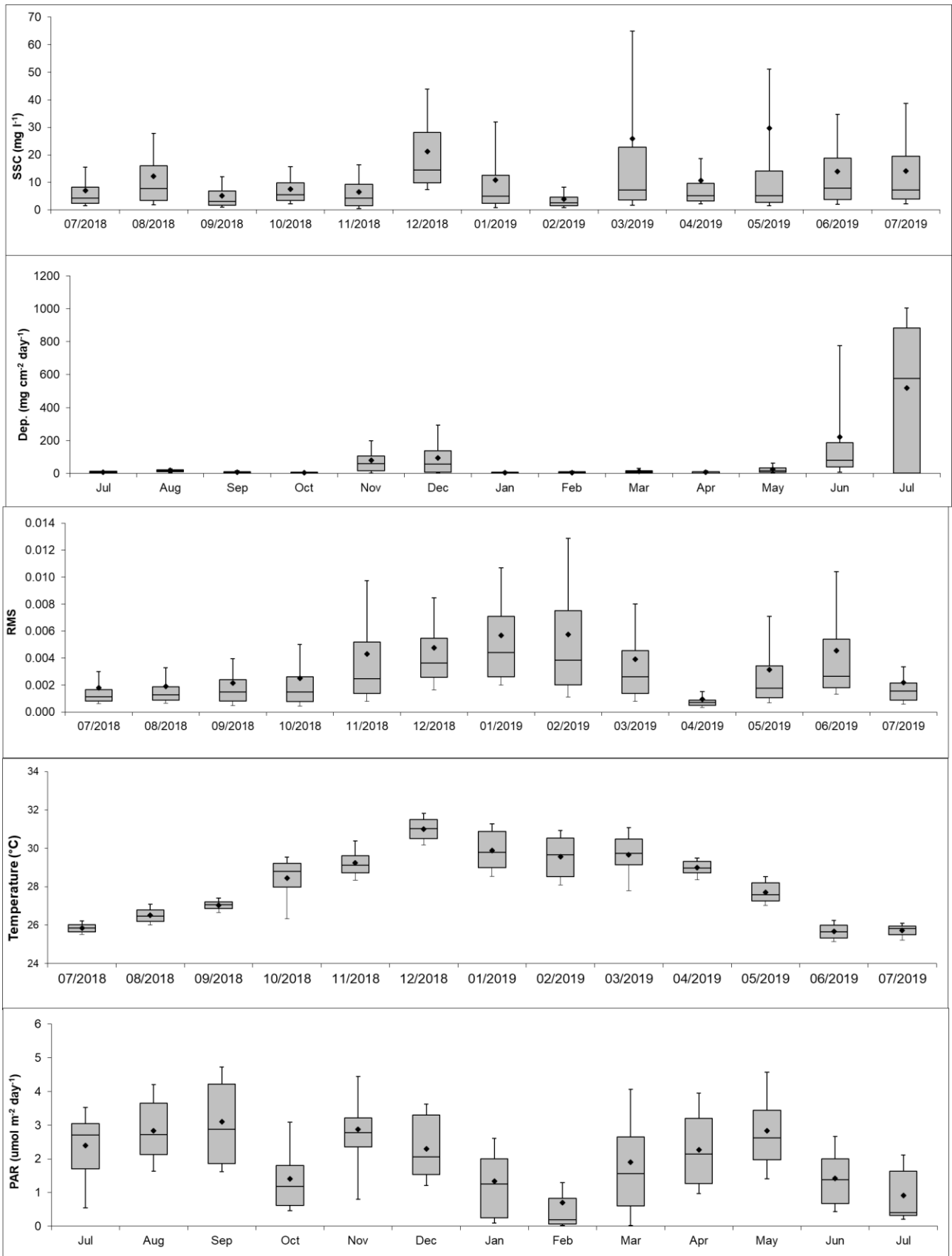
A1.3.2 WQ2

SSC	07/2018	08/2018	09/2018	10/2018	11/2018	12/2018	01/2019	02/2019	03/2019	04/2019	05/2019	06/2019	07/2019
Mean	2.14	40.54	2.17	5.77	6.08	21.82	106.95	419.40	63.04	21.06	19.48	17.97	10.45
median	1.22	3.76	1.86	4.69	4.02	12.82	42.96	363.52	7.44	17.49	8.22	9.39	4.70
min	0.00	0.00	0.00	0.46	0.00	1.05	0.00	0.70	0.00	0.00	0.42	0.00	0.51
lower	0.56	1.04	1.20	3.43	1.84	6.05	5.77	230.73	2.34	8.88	4.94	3.87	2.79
upper	2.50	30.25	2.80	6.87	7.86	27.80	160.34	504.02	47.14	29.96	27.88	22.35	13.16
max	25.17	619.27	13.86	35.86	52.99	240.33	1420.88	4817.42	925.66	688.95	103.07	633.20	106.37
90th percentile	4.49	148.07	4.08	10.47	14.06	49.21	289.16	703.71	211.81	40.71	55.97	46.81	23.99
10th percentile	0.16	0.19	0.64	2.53	0.71	3.86	1.11	147.84	1.12	3.96	3.99	1.96	1.65
n	2447	4370	2766	4463	3856	3240	2198	2929	4403	4179	4358	4313	1116
St. Dev	3.01	83.05	1.53	3.70	6.45	25.32	151.74	369.85	129.55	19.54	21.41	26.01	14.30
St. Error	0.06	1.26	0.03	0.06	0.10	0.44	3.24	6.83	1.95	0.30	0.32	0.40	0.43

Dep. (mg cm^{-2} day^{-1})	07/2018	08/2018	09/2018	10/2018	11/2018	12/2018	01/2019	02/2019	03/2019	04/2019	05/2019	06/2019	07/2019
Mean	3.11	2.77	1.97	10.57	30.99	80.99	3.88	22.36	81.58	36.03	80.28	122.72	38.72
median	2.69	3.01	1.03	7.06	27.33	17.13	2.94	10.69	67.47	22.43	12.94	28.75	19.42
min	1.52	0.06	0.15	0.58	1.71	1.45	0.51	5.13	12.80	0.53	2.16	1.84	4.80
lower	2.22	0.27	0.57	2.16	9.56	8.51	1.36	7.70	38.96	7.17	6.92	14.09	10.35
upper	3.67	4.60	2.07	13.09	43.61	153.08	4.11	21.84	124.25	59.90	89.60	103.46	40.70
max	7.65	6.33	11.42	57.32	93.81	384.63	12.63	81.61	228.40	156.81	403.00	706.17	170.04

90th percentile	4.40	5.34	3.66	25.10	62.81	217.90	9.46	46.45	160.29	76.80	283.15	404.04	69.79
10th percentile	1.76	0.11	0.37	0.87	4.61	4.35	0.72	6.48	19.59	3.12	5.01	5.55	7.71
n	17	30	20	30	26	22	15	7	31	30	31	30	9
St. Dev	1.50	2.17	2.63	12.07	24.60	109.34	3.66	27.01	56.83	37.40	127.87	209.44	51.47
St. Error	0.36	0.40	0.59	2.20	4.82	23.31	0.95	10.21	10.21	6.83	22.97	38.24	17.16

RMS	07/2018	08/2018	09/2018	10/2018	11/2018	12/2018	01/2019	02/2019	03/2019	04/2019	05/2019	06/2019	07/2019
Mean	0.012	0.014	0.010	0.012	0.020	0.058	0.096	0.129	0.050	0.008	0.011	0.013	0.011
median	0.010	0.012	0.008	0.008	0.012	0.036	0.061	0.070	0.029	0.007	0.009	0.012	0.010
min	0.002	0.002	0.002	0.000	0.001	0.003	0.001	0.002	0.001	0.000	0.001	0.000	0.003
lower	0.007	0.008	0.006	0.005	0.007	0.021	0.026	0.025	0.008	0.004	0.006	0.007	0.008
upper	0.015	0.017	0.012	0.015	0.025	0.063	0.127	0.200	0.059	0.010	0.014	0.018	0.014
max	0.055	0.086	0.079	0.070	0.212	0.619	0.691	0.624	0.492	0.050	0.104	0.058	0.046
90th percentile	0.020	0.026	0.018	0.025	0.049	0.128	0.232	0.362	0.125	0.016	0.021	0.024	0.018
10th percentile	0.005	0.006	0.004	0.003	0.005	0.013	0.010	0.009	0.005	0.003	0.004	0.005	0.006
n	2448	4384	2766	4463	4240	4458	4120	3982	4464	4207	4461	4316	1239
St. Dev	0.007	0.009	0.007	0.010	0.021	0.068	0.102	0.139	0.066	0.006	0.008	0.008	0.005
St. Error	0.000	0.000	0.000	0.000	0.000	0.001	0.002	0.002	0.001	0.000	0.000	0.000	0.000

Temperature	07/2018	08/2018	09/2018	10/2018	11/2018	12/2018	01/2019	02/2019	03/2019	04/2019	05/2019	06/2019	07/2019
Mean	25.57	26.19	26.91	28.63	29.83	30.95	29.86	29.40	29.65	28.79	27.61	25.67	25.42

median	25.52	26.16	26.93	29.13	29.69	31.02	29.81	29.42	29.58	28.77	27.50	25.62	25.34
min	24.85	25.38	25.97	25.81	28.38	29.17	27.68	27.71	27.50	27.88	26.74	24.92	24.71
lower	25.38	25.90	26.72	27.91	29.28	30.48	29.11	28.53	29.00	28.57	27.15	25.44	25.19
upper	25.70	26.47	27.13	29.51	30.21	31.44	30.79	30.09	30.38	28.97	28.11	25.87	25.62
max	26.63	27.55	27.78	30.45	35.95	32.46	33.53	31.34	31.37	29.59	28.88	26.88	26.29
90th percentile	26.01	26.73	27.29	29.85	31.13	31.86	31.15	30.71	30.93	29.26	28.32	26.17	25.91
10th percentile	25.27	25.67	26.49	26.49	28.91	29.99	28.44	28.19	28.49	28.39	26.98	25.25	25.04
n	2448	4384	2766	4448	4240	4458	4120	3976	4464	4207	4449	4307	1239
St. Dev	0.29	0.41	0.31	1.20	0.80	0.68	1.02	0.94	0.88	0.32	0.51	0.36	0.33
St. Error	0.01	0.01	0.01	0.02	0.01	0.01	0.02	0.01	0.01	0.00	0.01	0.01	0.01

PAR	07/2018	08/2018	09/2018	10/2018	11/2018	12/2018	01/2019	02/2019	03/2019	04/2019	05/2019	06/2019	07/2019
Mean	5.28	4.48	7.34	3.93	4.93	1.32	2.12	2.15	1.31	3.90	10.97	2.63	1.80
median	5.65	4.26	7.33	3.64	4.39	1.01	0.12	0.67	1.00	4.34	11.75	2.17	1.59
min	2.21	2.06	5.84	2.04	0.47	0.12	0.00	0.00	0.00	0.61	3.17	0.27	0.81
lower	3.99	3.31	6.69	3.07	3.54	0.51	0.12	0.00	0.12	2.76	6.25	1.43	1.11
upper	6.74	5.71	8.15	5.00	6.58	1.61	0.63	2.50	2.28	5.06	14.82	3.16	2.21
max	7.37	7.84	8.54	5.88	9.31	3.87	16.96	12.03	4.47	7.51	19.67	9.59	3.34
90th percentile	6.87	6.87	8.35	5.58	8.53	3.16	6.68	7.29	3.13	5.40	17.47	4.60	3.04
10th percentile	3.01	2.70	6.17	2.54	1.31	0.19	0.00	0.00	0.00	1.03	4.72	0.60	0.95
n	17	30	19	31	30	31	28	28	31	28	31	30	9
St. Dev	1.65	1.58	0.86	1.16	2.51	1.14	4.59	3.45	1.32	1.85	5.07	2.03	0.88
St. Error	0.40	0.29	0.20	0.21	0.46	0.21	0.87	0.65	0.24	0.35	0.91	0.37	0.29
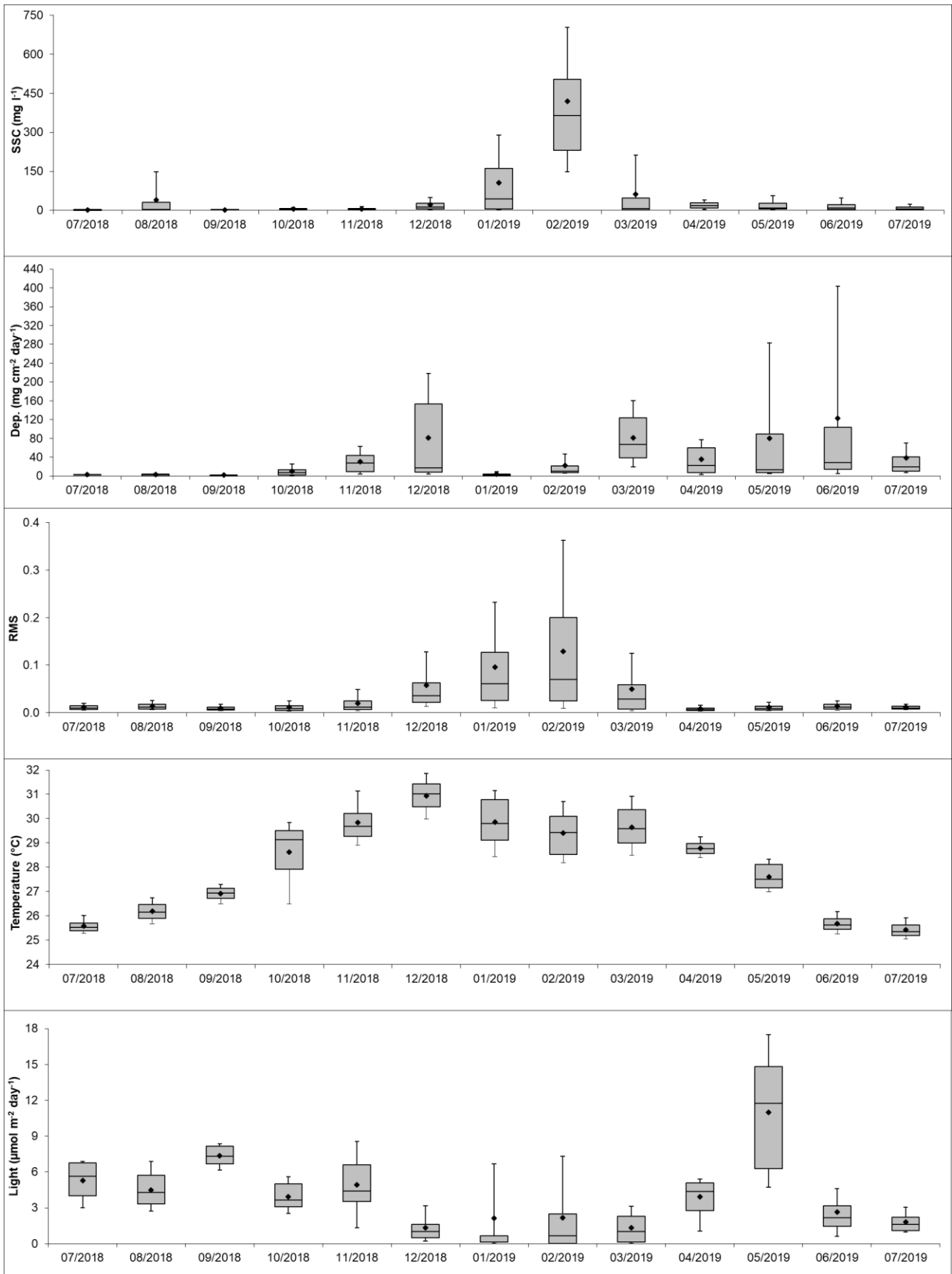
A1.3.3   WQ3

SSC	07/2018	08/2018	09/2018	10/2018	11/2018	12/2018	01/2019	02/2019	03/2019	04/2019	05/2019	06/2019	07/2019
Mean	2.49	7.05	1.97	2.43	1.78		1.45			1.13	1.70	5.23	1.96
median	2.32	5.79	1.83	2.04	1.44		0.91			1.09	0.92	3.12	1.87
min	0.09	3.46	0.00	0.00	0.00		0.00			0.00	0.00	0.05	0.50
lower	1.36	5.05	1.11	1.32	0.79		0.35			0.82	0.51	2.18	1.41
upper	3.40	7.05	2.64	3.10	2.48		2.08			1.35	1.70	5.91	2.39
max	10.22	79.03	10.42	24.11	15.45		8.73			5.76	58.20	56.70	7.29
90th percentile	4.33	10.04	3.58	4.30	3.52		3.81			1.70	3.05	11.96	2.94
10th percentile	0.83	4.60	0.43	0.84	0.38		0.10			0.53	0.25	1.42	1.10
n	2447	3983	2783	2319	4101	0	761	0	0	3681	4451	4311	1367
St. Dev	1.38	4.76	1.25	1.71	1.42		1.52			0.55	3.29	5.68	0.76
St. Error	0.03	0.08	0.02	0.04	0.02		0.06			0.01	0.05	0.09	0.02

Dep. (mg cm^{-2} day^{-1})	07/2018	08/2018	09/2018	10/2018	11/2018	12/2018	01/2019	02/2019	03/2019	04/2019	05/2019	06/2019	07/2019
Mean	123.69		64.87	22.19	21.97		15.17	41.50	44.68	15.90	48.28	82.59	57.92
median	123.69		33.29	12.46	15.94		0.64	26.09	40.48	13.55	49.07	56.78	53.10
min	72.69		0.63	1.25	3.05		0.06	0.43	12.21	0.61	5.40	21.75	38.33
lower	98.19		21.83	7.26	7.28		0.29	11.67	35.49	8.22	20.63	32.65	45.08
upper	149.19		63.75	32.55	32.97		13.19	56.13	50.46	19.26	72.84	124.47	68.00
max	174.69		320.26	78.02	79.70		101.40	218.69	86.29	54.07	123.77	278.51	94.51

90th percentile	164.49		171.35	44.69	47.43		46.86	60.83	67.52	34.94	82.50	169.71	74.58
10th percentile	82.89		11.37	4.95	4.63		0.21	6.23	26.61	3.42	8.14	24.71	42.59
n	2	0	22	31	25	0	15	15	9	26	31	30	10
St. Dev	72.12		77.11	21.09	19.85		29.09	53.37	20.88	12.82	31.41	65.62	17.26
St. Error	51.00		16.44	3.79	3.97		7.51	13.78	6.96	2.51	5.64	11.98	5.46

RMS	07/2018	08/2018	09/2018	10/2018	11/2018	12/2018	01/2019	02/2019	03/2019	04/2019	05/2019	06/2019	07/2019
Mean	0.012	0.014	0.009	0.007	0.012		0.117	0.156	0.055	0.009	0.014	0.020	0.008
median	0.009	0.009	0.008	0.007	0.007		0.070	0.085	0.027	0.007	0.008	0.014	0.007
min	0.001	0.001	0.001	0.001	0.001		0.002	0.000	0.000	0.000	0.000	0.000	0.000
lower	0.007	0.006	0.006	0.005	0.005		0.014	0.025	0.008	0.005	0.005	0.007	0.005
upper	0.014	0.016	0.011	0.009	0.011		0.183	0.236	0.061	0.011	0.017	0.029	0.009
max	0.075	0.123	0.058	0.036	0.128		0.768	1.034	0.729	0.055	0.144	0.113	0.033
90th percentile	0.023	0.033	0.016	0.012	0.029		0.292	0.429	0.144	0.018	0.031	0.044	0.012
10th percentile	0.005	0.004	0.004	0.004	0.004		0.008	0.008	0.005	0.004	0.004	0.004	0.004
n	2448	4464	4306	4459	4101	0	2221	4017	4464	4312	4453	4315	1368
St. Dev	0.009	0.014	0.006	0.004	0.014		0.126	0.173	0.080	0.007	0.015	0.017	0.003
St. Error	0.000	0.000	0.000	0.000	0.000		0.003	0.003	0.001	0.000	0.000	0.000	0.000

Temperature	07/2018	08/2018	09/2018	10/2018	11/2018	12/2018	01/2019	02/2019	03/2019	04/2019	05/2019	06/2019	07/2019
Mean	25.28	25.79	26.56	27.61	28.46		30.08	28.98	29.71	29.13	27.96	25.67	25.14

	07/2018	08/2018	09/2018	10/2018	11/2018	12/2018	01/2019	02/2019	03/2019	04/2019	05/2019	06/2019	07/2019
median	25.26	25.78	26.59	27.71	28.31		30.24	28.79	29.70	29.10	27.78	25.53	25.13
min	24.88	25.24	25.96	26.18	27.35		28.80	28.20	27.81	27.98	27.05	24.91	24.72
lower	25.12	25.64	26.43	27.08	28.01		29.30	28.54	29.34	28.95	27.43	25.39	25.08
upper	25.44	25.93	26.70	28.18	28.71		30.80	29.32	30.27	29.26	28.69	25.69	25.19
max	25.69	26.22	27.20	28.95	30.76		36.04	31.19	31.36	29.86	29.07	27.25	25.38
90th percentile	25.57	26.04	26.80	28.40	29.53		30.97	29.94	30.74	29.46	28.85	26.60	25.24
10th percentile	25.04	25.53	26.20	26.65	27.68		29.15	28.36	28.49	28.87	27.25	25.23	25.06
n	2448	4464	4306	4447	4101	0	2221	4011	4464	4312	4446	4315	1368
St. Dev	0.20	0.20	0.23	0.66	0.69		0.77	0.60	0.78	0.21	0.60	0.48	0.09
St. Error	0.00	0.00	0.00	0.01	0.01		0.02	0.01	0.01	0.00	0.01	0.01	0.00

PAR	07/2018	08/2018	09/2018	10/2018	11/2018	12/2018	01/2019	02/2019	03/2019	04/2019	05/2019	06/2019	07/2019
Mean	2.21	1.25	1.29	2.01	1.97		2.92	1.43	1.08	2.39	1.38	0.29	0.61
median	2.16	1.06	1.28	1.76	1.97		1.25	0.87	0.64	2.33	1.21	0.24	0.63
min	1.37	0.36	0.38	1.25	0.89		0.59	0.00	0.00	0.53	0.09	0.00	0.51
lower	1.79	0.81	0.98	1.63	1.69		0.69	0.19	0.12	1.26	0.72	0.09	0.59
upper	2.69	1.76	1.61	2.41	2.30		3.97	2.48	1.83	3.02	1.84	0.44	0.66
max	3.11	2.30	2.43	3.17	2.76		8.96	6.45	5.42	4.99	3.24	0.94	0.67
90th percentile	2.88	1.89	1.96	2.67	2.55		8.10	3.29	2.28	4.25	2.66	0.52	0.66
10th percentile	1.55	0.65	0.46	1.42	1.44		0.62	0.03	0.00	0.83	0.41	0.05	0.52
n	17	31	30	31	28	0	15	28	31	30	31	30	10
St. Dev	0.54	0.53	0.55	0.54	0.44		3.04	1.55	1.25	1.25	0.85	0.24	0.06
St. Error	0.13	0.10	0.10	0.10	0.08		0.78	0.29	0.22	0.23	0.15	0.04	0.02
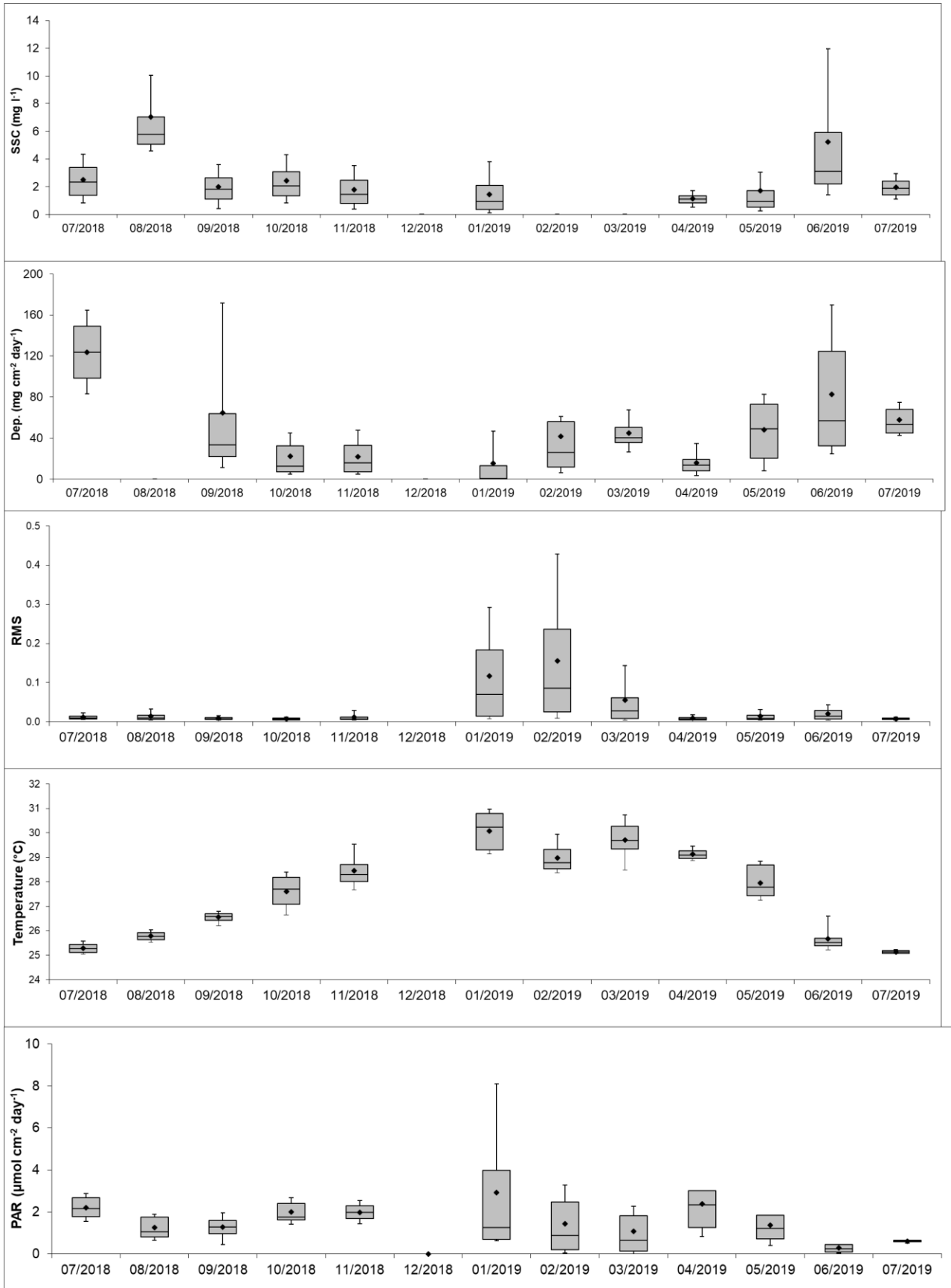
A1.3.4 WQ4

SSC	07/2018	08/2018	09/2018	10/2018	11/2018	12/2018	01/2019	02/2019	03/2019	04/2019	05/2019	06/2019	07/2019
Mean	15.25	13.71	7.71	12.78	71.38	287.84	123.43	19.91	85.33	21.95	47.07	239.44	132.15
median	7.21	7.19	4.31	9.10	16.97	56.68	24.61	13.08	34.74	10.54	20.77	39.76	35.06
min	0.00	0.00	0.00	0.00	0.00	4.95	0.00	0.00	0.00	0.00	0.00	0.00	0.00
lower	3.53	3.35	1.95	5.36	7.87	24.75	8.61	8.06	13.07	5.05	8.35	16.78	14.20
upper	16.60	19.08	9.78	15.50	42.16	153.26	59.34	21.88	102.43	26.38	51.72	142.06	113.53
max	372.42	215.61	84.79	133.28	5154.75	5557.21	7354.25	195.72	2111.76	1389.49	2681.88	5018.73	1888.46
90th percentile	38.39	34.33	19.55	27.24	107.94	657.34	126.95	38.54	202.77	52.82	96.28	501.08	317.32
10th percentile	1.47	1.97	0.97	2.66	3.37	14.54	0.88	3.56	6.51	2.69	4.33	8.78	8.37
n	2443	4377	2728	4416	1821	4426	777	198	4394	4259	4412	4316	1244
St. Dev	23.66	16.10	9.20	12.75	346.33	716.67	585.61	25.42	143.00	37.51	116.45	646.15	269.33
St. Error	0.48	0.24	0.18	0.19	8.12	10.77	21.01	1.81	2.16	0.57	1.75	9.84	7.64

Dep. (mg cm^{-2} day^{-1})	07/2018	08/2018	09/2018	10/2018	11/2018	12/2018	01/2019	02/2019	03/2019	04/2019	05/2019	06/2019	07/2019
Mean	16.76	102.22	44.12	90.89	81.68	49.86	119.24	17.37	218.23	106.12	135.71	405.12	374.75
median	9.09	81.28	19.10	80.31	42.45	31.14	75.05	17.37	177.62	95.45	102.38	191.61	364.66
min	1.54	9.19	1.22	9.51	16.68	2.80	2.53	17.37	9.05	24.48	8.31	5.55	91.53
lower	3.90	29.19	5.99	33.41	28.61	13.42	38.41	17.37	94.90	79.22	46.07	92.49	273.26
upper	23.53	147.89	42.69	135.74	86.46	63.55	149.15	17.37	310.84	108.88	154.76	704.08	489.88
max	52.68	315.49	207.52	279.87	330.94	240.29	377.19	17.37	697.42	304.00	562.46	1273.80	656.11

90th percentile	42.74	206.99	122.72	153.41	176.83	111.82	350.72	17.37	371.39	174.97	294.16	999.71	634.42
10th percentile	2.78	16.74	3.04	29.39	21.29	6.80	5.89	17.37	29.33	42.01	40.63	44.69	156.38
n	16	28	18	20	12	29	23	1	31	18	23	30	9
St. Dev	17.06	83.22	58.80	68.02	92.73	53.75	122.49		165.54	65.79	131.62	405.55	192.57
St. Error	4.26	15.73	13.86	15.21	26.77	9.98	25.54		29.73	15.51	27.44	74.04	64.19

RMS	07/2018	08/2018	09/2018	10/2018	11/2018	12/2018	01/2019	02/2019	03/2019	04/2019	05/2019	06/2019	07/2019
Mean	0.002	0.002	0.002	0.002	0.002	0.002	0.003	0.005	0.005	0.002	0.001	0.002	0.002
median	0.001	0.001	0.001	0.001	0.001	0.002	0.002	0.004	0.004	0.001	0.001	0.001	0.001
min	0.000	0.000	0.000	0.000	0.000	0.000	0.000	0.000	0.000	0.000	0.000	0.000	0.000
lower	0.001	0.001	0.001	0.001	0.001	0.001	0.001	0.002	0.002	0.001	0.001	0.001	0.000
upper	0.002	0.002	0.002	0.002	0.002	0.003	0.004	0.007	0.008	0.002	0.001	0.002	0.001
max	0.063	0.037	0.031	0.033	0.035	0.037	0.053	0.127	0.053	0.052	0.028	0.046	0.035
90th percentile	0.003	0.003	0.003	0.003	0.003	0.004	0.006	0.010	0.009	0.003	0.002	0.003	0.002
10th percentile	0.000	0.000	0.000	0.000	0.000	0.001	0.001	0.001	0.001	0.000	0.000	0.000	0.000
n	2448	4382	2729	4448	4242	4464	4271	3880	4464	4316	4460	4318	1245
St. Dev	0.003	0.002	0.002	0.003	0.002	0.002	0.003	0.006	0.005	0.004	0.002	0.003	0.004
St. Error	0.000	0.000	0.000	0.000	0.000	0.000	0.000	0.000	0.000	0.000	0.000	0.000	0.000

Temperature	07/2018	08/2018	09/2018	10/2018	11/2018	12/2018	01/2019	02/2019	03/2019	04/2019	05/2019	06/2019	07/2019
Mean	25.89	26.52	26.78	28.59	30.05	30.96	29.88	29.50	29.65	29.03	27.71	25.64	25.63

median	25.92	26.56	26.82	29.07	29.95	31.01	29.85	29.47	29.69	29.05	27.61	25.65	25.70
min	24.92	23.88	24.89	25.09	27.68	29.21	27.91	24.78	26.48	27.61	26.30	24.52	24.17
lower	25.69	26.23	26.52	27.76	29.58	30.48	29.01	28.41	29.13	28.78	27.22	25.31	25.33
upper	26.13	26.85	27.09	29.60	30.57	31.44	30.89	30.45	30.54	29.35	28.24	25.95	25.92
max	26.86	27.62	27.96	30.63	37.55	32.67	36.65	32.54	32.11	30.43	29.42	27.10	26.68
90th percentile	26.29	27.08	27.34	29.95	31.13	31.78	31.24	30.95	31.11	29.50	28.53	26.20	26.16
10th percentile	25.42	25.97	26.14	26.36	29.17	30.09	28.57	28.06	27.68	28.47	26.96	25.05	25.06
n	2448	4382	2729	4448	4242	4464	4271	3872	4464	4307	4446	4298	1245
St. Dev	0.33	0.46	0.48	1.31	0.76	0.64	1.06	1.15	1.18	0.42	0.61	0.45	0.42
St. Error	0.01	0.01	0.01	0.02	0.01	0.01	0.02	0.02	0.02	0.01	0.01	0.01	0.01

PAR	07/2018	08/2018	09/2018	10/2018	11/2018	12/2018	01/2019	02/2019	03/2019	04/2019	05/2019	06/2019	07/2019
Mean	25.89	26.52	26.78	28.59	30.05	30.96	29.88	29.50	29.65	29.03	27.71	25.64	25.63
median	25.92	26.56	26.82	29.07	29.95	31.01	29.85	29.47	29.69	29.05	27.61	25.65	25.70
min	24.92	23.88	24.89	25.09	27.68	29.21	27.91	24.78	26.48	27.61	26.30	24.52	24.17
lower	25.69	26.23	26.52	27.76	29.58	30.48	29.01	28.41	29.13	28.78	27.22	25.31	25.33
upper	26.13	26.85	27.09	29.60	30.57	31.44	30.89	30.45	30.54	29.35	28.24	25.95	25.92
max	26.86	27.62	27.96	30.63	37.55	32.67	36.65	32.54	32.11	30.43	29.42	27.10	26.68
90th percentile	26.29	27.08	27.34	29.95	31.13	31.78	31.24	30.95	31.11	29.50	28.53	26.20	26.16
10th percentile	25.42	25.97	26.14	26.36	29.17	30.09	28.57	28.06	27.68	28.47	26.96	25.05	25.06
n	2448	4382	2729	4448	4242	4464	4271	3872	4464	4307	4446	4298	1245
St. Dev	0.33	0.46	0.48	1.31	0.76	0.64	1.06	1.15	1.18	0.42	0.61	0.45	0.42
St. Error	0.01	0.01	0.01	0.02	0.01	0.01	0.02	0.02	0.02	0.01	0.01	0.01	0.01

A1.4 Marotte current meter animations

Link to short video:

https://jamescookuniversity-my.sharepoint.com/:v:/r/personal/rachael_macdonald_jcu_edu_au/Documents/NQBP%20Ambient%20Marine%20Water%20Quality%20Monitoring%20Program/Weipa/Marotte%20video/Weipa_cm2018-2019_short.avi?csf=1&e=gVVlfj

Link to long video:

https://jamescookuniversity-my.sharepoint.com/:v:/r/personal/rachael_macdonald_jcu_edu_au/Documents/NQBP%20Ambient%20Marine%20Water%20Quality%20Monitoring%20Program/Weipa/Marotte%20video/Weipa_cm2018-2019_long.avi?csf=1&e=iHUAbq
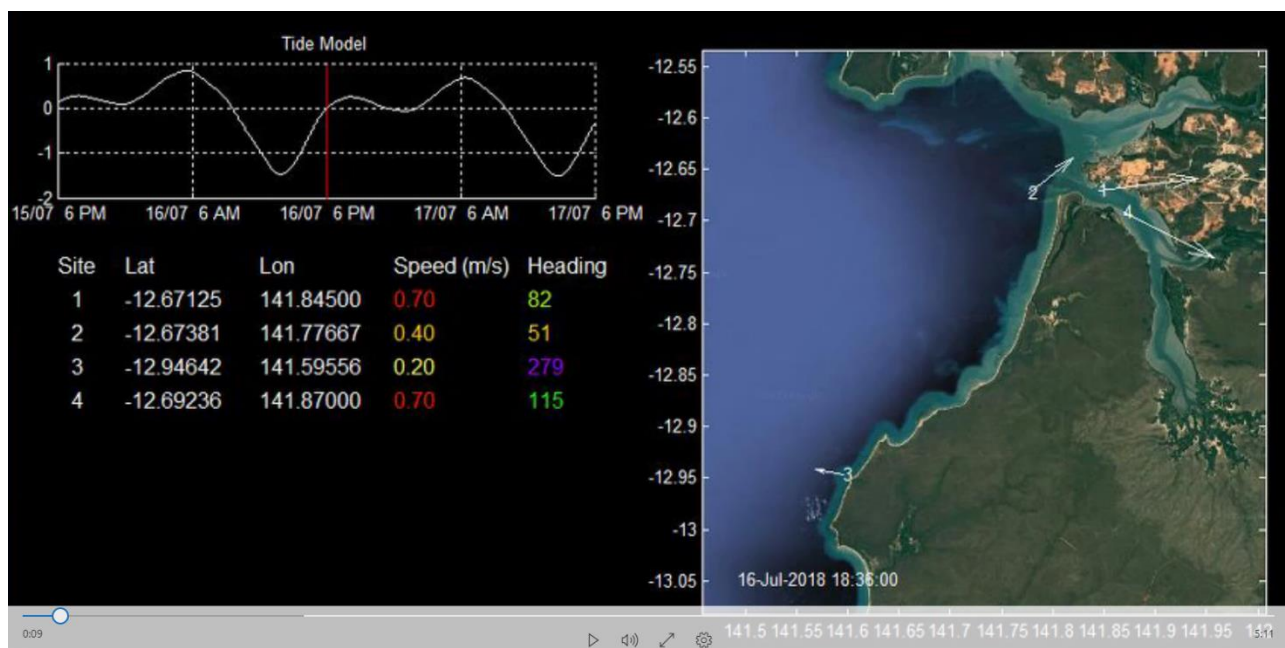

Figure A1.4.1   Example screengrab from current speed and direction animations